TECHNICAL REPORT STANDARD TITLE PAGE

1. Report No.	2. Government Accession No.	3. Recipient's Catalog No.

4. Title and Subtitle	5. Report Date
INFLUENCE OF WATER DEPTHS ON FRICTION PROPERTIES OF VARIOUS PAVEMENT TYPES	August 1974
	6. Performing Organization Code
7. Author(s)	8. Performing Organization Report No.
Bob M. Gallaway, Jerry G. Rose, William W. Scott, Jr. and Robert E. Schiller	RESEARCH REPORT 138-6
9. Performing Organization Name and Address	10. Work Unit No.
Texas Transportation Institute Texas A&M University College Station, Texas 77843	11. Contract or Grant No.
	13. Type of Report and Period Covered
12. Sponsoring Agency Name and Address	Interim - Sept. 1968 August 1974
Texas Highway Department P. O. Box 5051 Austin, Texas 78763	14. Sponsoring Agency Code Research Study 2-8-69-138

15. Supplementary Notes

Research done in cooperation with DOT, FHWA.
Research Study Title: "Vehicle-Pavement Interaction"

16. Abstract

Reported herein are the results of the final phase of THD Study 2-8-69-138. This phase of the study is concerned with the effect of various water depths (obtained with a rain simulator) on the friction properties of various pavement textures at different levels of vehicular speeds and tire-tread depths, tire pressures, and tire types. Equations relating these variables are also developed and the relative effects of the variable determined. Tabular and figurative methods are utilized to present the results.

Background information and pertinent past research pertaining to effects of water depth on pavement friction are given.

Sixteen different types of surfaces were tested, including full scale prototypes and regular pavements built under normal contracts. The surfaces, located at the Texas A&M Research Annex, are 600 feet long and 24 feet wide. Friction tests were conducted on each surface at several water depths for various combinations of tire type, tire-tread depth, tire pressure, and vehicle speed. Multiple regression analyses were used to assess the effects of the variables on friction properties of the different surfaces. A series of twenty-five tables included in the report presents the summarized data of the study.

Pavement water depth was found to significantly affect skid numbers at 60 mph. For a tire-tread depth of 0.31 in. and a texture of 0.033 in., increasing the water depth from 0.023 to 0.87 in. decreased the 60-mph skid numbers by 36 percent (See Table 3-17.) Increases in tire-tread depth and surface texture increased skid numbers; whereas, increases in vehicle speed decreased skid numbers.

(continued on separate page).

17. Key Words	18. Distribution Statement

19. Security Classif. (of this report)	20. Security Classif. (of this page)	21. No. of Pages	22. Price
Unclassified	Unclassified	124	

Form DOT F 1700.7 (8-69)

The findings and conclusions contained herein will be useful to the highway engineer in determining proper geometric designs and paving materials commensurate with acceptable pavement friction characteristics and service demands. Suggestions for further research are also included.

INFLUENCE OF WATER DEPTHS ON FRICTION PROPERTIES OF VARIOUS PAVEMENT TYPES

by

Bob M. Gallaway
Research Engineer

Jerry G. Rose
Research Assistant

William W. Scott, Jr.
Research Assistant

and

Robert E. Schiller
Research Engineer

Research Report Number 138-6
Vehicle-Pavement Interaction Study
Research Study Number 2-8-69-138

Sponsored by
the Texas Highway Department
in Cooperation with
U. S. Department of Transportation
Federal Highway Administration

August 1974

TEXAS TRANSPORTATION INSTITUTE
Texas A&M University
College Station, Texas

DISCLAIMER

The contents of this report reflect the views of the authors who are responsible for the facts and the accuracy of the data presented herein. The contents do not necessarily reflect the official views or policies of the Federal Highway Administration. This report does not constitute a standard, specification, or regulation.

ACKNOWLEDGEMENTS

In the collection of the data and the preparation of the report the authors are sincerely indebted to the assistance of several dedicated individuals without whose help this task probably would not have been completed.

Messrs. E. V. Kristaponis and W. J. Lindsay of the Federal Highway Administration and Messrs. Kenneth Hankins, J. F. Nixon, C. L. Gass, and R. L. Tyler, of the Design Division of the Texas Highway Department (THD), are due well deserved thanks for their input and overview of the research.

Responsibility for running the skid test equipment was lodged primarily in the hands of Messrs. A. B. Hubbard and B. D. Cannody, THD Austin. These men are commended for their fine help.

Splendid help was furnished by THD District 17 personnel. Special thanks go to Messrs. J. G. Hanover, J. G. Long, J. O. Sloan, and J. H. Young.

Texas Transportation Institute personnel and University student assistance are gratefully acknowledged. Particular thanks go to Messrs. A. J. Stocker, D. L. Ivey, H. Tomita, L. W. Presswood, B. W. Jubela, P. H. Harris, Jr., and R. J. Holmgreen. Special thanks are due Mr. L. J. Horn of TTI Publications for editing, preparing, and publishing the report.

ABSTRACT

Reported herein are the results of the final phase of THD Study 2-8-69-138. This phase of the study is concerned with the effect of various water depths (obtained with a rain simulator) on the friction properties of various pavement textures at different levels of vehicular speeds and tire-tread depths, tire pressures, and tire types. Equations relating these variables are also developed and the relative effects of the variable determined. Tabular and figurative methods are utilized to present the results.

Background information and pertinent past research pertaining to effects of water depth on pavement friction are given.

Sixteen different types of surfaces were tested, including full scale prototypes and regular pavements built under normal contracts. The surfaces, located at the Texas A&M Research Annex, are 600 feet long and 24 feet wide. Friction tests were conducted on each surface at several water depths for various combinations of tire type, tire-tread depth, tire pressure, and vehicle speed. Multiple regression analyses were used to assess the effects of the variables on friction properties of the different surfaces. A series of twenty-five tables included in the report presents the summarized data of the study.

Pavement water depth was found to significantly affect skid numbers at 60 mph. For a tire-tread depth of 0.31 in. and a texture of 0.033 in., increasing the water depth from 0.023 to 0.87 in. decreased the 60-mph skid numbers by 36 percent (See Table 3-17.) Increases in tire-tread depth and surface texture increased skid numbers; whereas, increases in vehicle speed decreased skid numbers.

The findings and conclusions contained herein will be useful to the highway engineer in determining proper geometric designs and paving materials commensurate with acceptable pavement friction characteristics and service demands. Suggestions for further research are also included.

OBJECTIVES AND SCOPE

The objectives of this research were:

1. To examine the effects of various water depths on the friction properties of various surface textures at different levels of vehicular speeds and tire pressures, tire types and tire-tread depths;

2. To develop an equation relating water depth, surface texture, vehicular speeds, tire-tread depth, tire pressure and tire type to friction number, and;

3. To recommend means by which the findings and conclusions contained herein can be implemented by the highway engineer in determining proper geometric designs and paving materials commensurate with acceptable pavement friction characteristics and service demands.

SUMMARY OF FINDINGS AND RESULTS

1. Vehicle speed, tire type, tire-tread depth, tire pressure, surface texture, and water depth were found to affect skid numbers as discussed below. The equation selected as the final model, based on R^2, the physical constraints, simplicity of expression and inclusion of all four independent variables, namely, MPH, TD, WD, and TXD is given below.

$$SN = 135.121\, X_4 + 563.655\, X_5$$

$$= 135.121\, \frac{TD^{0.06}}{MPH^{0.72}} + 563.655\, \frac{TXD^{0.05}}{MPH^{0.72}\,(25.4WD + 2.5)^{0.08}}$$

$$= \frac{135}{MPH^{0.72}} \left[TD^{0.06} + \frac{4.18\; TXD^{0.05}}{(25.4WD + 2.5)^{0.08}} \right]$$

where

SN = skid number at corresponding speed;

MPH = vehicle speed (mph);

TD = tire-tread depth (in.);

TXD = average surface-texture depth (in.);

WD = water depth above top of texture (in.).

Other data groups are regressed using the same procedures. Final models for each data group are shown below. Plots of these models are included in Appendix of the main report.

Select Regression (Pads 1, 3, 4, 5, 6, 7, 8)

ASTM 32 psi

$$SN = \frac{135}{MPH^{0.72}} \left[TD^{0.06} + \frac{4.18\; TXD^{0.05}}{(25.4WD + 2.5)^{0.08}} \right] \qquad \text{Equation 1.}$$

Comm. 32 psi

$$SN = \frac{186}{MPH^{0.83}} \left[\frac{TD^{0.07} \quad TXD^{0.01}}{(25.4WD + 2.5)^{0.16}} + 2.49 \right] \qquad \text{Equation 2.}$$

$(N = 735, R^2 = 0.933, SE = 9.47, DF = 2/733, F = 5131)$

ASTM 24 psi

$$SN = \frac{154}{MPH^{0.77}} \left[TD^{0.05} + \frac{4.71 \quad TXD^{0.09}}{(25.4WD + 2.5)^{0.09}} \right] \qquad \text{Equation 3.}$$

$(N = 228, R^2 = 0.942, SE = 10.32, DF = 2/226, F = 1825$

Comm. 24 psi

$$SN = \frac{234}{MPH^{0.86}} \left[\frac{TD^{0.06} \quad TXD^{0.07}}{(25.4WD + 2.5)^{0.13}} + 2.49 \right] \qquad \text{Equation 4.}$$

$(N = 732, R^2 = 0.937, SE = 8.79, DF = 2/730, F = 5441)$

Other equations were developed specifically for low friction surfaces and portland cement concrete finishes.

2. Increases in water depths were not found to affect skid numbers significantly at 20 and 40 mph speeds; however, significant decreases in skid numbers with increases in water depths were found when skid numbers at 60 mph were used in the analysis. This is not meant to imply that the absence or presence of a water film has no influence on friction numbers at any speed, since these results are based on data taken only after the surface was completely wetted.

3. Surface texture and skid numbers were positively related. The effect was very pronounced at the lower texture values where slight increases in texture produced large increases in skid numbers.

4. Tire-tread depth and skid numbers were also positively related, particularly at the lower tread depths. The effect became less evident at tread depths greater than 0.20-inch.

5. Vehicle speed had a very significant effect on skid numbers. Higher speeds were associated with lower skid numbers. The reader is referred to Tables 3-1 through 3-25 and Figures 3-1 through 3-48 for more information on Items 1 through 5 .

6. Under simulated rain the 60 mph performance of all surfaces (with the associated variables studied) was rather poor. At speeds in this range, skid numbers are highly dependant on water film thickness up to some critical value. Additional water beyond this amount (depth) appears to have only a minor effect on these higher speed skid numbers.

7. From the results of this study the need for adequate drainage at the tire-pavement interface is critical at speeds in excess of 40-50 mph. Macro-texture values in the 0.04 to 0.05 should be considered minimum for high speed facilities. Values above this range are recommended.

8. Tread depth exercised a strong influence on the skid number. The magnitude of the effect varied as expected with water depth, speed and amount of macrotexture.

IMPLEMENTATION

The findings of this study have been given extensive exposure, and partly as a result of these findings, specifications for drainage at the tire-pavement interface have been included in an ever increasing number of design and construction procedures.

Data from this study have conclusively shown that skid numbers obtained by use of locked wheel trailers of the ASTM 274-70 type can be misleading as barometers of pavement performance at high speeds under inclement weather conditions. Efforts are now being made to determine whether or not correlations exist between skid number and speed using the standard internal watering system of the ASTM trailer and skid number speed gradients under simulated rain exists. From information presented in the study, the researchers confirmed a previous conclusion that the widely used skid trailer is primarily a survey and inventory device and is not necessarily suitable for determining possible hazards in the actual skid characteristics of pavements during rainy weather. The need for continued and extended implementation of wet weather advisory speed warnings is emphasized. Macrotexture values in the 0.04 to 0.05 range are recommended for high speed traffic and values above this range should be sought wherever it is technically and economically practical. Adequate microtexture is considered necessary at all reasonable vehicle speeds.

TABLE OF CONTENTS

LIST OF FIGURES

LIST OF FIGURES (CONTINUED)

LIST OF FIGURES (CONTINUED)

LIST OF FIGURES (CONTINUED)

LIST OF TABLES

LIST OF TABLES

LIST OF TABLES

INTRODUCTION

Safety on our nation's highways is a topic of utmost importance to the driving public. Concern for the prevention of traffic accidents is evidenced by every responsible agency from the Department of Transportation at the federal level to local highway authorities. The causes of traffic accidents are numerous, but the results are the same--costly destruction of property, incalculable human suffering, and an annual death toll exceeding 50,000 lives. Trends in the causes of traffic accidents have been discovered; research has been, and will continue to be, conducted in an effort to solve the problems which bring about this senseless loss of resources.

Among those topics which have received considerable attention over the past 30 to 40 years is the problem of providing roadway pavement surfaces which will provide adequate tire-gripping capabilities when wet under normal operating conditions, thus reducing the occurrence of accidents attributed to skidding. Skidding is the phenomenon which occurs when vehicle wheels lose traction with the pavement resulting in an increased stopping distance, loss of directional stability, and loss of operator control. It is obvious that this situation is of the utmost danger to the occupants of the skidding vehicle as well as to other persons or property which might be within range of the skidding vehicle.

Characteristically, a pavement becomes slippery when the prevailing conditions are such that water lubricates the tire-road surface contact area, when the inherently high skid resistance of a new surface has been worn and polished away by traffic, and/or when vehicle speeds are high enough to hydrodynamically reduce the tire-surface contact (and thus the available

friction) below the level required for vehicle maneuvers (1)*. Dearinger and Hutchinson (2) suggest that although the details of the slipperiness-skid resistance problem are quite complex, most automobile accidents involving skidding are due simply to the unfortunately common combination of wet pavement and an attempt by the driver to perform a maneuver (braking, cornering, accelerating) at a speed too high for the conditions. The frequency of occurence of this combination of circumstances has risen sharply in the past few years with continuing increases in traffic volumes and higher average vehicle speeds.

*Underlined numbers in parentheses refer to references in the Bibliography.

Chapter I

REVIEW OF LITERATURE

American highway engineers have been studying the vehicle skidding problem, particularly resistance to skidding offered by pavement surfaces, for several decades. In fact, initial technical papers (3, 4) written on the subject 30 to 40 years ago include many of our present day ideas. However, the problem was not considered to be serious since most pavement types were adequate for the low volume, low speed traffic which existed at that time. Today, as a result of increasing traffic volumes and speeds, the skidding problem is rapidly gaining in significance. Nationally, the average number of wheel passes over the same pavement section increased approximately 50 percent from 1950 to 1960 (5). Indications are that an even larger increase was experienced during the past decade. The average vehicle speed today is approximately 16 mph greater than in 1941, which is an increase of about 1 percent per year. Today's average speed for dry, modern rural highways is about 46 mph with 47 percent of all vehicles exceeding 60 mph and 12 percent exceeding 70 mph, with only a 1- or 2-mph reduction in speed on wet pavement (5, 6).

A recent survey by Highway Research Board Committee D-B4 Task Group (7), stated that "...slippery pavements were recognized as a problem of major concern in 22 states, moderate concern in 24 states, and minor concern in 2 states." The HRB survey (7), with 48 states reporting, also revealed that "...42 states were using accident data for the detection or selection of slippery pavements,...that 32 states were using skid test data as a criterion for resurfacing or deslicking,...and that 30 states were presently

conducting a research program on pavement slipperiness." By contrast, a 1958 HRB survey (8) conducted on behalf of Highway Research Board Committee D-1 on Mineral Aggregates revealed that "...only 10 of 47 state highway departments querried were actively conducting studies involving the measurement of pavement skid resistance." More than two million dollars were spent during 1972 by various research agencies in the United States on the development of knowledge on roadway vehicle interaction, particularly on skidding--causes, effects, and prevention.

Comprehensive assessments of the role of slippery pavements and skidding in highway accidents are scarce due partially to inadequate or confusing accident-reporting systems. Data extracted from a British study (9) indicated that skidding of one or more vehicles was involved in about 16 percent of all accidents reported. Of the accidents occurring on wet roads (31 percent of the total), 27 percent involved skidding. A recent British study revealed a general linear relationship between skid resistance and accident risk (10). It was concluded from a Virginia highway accident study (11) that "as high as forty percent of all accidents involve skidding." "In about one-third of these accidents (13 percent of the total accidents), skidding occurs before brake application."

Studies of the locations of individual skidding accidents on wet roads have shown that 'wet skids' tend to cluster on short stretches of road and the significance of these clusters may be judged by comparing the skidding rates at the individual sites with an acceptable standard (12, 13). More specifically, very strong correlation between precipitation and accident involvement rate has been found (14). In the United States it is estimated that accidents involving cases where skidding is the primary cause result

in an annual loss of life of nearly 3,000 persons with an additional 100,000 persons receiving disabling injuries (15).

A 1966 Arthur D. Little, Inc. report (16), which, in the authors' opinions, is the most comprehensive study of traffic safety information ever attempted, stated that:

> Skidding has emerged as a factor of major importance to the overall traffic safety problem, and the surface characteristic of principal concern appears to be the frictional properties of the road surface, both wet and dry. While there is evidence that skidding is involved in a high proportion of accidents, current methods of reporting accidents are believed to be inadequate to determine the true extent of this factor. Since skidding occurs in many accidents, either before or after braking, it is generally overlooked as a 'cause' in most accident reports. There is a tendency to list more obvious 'causes' such as 'failure to negotiate the curve' or 'lost control of car' which are in fact not causes but results; therefore, no accurate record is maintained of the kind and the degree of skidding involvement.

Thus it can be concluded from the above quote that skidding and associated problems are actually contributing causes of more accidents than attributed by current methods of reporting accidents. Even so, analyses of accident records indicate that the incidence of total accidents, as well as accidents directly involving skidding, does increase significantly with decreasing friction coefficients between the pavement and the tire.

The shorter the distance required to stop a vehicle in emergency situations, and the higher the force to provide adequate cornering, the better the resultant chance to avoid or reduce the severity of accidents. And, as stopping distance and cornering capability are direct functions of

friction coefficient, a uniform high value of friction coefficient is becoming more and more important.

Any moving object, including a wheeled vehicle, produces kinetic energy at a rate increasing with the square of its velocity. Dissipation of this energy is required in order for the moving body to come to rest. In the case of the wheeled vehicle, energy (neglecting wind resistance and change in elevation) is dissipated between the tire and the pavement and in the braking system by the creation of a friction force opposing the direction of motion of the vehicle. After wheel lockup the total friction force available to oppose the motion of the vehicle must be generated at the tire-pavement interface.

The skid resistance coefficient is related to the stopping distance of a vehicle by the expression $D = \frac{V^2}{30f}$, where D is the stopping distance in feet, V is the vehicle speed in miles per hour, and f is the coefficient of friction. The stopping distance can therefore be decreased by increasinc the skid resistance coefficient which results in better vehicle control (17). High pavement friction means a greater margin of safety in both stopping and directional control of the vehicle. The higher this margin the better because side friction or directional control and forward or stopping friction are not two separate reservoirs of safety to draw upon in an emergency; they are one reservoir of tire-gripping capability provided by the road surface. Once all of the force is applied in the form of a forward skid, there is, for all practical purposes, none left for directional control or steering of the vehicle.

Technical discussion currently is focused upon acceptable minimum pavement skid-resistance values. Recently, even the courts have been

faced with decisions in this area; however, all answers in this area of concern are relative to the degree of safety intended.

The achievement of adequate pavement skid resistance is a result of the driver's responses and the interaction between the pavement and tire. This discussion, however, deals only with the pavement, disregarding variations in friction which may be due to variations in tire design, vehicle parameters, and driver characteristics.

The main causes of pavement slipperiness are many and varied, but in very general terms are due to 1) the presence of water of other friction reducing materials in the tire-pavement contact area which, with increasing vehicle speeds, lowers the obtainable frictional drag and raises the frictional demand, and 2) higher traffic volumes which, through pavement wear and aggregate polish, drastically reduce built-in friction potential of most new pavement-surface types. Many parameters affect the interactions at the tire-pavement interface. Considered to have major effects are: 1) mode of operation, i.e. rolling, skidding, or sliding, 2) pavement-surface characteristics, mainly macro- and microscopic roughness and drainage capability, 3) water-film thickness at the interface, 4) tire-tread depth and elastic and damping properties of the tire rubber, and 5) vehicle speed.

Many published research findings have indicated that, neglecting contamination, practically all pavement surfaces exhibit adequate friction for normal stopping and cornering maneuvers when dry. When wet, however, the same pavements will inevitably exhibit friction values that are

lower and cover a much wider range of values. At the upper end of the range the wet values may approach the dry; whereas, at the lower end, the wet values may approach or be lower than that of ice. Although the details of the pavement slipperiness problem are quite complex, it is apparent that relative abilities of pavement-surface types to permit effective escape of water from under the tire vary tremendously. When several different surface types have been subjected to similar traffic conditions with accompanying relative variation in friction properties, then the ultimate conclusion must be that certain inherent properties of particular surface types largely determine their ultimate friction properties. The revelance of these properties as factors demands some discussion.

Relevant Surface Factors

Attempts have been made to characterize properties affecting friction of pavement-surface types using qualitative terms such as surface macrotexture, aggregate size, shape, microtexture, and mineralogy; and drainage characteristics of the total surface. Although the relative magnitude of their influences has not been universally accepted, it is generally agreed that these characteristics largely determine the ultimate friction properties of surfaces. It is the authors' opinion that the importance of these characteristics rests primarily in their ability to assist in the escape of water from the tire-pavement interface.

The importance of the type and magnitude of surface texture on the friction properties of pavement surfaces has been studied by several researchers (1, 18, 19, 20, 21). Pavement surface texture refers to the distribution and the geometrical configuration of the individual surface aggregates. There is not sufficient agreement among the various researchers to adopt a standard nomenclature for discussing textural parameters. However, general practice today favors the use of the terms macroscopic texture (macrotexture) which refers to that part of the pavement surface as a whole or the large-scale texture caused by the size and shape of the surface aggregate, and microscopic texture (microtexture) which refers to the fine-scaled roughness contributed by individual small asperities on the individual aggregate particles.

Researchers have conflicting claims on the relative merits of macro- and microtexture. Some contend that a high level of macrotexture is essential to provide the pavement drainage at high speeds (22), whereas, microtexture provides the main texture contribution for a given friction level. Still others believe that a combination of both macro- and microtexture is most desirable (1, 23).

Kummer and Meyer (1) proposed the classification shown in Fig. 1-1, which delineates the two roughness types that affect the friction of pavement surfaces. Friction is denoted by skid number which is the coefficient of friction multiplied by 100 and expressed as a whole number. Although five surface types are classified, only three levels of macrotexture, i.e., smooth, fine, and coarse, are identified since types 2 and 3

and types 4 and 5, respectively, are the same as far as macrotexture is concerned. A given level of macrotexture as measured by the majority of existing test methods does not appear to adequately assess the degree of roundness or grittiness the individual aggregates possess.

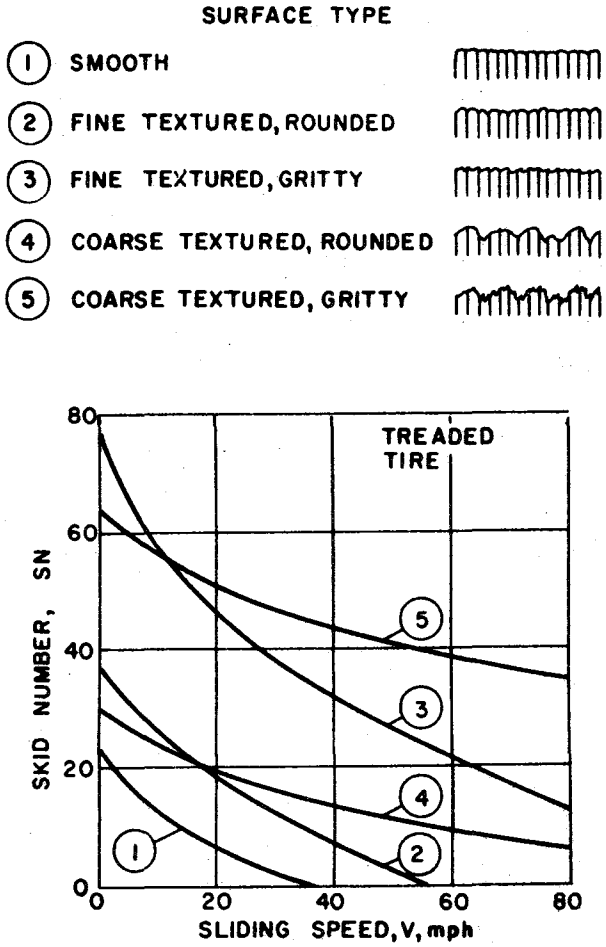

Figure 1. Classification of pavement surfaces according to their friction and drainage properties (1).

Macro- and microtexture, respectively, provide for gross surface drainage and subsequent puncturing of the water film. Another factor which acts in combination with macro- and microtexture is internal drainage of the pavement surface itself. Goodwin (24), Hutchinson (25), and Gallaway (23), among others, have postulated that high-void content surfaces, porous pavements, or vesicular aggregates would provide internal escape paths for water under a tire and thus lessen hydrodynamic pressure build up. This would result in better tire-gripping capability and increased traction, particularly at higher speeds, while decreasing the need of macrotexture for providing initial, gross drainage. Research directed toward measuring dynamic drainage capabilities of pavement surfaces is in the experimental stage (25). The demonstrated danger of using data obtained by use of the standard ASTM trailer with its regularly used internal watering system for predicting skid numbers at speeds above 40 mph on naturally wetted (rain slick) surfaces appears to have been shown.

With respect to the size of the coarse aggregate, the majority opinion seems to be that finer mixes are superior to coarser ones, at least in bituminous construction (26, 27). However, the advantages of fine mixes are not always apparent, and some investigators have suggested that particle size has actually little or no effect on frictional characteristics (28, 29).

The shape of the aggregate particles is a significant factor in skid-resistance considerations. The individual particles should be angular and sharp in order to give a gritty, sandpaper-like texture, (30, 31, 32). Skid resistance measurements have been found to be about 25 percent higher for bituminous mixes containing angular aggregates than for those containing

rounded aggregates (29). The importance of the aggregate shape has also been borne out by laboratory experiments (33, 34).

If aggregates are to retain their shape under traffic and weathering, the particles should be hard and must resist polishing. It has been found (35) that the skid resistance increases with increasing silicate content and decreasing carbonate content in calcareous aggregate. Since calcite has a hardness of three, (on the moh scale of 1 to 10 with 10 for diamond) pure limestones are susceptible to polishing by just about any kind of grit in the road debris. And since quartz has a hardness of seven, quartz sandstones are much less susceptible to polishing by mineral abrasives abundantly present in the road surface.

Wear and polishing under traffic result in skid-resistance variations across the width of the road (36); these may lead to skidding accidents regardless of the actual minimum value. It has been calculated (37) that if the coefficient of friction is 0.40 along one wheelpath and 0.60 along the other, a 3000 pound vehicle would turn about seventeen degrees in a locked-wheel stop from 40 mph. This problem may be further accentuated on multilane highways where the driving lane is normally more slippery that the passing lane (38, 39).

Since the nature of the wear is directly related to the resistance of the surface aggregate to polishing, wear can actually be desirable on road surfaces. Differential wear, due to variation in hardness of the aggregate constituents and/or matrix (31, 40), greatly contributes to the retention of the rough texture. Particle-by-particle wear, during which aggregate particles are dislodged from the surface before they get excessively polished, continuously rejuvenates the surface (32,41). In addition, particle-by-particle wear does not just insure prolonged skid resistance

but distributes the energy of stopping to the brakes, tires, and road surface--therefore providing instantaneously-high skid-resistance.

Tire-Pavement Friction Mechanism

Application of the classical theories of friction to the tire-pavement situation has failed to assess the nature of skid resistance properly, primarily due to the fact that rubber is a viscoelastic material. Laboratory work in Great Britain by Giles and Sabey (42, 43) introduced the present theory of tire-pavement friction. A unified theory of rubber friction, as proposed by Kummer (44) and supported by Meyer and others (45, 46, 47) refined the earlier work of the other researchers and is generally considered today to constitute the state of knowledge of the problem.

The frictional force generated between the tire and the pavement is made up of two components; a force attributable to adhesion between tire and pavement, and a force attributable to hysteresis losses in the tire rubber caused by deformation of the tire as it rolls or slides across an irregular surface. Both forces are functions of molecular activity within the tire rubber.

The adhesion component is generated by the junctions of rubber and surface molecules created primarily by Van der Waals forces of attraction. These junctions produce a shearing resistance at the tire-pavement interface. Therefore, adhesion forces are dependent upon the magnitude of the shearing resistance and upon the area of contact between the tread rubber and the pavement surface. The hysteresis force is generated by the deformation of the tire rubber which produces a pressure difference between the two sides of the intruding surface projections (or asperities as they are

commonly termed) when the rubber rebounds less vigorously than it is displaced. Hysteresis forces depend largely upon the quantity of rubber being deformed and on the damping properties of the rubber. Figure 2 (1) illustrates these two components in a simplified fashion. In this figure F_{ai} and F_{hi} are the two principal components of rubber friction, adhesion and hysteresis forces. The symbol E_{ai} represents the evergy released when the junctions between the rubber and pavement surface molecules are formed and then ruptured during the adhesion process. The symbol E_{hi} represents the energy loss due to the excitation of the chain-like rubber molecules caused by deformation of the tire rubber, or the hysteresis loss. Both types of energy loss are in the form of heat (1).

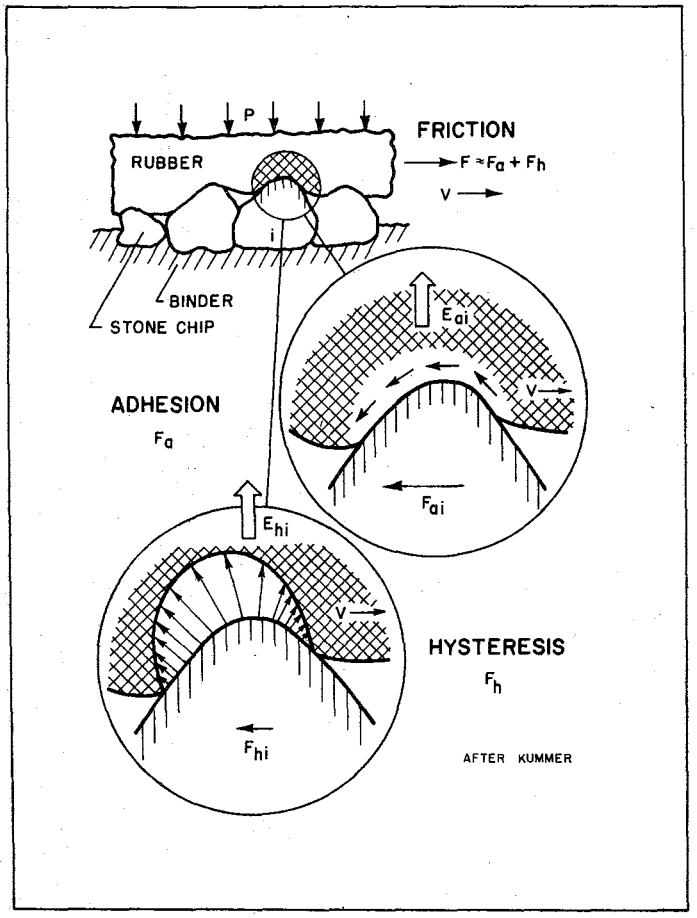

Figure 1-2 The two principal components of rubber friction: ashesion and hysteresis (1).

Figure 1-3 (1) summarizes the work of many researchers in both Europe and the United States. The figure shows that the dry friction level of a pavement is either independent of or increases slightly with vehicle speed. This is due to the complementary effects of the adhesion and hysteresis components of friction (1). The figure also illustrates the rapid decay

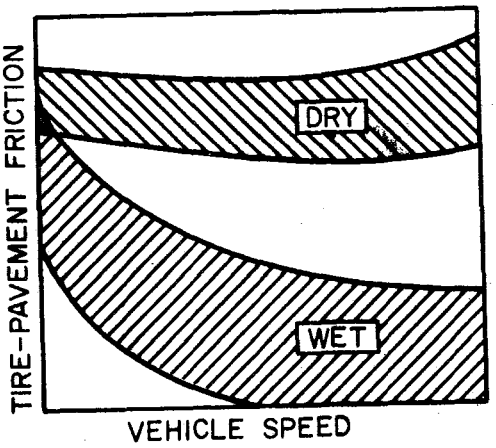

Figure 1-3 Frictional trends for slipping and skidding tires on dry and wet pavements (1).

of frictional resistance on wet pavements as speed increases, indicating the obvious danger of wet pavements with regard to skid resistance. Figure 1-4 (44) shows the relative contribution of the adhesion and hysteresis components on dry surfaces as speed increased and demonstrates that the adhesion component provides the greater contribution to total friction for speeds below about 50 mph. Since the adhesion component depends for its magnitude on contact area available to generate shearing forces, the intrusion of water into this contact area drastically reduces the adhesion components leaving only hysteresis forces to oppose sliding or skidding. Thus, removal of the water from the pavement can significantly increase

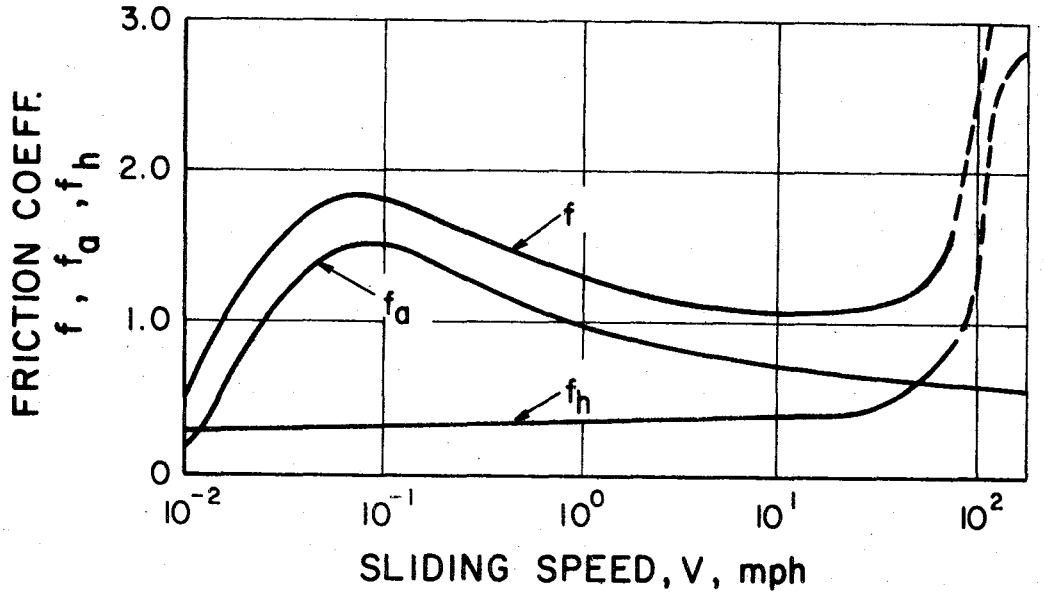

Figure 1-4 Contributions of adhesive and hysteresis friction to the total tire friction (44).

the skid resistance of the pavement. Conversely removal of the pavement (by grooving for example) can reduce the skid resistance of a pavement.

The phenomenon of hydroplaning has received much attention from some skid-resistance researchers. Hydroplaning occurs when the tire is completely separated from contact with the pavement surface by a water film, resulting in essentially zero friction being generated between the tire and pavement (17, 48). This phenomenon has been especially noticeable on flooded runways when aircraft land at high speeds.

When a tire rolls or slides across a wet pavement, water is removed from the tire-pavement interface in three steps, as shown in Figure 1-5 (49, 50,51). As the tire moves over the surface, the bulk of the water is removed by the normal force of the tire squeezing the water outside the tire footprint through drainage channels in the pavement or into the grooves in the tire tread. However, a thin film of water, on the order of a thousandth of an inch, remains tenaciously bound to the pavement surface. Very high

localized pressures caused by smaller pavement asperities against the tire surface then may serve to puncture this thin water "squeeze-film" to permit intimately dry tire-pavement contact (51).

When the depth of water is too great to be removed by this action, "dynamic" hydroplaning occurs. A second type, "viscous" hydroplaning occurs when, either due to the smoothness of the tire or the lack of surface asperities, the tire rides on the microfilm of water remaining at the surface (48).

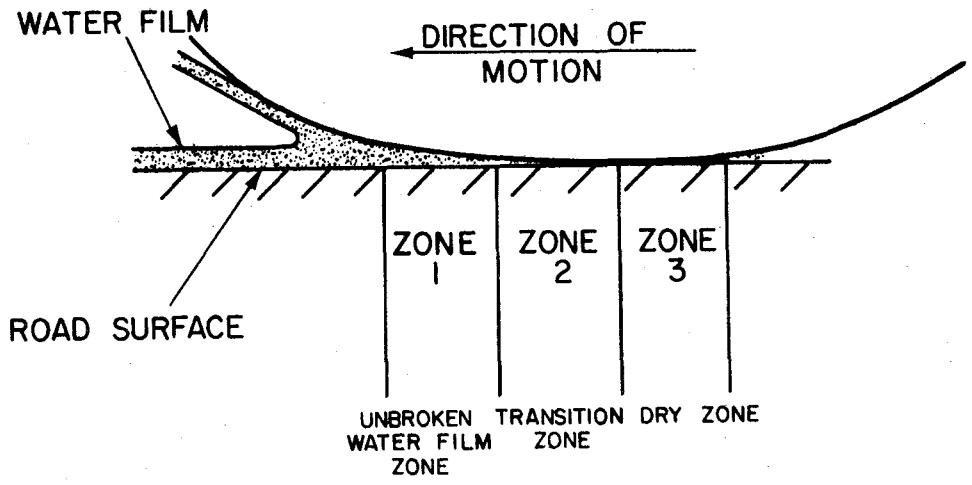

Figure 1-5 The three zones of the contact area of a tire (51).

The depth of water required for hydroplaning varies mainly with the tire tread design and tread depth and the textural characteristics of the pavement surface. There is some question (48) as to the danger of automobile skidding due to dynamic hydroplaning since complete or near complete flooding of the roadway is required to sustain this phenomenon. However, viscous hydroplaning is believed (48, 49) to be an ever present threat, since only enough water to form an extremely thin film at the surface of individual particles is needed to produce it. Actual field

data taken in simulated rain will be presented later in this report to show meaningful data in this area.

Previous Research

Pavement dampness has been found to reduce the friction level from its dry value, but the frictional coupling is not speed-dependent because there is no bulk water to be removed and no thin film to be displaced. The friction level of a pavement covered by a visible water film is speed-sensitive because the presence of the fluid film makes it progressively more difficult for the tread to make contact with the pavement, even though no bulk displacement of water takes place. If, however, the geometric features of the pavement surface are obliterated by water, both processes occur together and thereby increase the friction-speed gradient in an alarming manner for many highly textured pavements subjected to simulated rain.

The change of the friction-speed gradient at 30 mph when a pavement is flooded has been experimentally verified by Kummer and Meyer (1) on a Type 4 Pennsylvania surface (Fig. 1-6). The test site was especially selected for a straight approach and exit to permit speeds up to 60 mph, and for levelness to assure a uniform water depth. The water was contained in a trough 32 in. wide and 200 ft. long, made of wooden strips 3/4 in. high and 1/2 in. wide. The strips were nailed to the asphaltic pavement with 2-in. concrete nails and sealed with putty. For this test series the single-wheel trailer of the Penn State road friction tester was mounted at the center of the towing vehicle, so that the truck tires straddled the trough on the outside and the fluid depth could not affect the safe operation of the truck. The water depth was varied by changing the flow rate from a supply pump, and was controlled by depth gages.

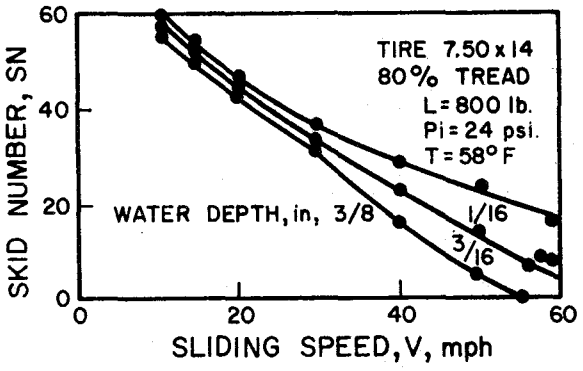

Figure 1-6 Demonstration of gradient increase due to penetration of fluid wedge into tire contact area (1).

Results from the British Road Research Laboratory research (52) indicate that the skid resistance at a given speed decreases initially with increasing water-film thickness, but stabilizes on most pavements when the film thickness exceeds 0.010 in. (Fig. 1-7). The Road Research Laboratory regards a 0.020-in. film thickness as sufficient for skid-resistance measurements.

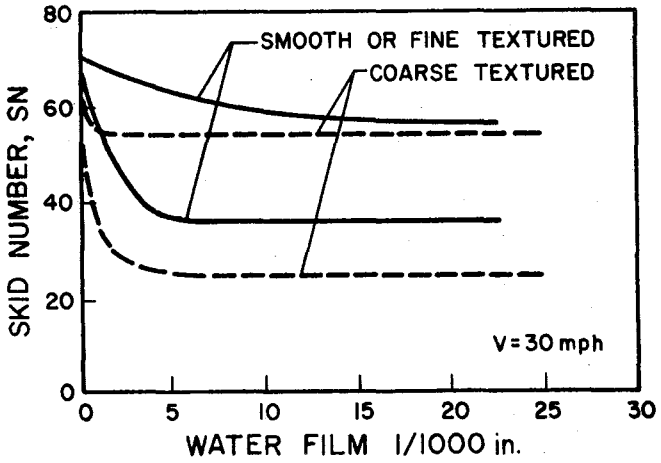

Figure 1-7. Water-film thickness and skid resistance (52).

Chapter II

TEST FACILITIES AND PROCEDURES

Surface Types

Nine different types of pavement surfaces were constructed. These surfaces, including four hot mix asphalt concrete surfaces, one portland cement concrete surface, two surface treatments, a painted portland cement concrete surface, and one sealed surface, are located at the Texas A&M Research Annex on property previously used by the United States government as a jet-trainer airfield. An overall layout of the facilities is shown in Figure 2-1.

The test surfaces were placed on existing concrete pavement near the center of a flat section of Runway B, which is 150 feet wide by 7000 feet long. A general view and inclusive details are shown in Figures 2-2 and 2-3, respectively.

Five surfaces, including three asphalt concrete, one seal, and a selected portion of the existing concrete runway, had been previously used (55, 53, 21, 54) for pavement-friction research. Four additional surfaces were constructed a few months prior to the testing sequence reported herein. The surfaces were constructed in accordance with Texas Highway Department specifications. Each surface is 24-feet wide by 600-feet long and has a cross slope of about 1/8-inch per foot.

The surface types were chosen so as to exhibit widely different friction levels, friction-velocity gradients, drainage capabilities, mineralogical properties, and textural classifications. Descriptions of each surface are presented in tabular form in Table 2-1 and close-range photographs are shown in Figure 2-4. The surfaces were cleaned and polished

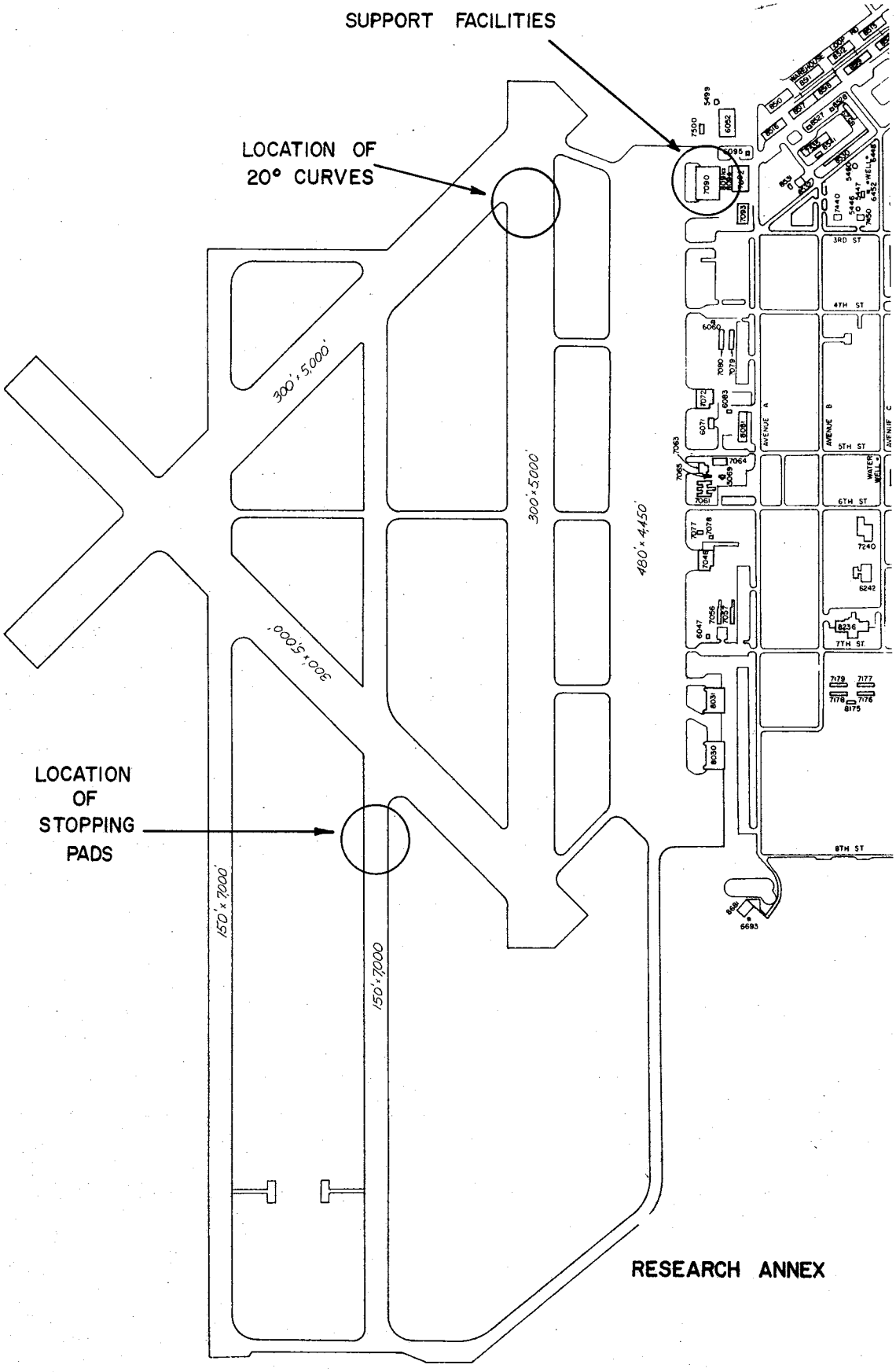

Figure 2-1. Overall layout of Texas A&M Research Annex.

prior to testing as indicated in Table 2-1 and shown in Figure 2-5. Test Pad No. 9 was prepared by applying two coats of white traffic paint to a segment of the portland cement concrete runway surface. The same surface types, with corresponding numbers, were used in a laboratory study reported previously (56). Textures obtained on corresponding surfaces differed slightly due to different field and laboratory compaction procedures.

Figure 2-2. Overall photograph of the test pads.

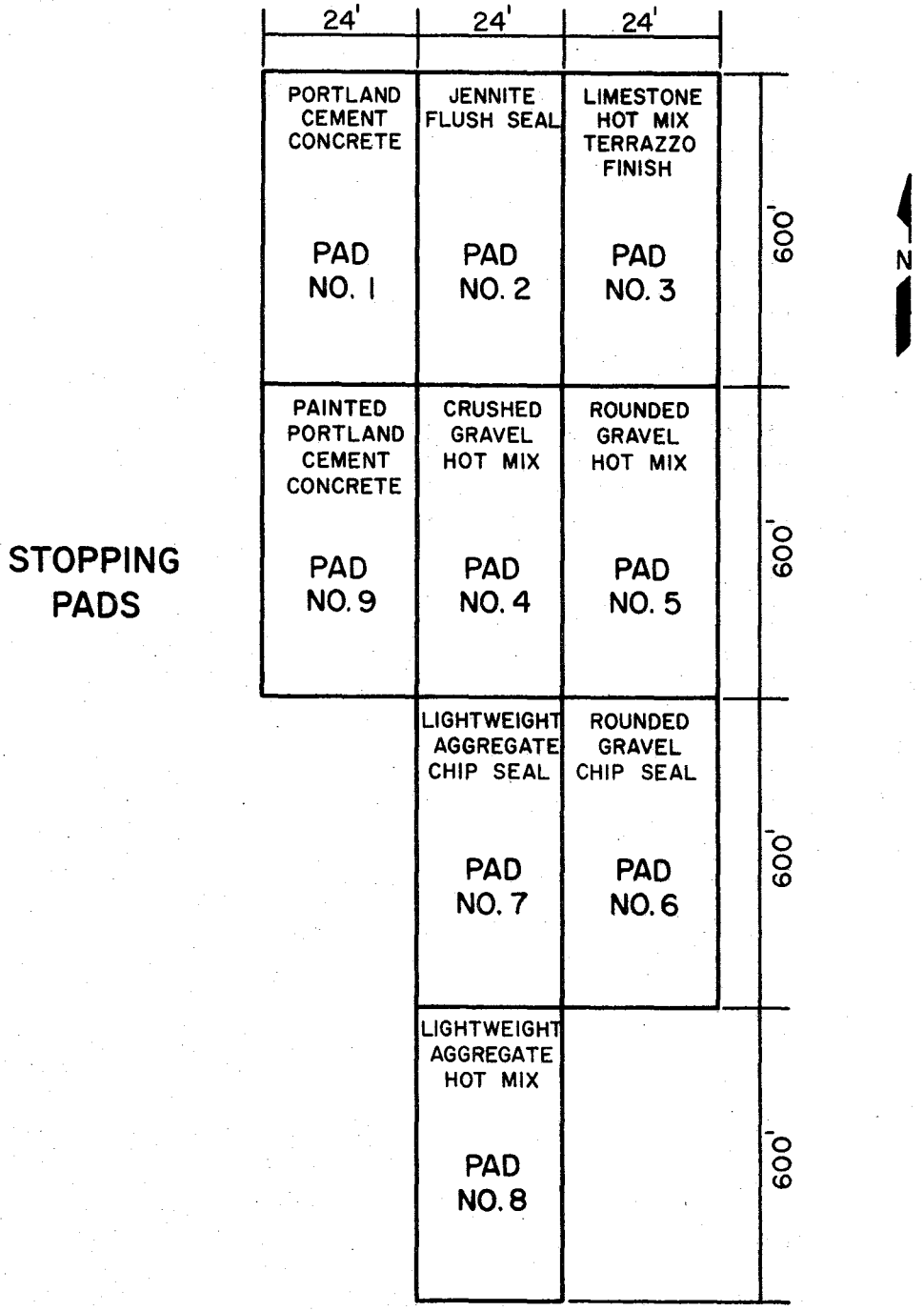

Figure 2-3. Drawing of the test pads.

Table 2-1

DESCRIPTION OF THE TEST SURFACES

Test Pad Number	Surface Types	Aggregate			Texas Highway Department Specifications	Construction Date	Preparation Prior to Testing (September 1970)	Average Texture Depth,** In.
		Weight Percent	Type	Maximum Size, in.				
1	Rounded Siliceous Gravel Portland Cement Concrete (Belt Finish)	67	Rounded Siliceous Gravel	1-1/2	(Existing Runway Surfaces)	1953	Cleaned with water and power broom	0.039
		33	Siliceous Sand					
2	Clay Filled Tar Emulsion (Jennite) Flushed Seal		No Aggregate		Type E*	1968	Scrubbed with water and rubber float	0.005
3	Crushed Limestone Aggregate Hot Mix Asphalt Concrete (Terrazzo Finish)	35	Coarse Crushed Limestone	1/2	Type D	1968	Ground with terrazzo machine and polished with water, fly ash, and rubber float	0.014
		30	Medium Crushed Limestone					
		25	Fine Crushed Limestone					
		10	Field Sand					
4	Crushed Siliceous Gravel Hot Mix Asphalt Concrete	60	Coarse Crushed Siliceous Gravel	1/4	Type F	1968	Polished with water, fly ash and rubber float	0.029
		20	Fine Crushed Siliceous Gravel					
		20	Field Sand					
5	Rounded Siliceous Gravel Hot Mix Asphalt Concrete	30	Coarse Rounded Siliceous Gravel	5/8	Type C	1968	Polished with water, fly ash and rubber float	0.024
		25	Fine Rounded Siliceous Gravel					
		35	Crushed Limestone Fines					
		10	Field Sand					
6	Rounded Siliceous Gravel Surface Treatment (Chip Seal)	100	Rounded Siliceous Gravel	1/2	Grade 4	1970	None	0.119
7	Synthetic Lightweight Aggregate Surface Treatment (Chip Seal)	100	Lightweight Aggregate (Fired Clay)	1/2	Grade 4	1970	None	0.148
8	Synthetic Lightweight Aggregate Hot Mix Asphalt Concrete	40	Lightweight Aggregate (Fired Clay)	1/2		1970	Scrubbed with detergent, water and broom and polished with water, fine sand and rubber float	0.022
		40	Lignite Boiler Slag Aggregate					
		20	Siliceous Field Sand					

*A 3/16 maximum size Type E mix composed of slag and limestone screenings was used as a base for the seal.

**Obtained by putty impression method.

Table 2-1 (Continued)

DESCRIPTIONS OF THE TEST SURFACES

Test Pad Number	Surface Types	Aggregate			Texas Highway Department Specifications	Construction Date	Preparation Prior to Testing (September 1970)	Average Texture Depth, ** In.
		Weight Percent	Type	Maximum Size, in.				
9	Rounded Siliceous Gravel Portland Cement Concrete (Belt Finish) Two Coats of Traffic Paint	67	Rounded Siliceous Gravel	1-1/2	(Existing Runway Surfaces)	1953	Cleaned with water and power broom	0.033

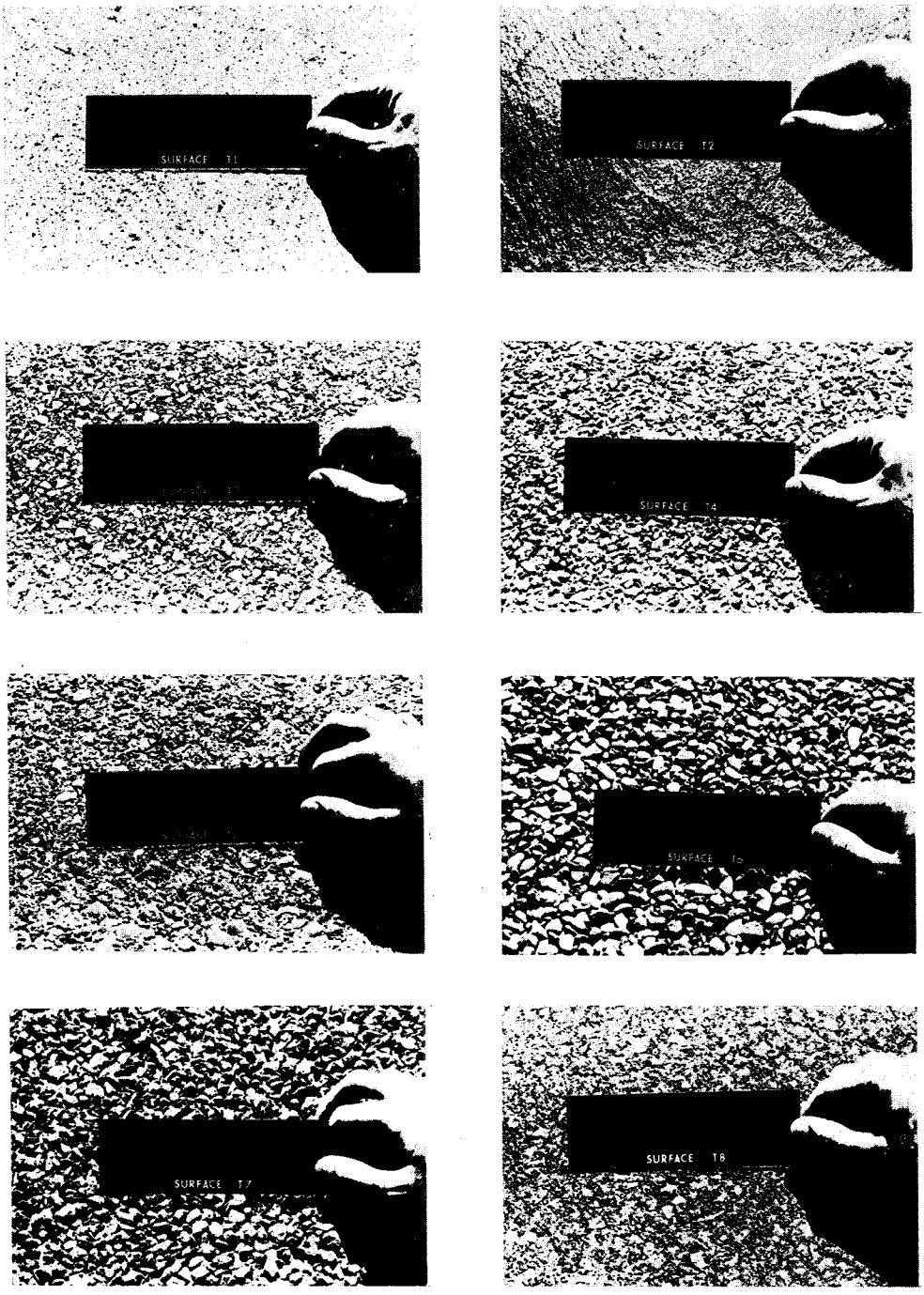

Figure 2-4. Close-Range Photographs of the Test Pads.

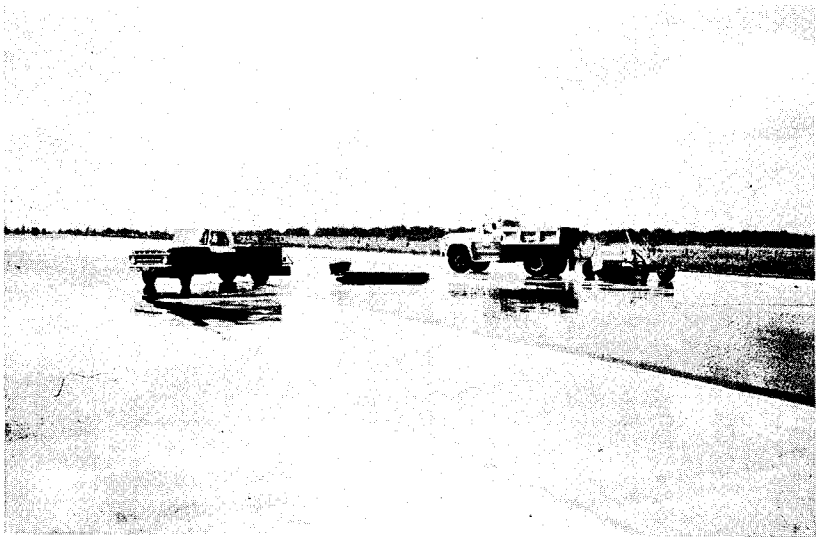

Figure 2-5. Equipment used for preparation of the surfaces.

Friction measurements with the skid trailer were conducted on surfaces Nos. 6, 7, 8, and 9 constructed during the final months of the testing sequence. Preparation and conditioning of the surfaces had advanced sufficiently to permit locked-wheel skids, particularly at various water depths and although data from these surfaces were not processed at the termination of the study, subsequent effort made it possible to include the additional data included in the report.

Also during the final months of the study the number of pavement surface types was enlarged to include seven experimentally developed surfaces on portland cement concrete. Detailed descriptions of these surfaces are given in Texas Highway Department Study 2-6-70-141.

Summarized descriptions of the seven surfaces are given in Table 2-1 of THD Research Report 141-2. It should be noted that the list includes a control which in this case represented the currently used burlap drag type of concrete pavement surfacing. The other surfacing techniques employed represent technically feasible methods of texturing portland cement concrete pavements during construction, that is, texture formation while the concrete is still in the plastic state. Photographs of five of these experimental surface textures are shown in Figures 2-6 through 2-10.

Fig. 2-6. Test Section F-1: Transverse broom finish (as constructed)

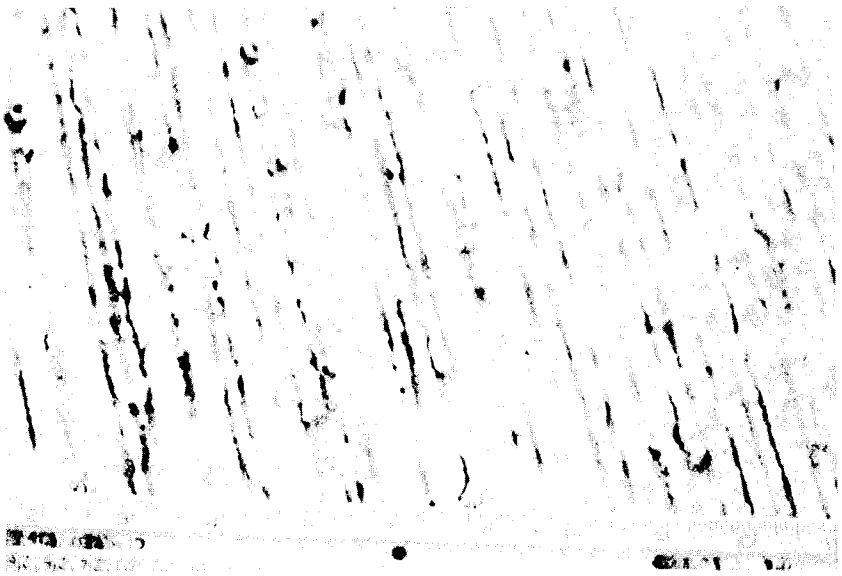

Fig. 2-7. Test Section F-4: Longitudinal tine finish (as Constructed)

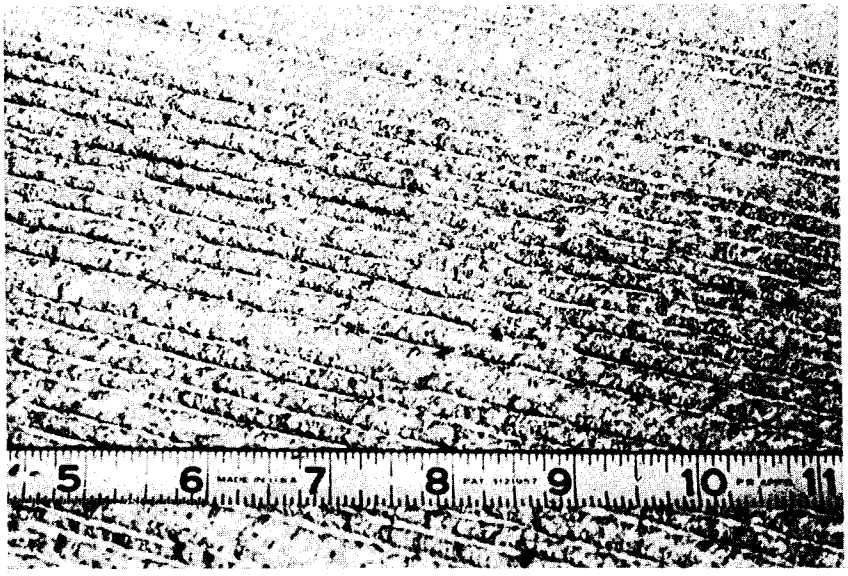

Fig. 2-8. Test Section F-5: Burlap drag plus longitudinal tine finish (as constructed)

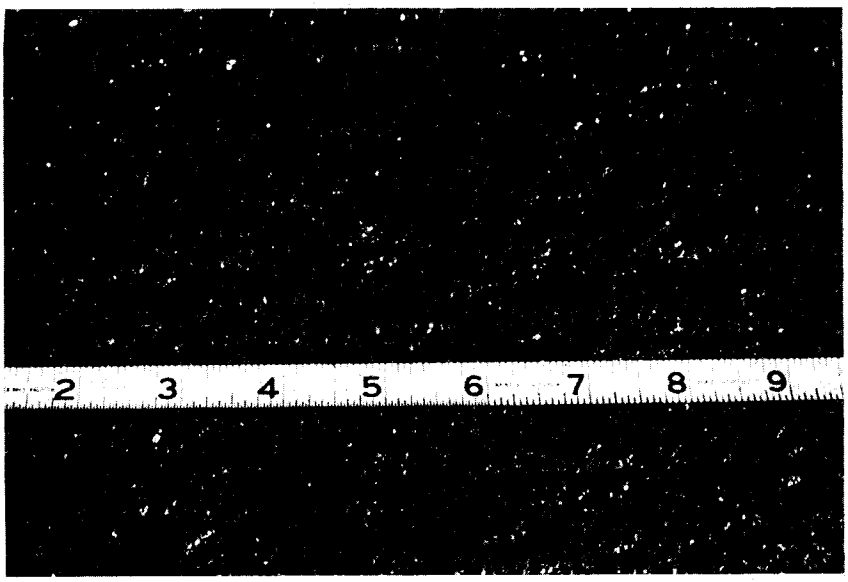

Figure 2-9. Test Section F-6: Burlap control finish (as constructed).

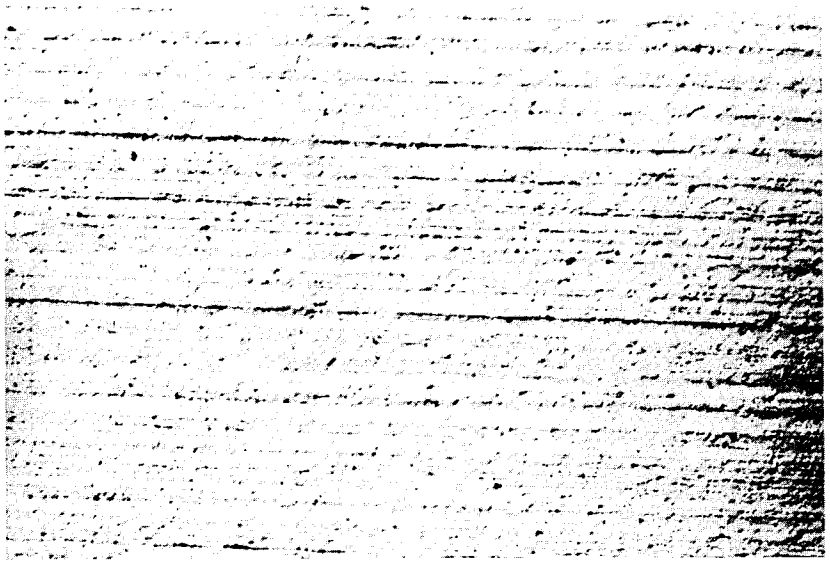

Figure 2-10. Test Section F-7: Transverse natural brush finish (as constructed).

Tires Used in Field Studies

The tires used in the study included the ASTM 14-inch standard skid resistance tire, the 15-inch interim standard ASTM skid tire, (the manufacture of this tire has been discontinued), and three commercial tires. All tires were tested at 24 and 32 psi inflation pressure.

The ASTM tires used included a range of tread depths from no tread to a full tread of 10/32 inches. The three commercial tires ranged in tread depth from no tread to tread depths of 9/32 inches.

Photographs of typical examples of the tire treads included are shown in Figures 2-11 through 2-20.

Although the sample of commercial tires used was quite limited, it is felt that the trends in performance on what might be considered typical wet pavement surfaces can be gained from the rather extensive data presented.

Tire tread patterns and rubber compounds have changed, and these changes are evidenced in their performance characteristics. However, from data presented by Kienle (57), it appears that tread improvements in the past decade have been meager. The current trend in rubber compounding (57) is toward better wear characteristics and improved traction, and both of these changes have strong public appeal.

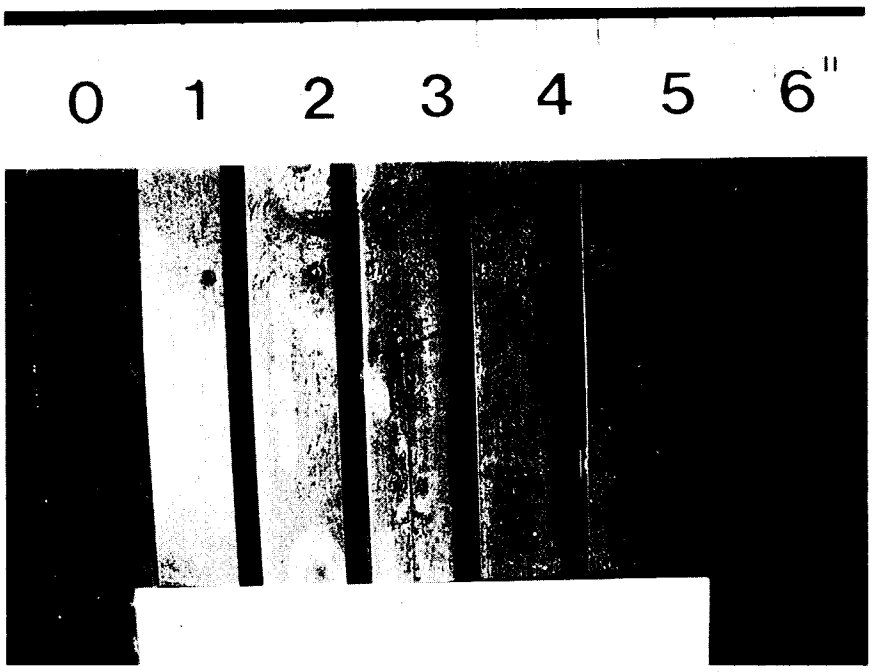

Figure 2-11. ASTM-full tread.

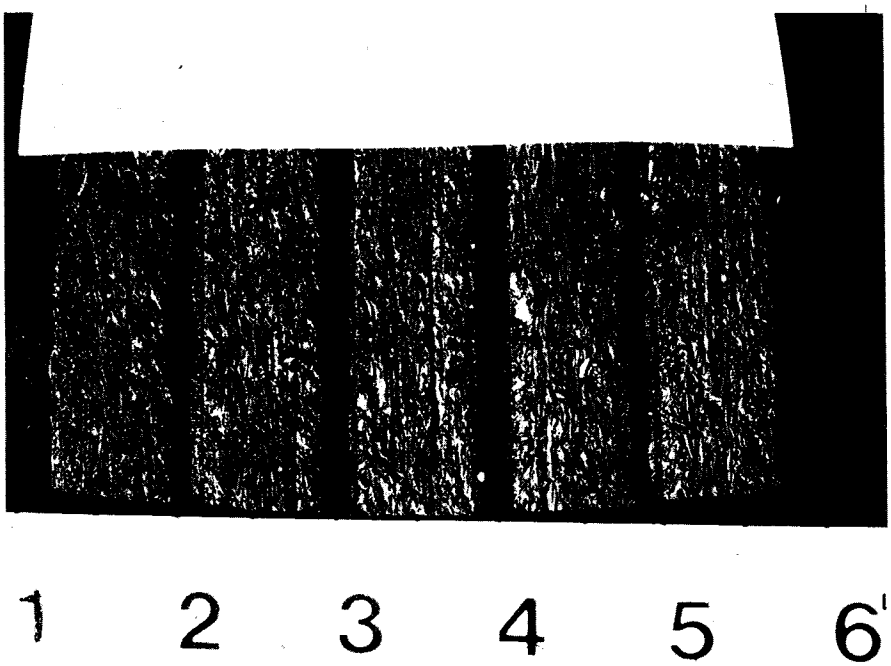

Figure 2-12. ASTM-medium tread.

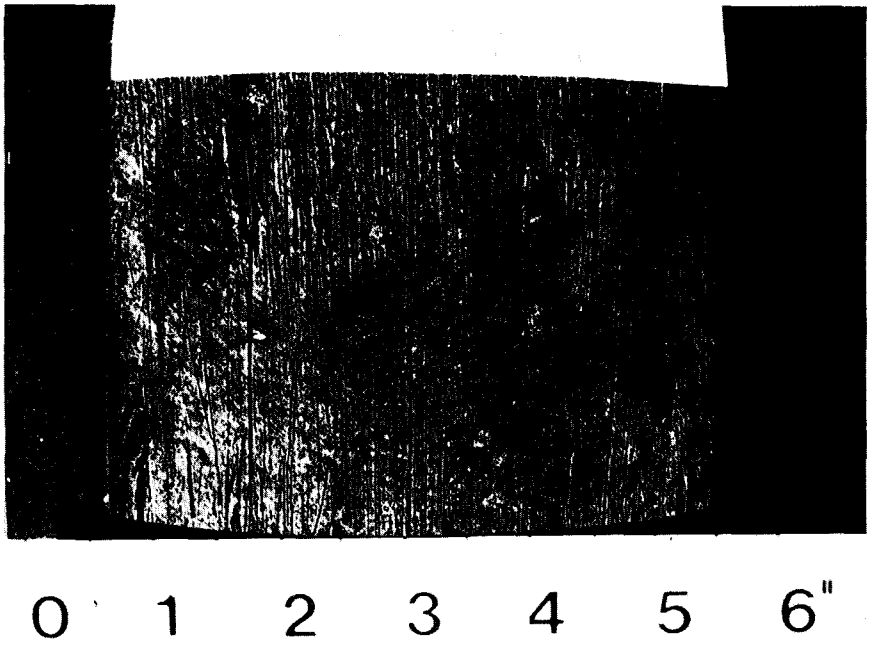

Figure 2-13. ASTM-bald tread

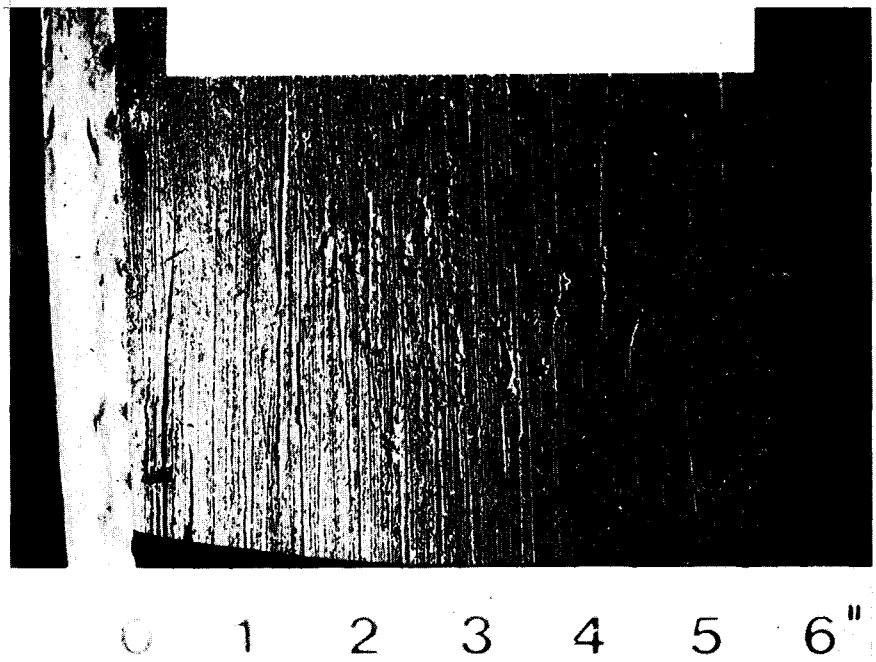

Figure 2-14. Jet Air II-slick tread.

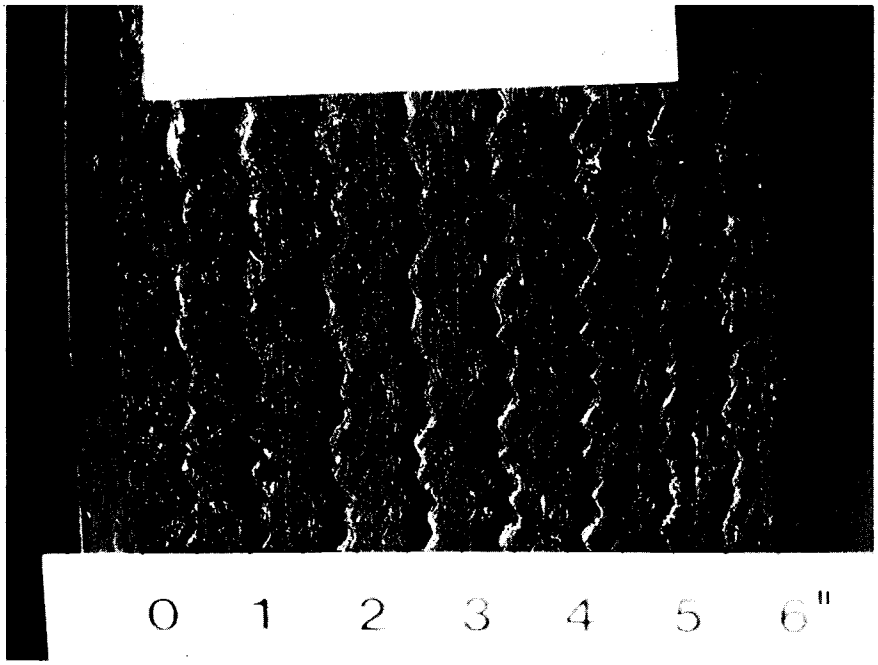

Figure 2-15. Goodyear Wide Oval F70-14-Medium Tread.

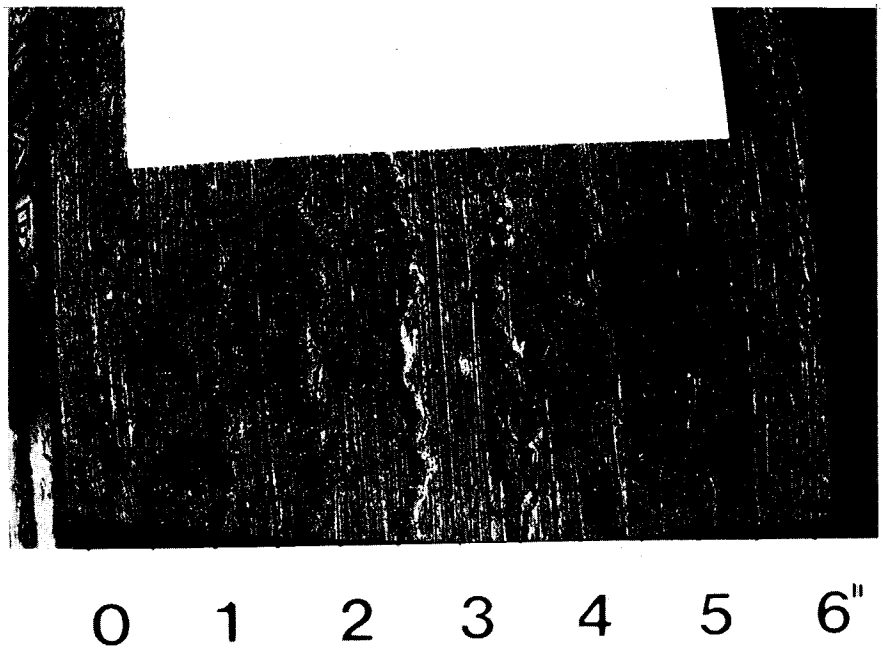

Figure 2-16. Goodyear Wide Oval-Slick Tread.

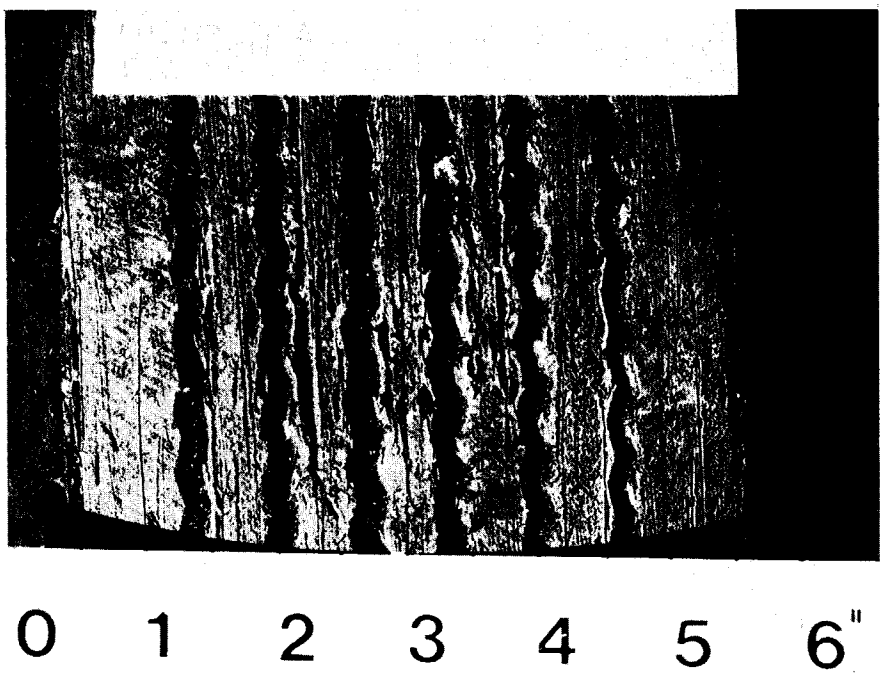

Figure 2-17. Uniroyal-Laredo Rain Tire-Medium Tread.

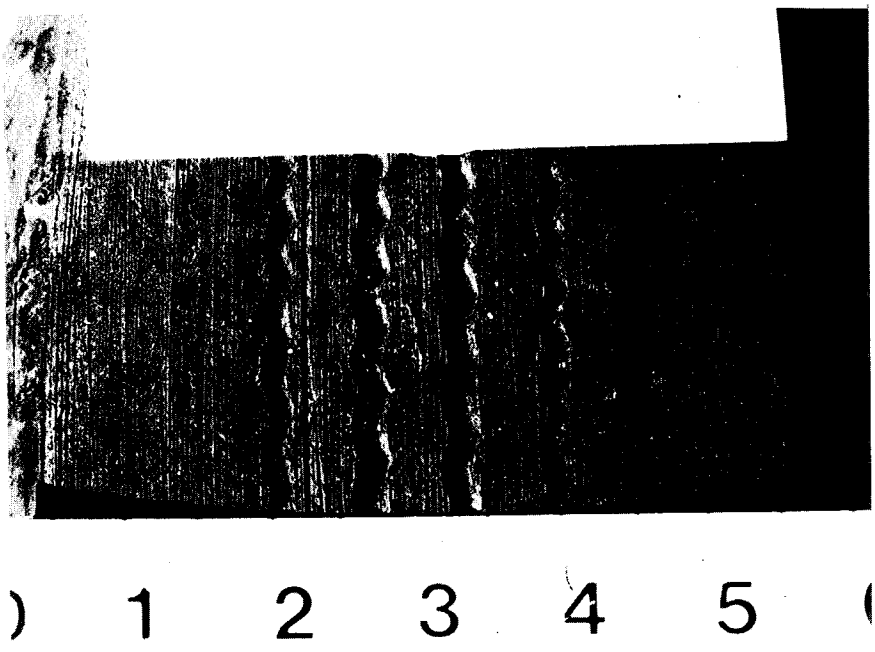

Figure 2-18. Uniroyal-Laredo Rain Tire-Minimum Tread.

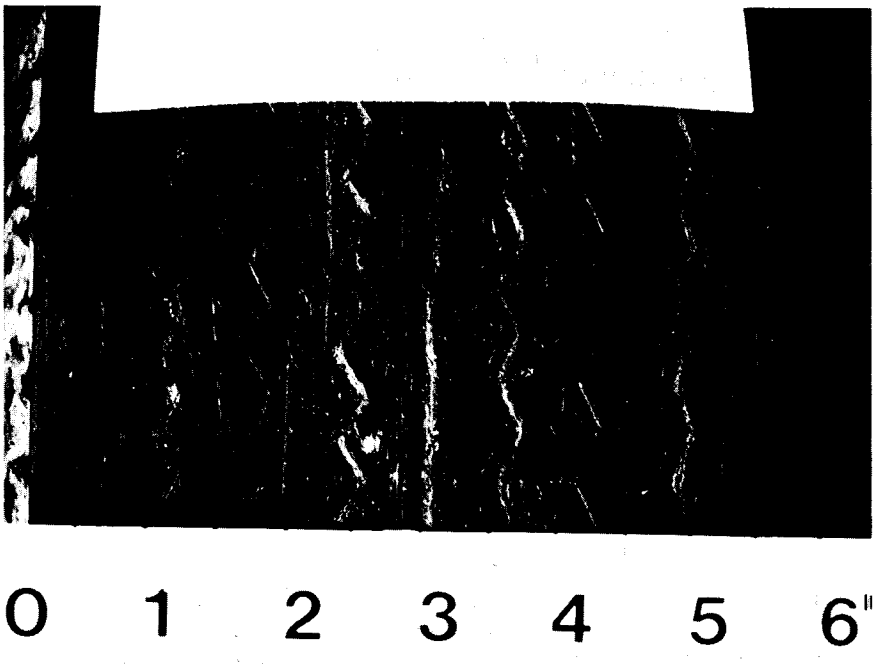

Figure 2-19. Jet Air II-Minimum Tread.

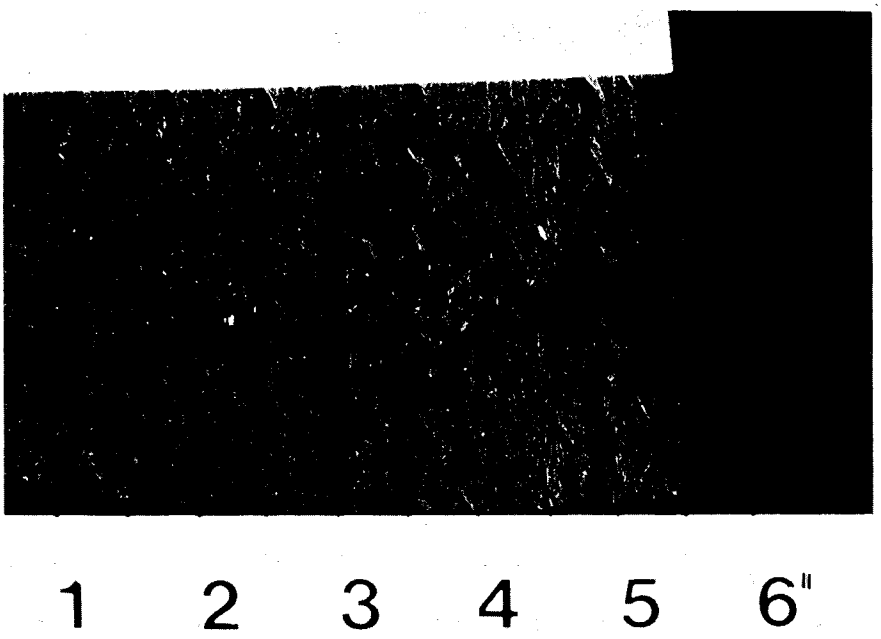

Figure 2-20. Jet Air II-Medium Tread .

Equipment

A general view of the rain simulator equipment used for wetting the surfaces is shown in Figure 2-21. The basic framework of the rain

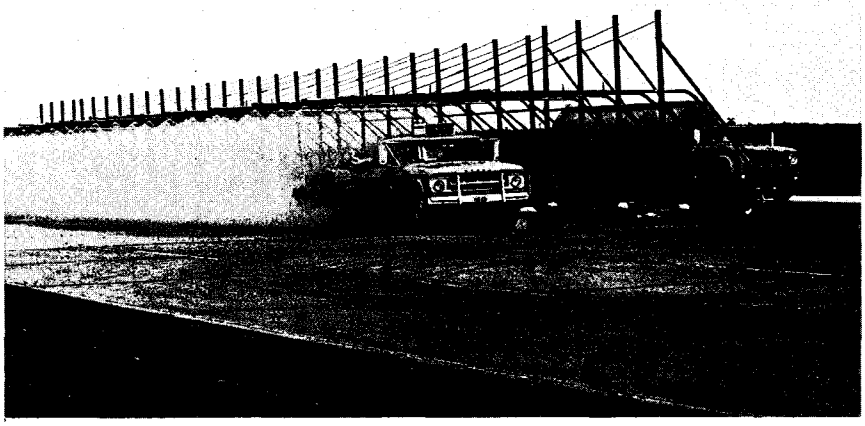

Figure 2-21. Equipment used for wetting and friction testing of the surfaces.

simulator was composed of 4-inch wide by 1-inch deep steel channels. A 4-inch diameter pipe served as the manifold with 2-inch diameter pipes used as feeder lines for the shrub-head nozzles. Eight 20-foot long sections of the rain simulator wetted an area approximately 210 feet long by 30 feet wide. Spray bars were spaced 6 feet apart with shrub-head nozzles directed downward and spaced at 6 ft. intervals along the spray bar. Hoze-type nozzles were attached to the upper side

of the spray bar and used for low intensity rainfall for initial tests, but were discontinued due to the adverse effects of light cross-winds. Detailed drawings of one section of the rainfall simulator are given in Figure 2-22 with a photograph of the nozzles given in Figure 2-23.

A 4000-gallon tank truck equipped with a high pressure pump was used for supplying water to the system. The number and type of nozzles and water pressure which were used to regulate rainfall intensity are noted in Table 2-2. Desired water depths were measured at various distances along the drainage path.

Rainfall intensities were deduced from the amount of water caught in metal cans during a twelve-minute interval. Twelve cans were placed at random locations under the rain simulator. Results are reported in inches-per-hour.

The friction measurements reported herein were obtained with the Texas Highway Department research skid trailer which conforms substantially to ASTM standards (E27-65T)* and utilizes 14-inch ASTM Standard tires (E249-66) inflated to 24 psi. The drag forces are measured with strain gages and the internal-watering system, when used, utilizes a centrifugal pump which applies a water film approximately 0.020-inches in thickness to the pavement surface. The development and calibration of the trailer may be reviewed in departmental research reports published earlier by the Texas Highway Department (58, 59). Figure 2-21 depicts the

*Part 11, 1970 Annual Book of ASTM Standards, American Society for Testing and Materials, 1916 Race Street, Philadelphia, Pa.

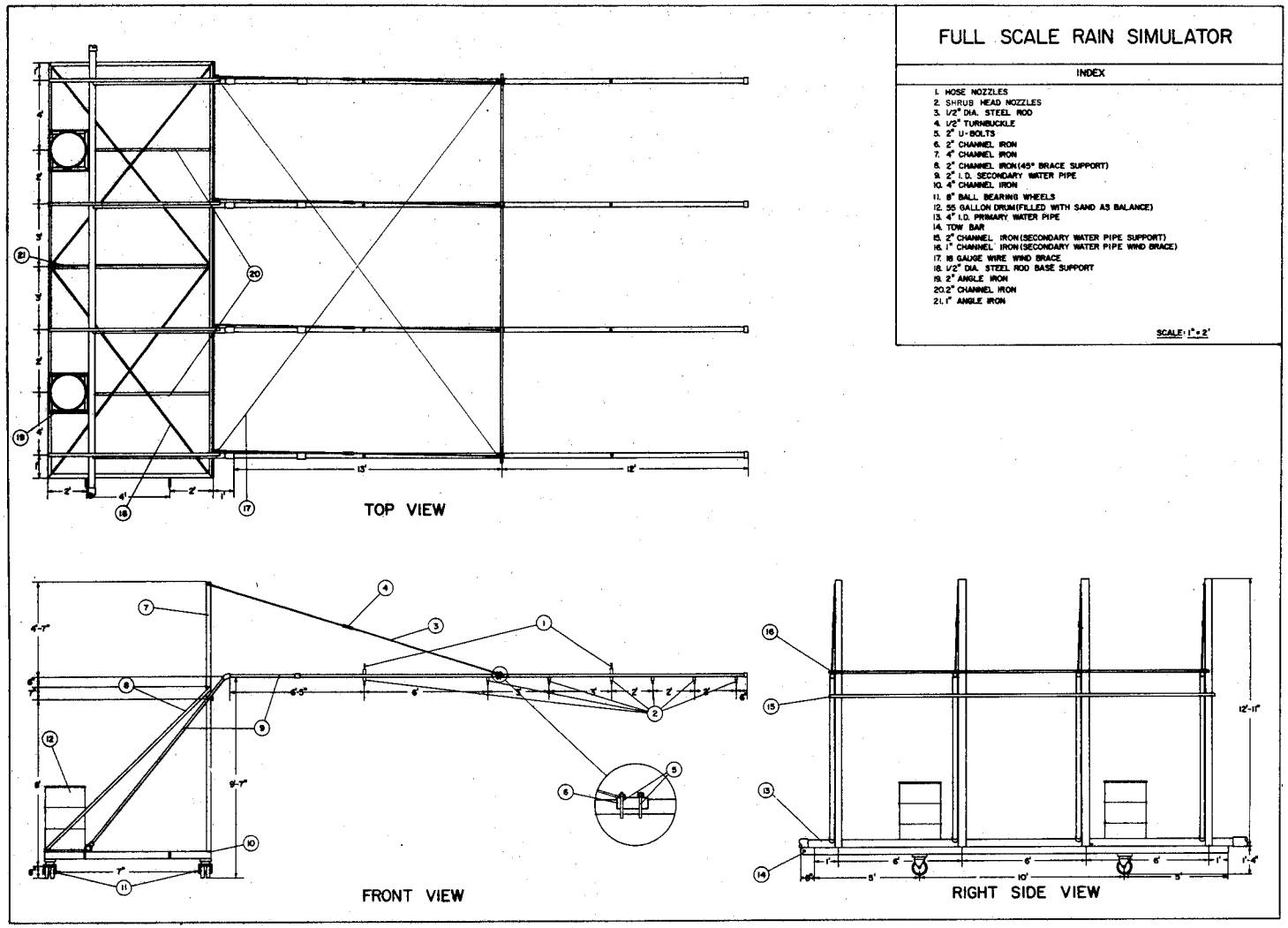

Figure 2-22. Detailed drawing of one section of the rain simulator.

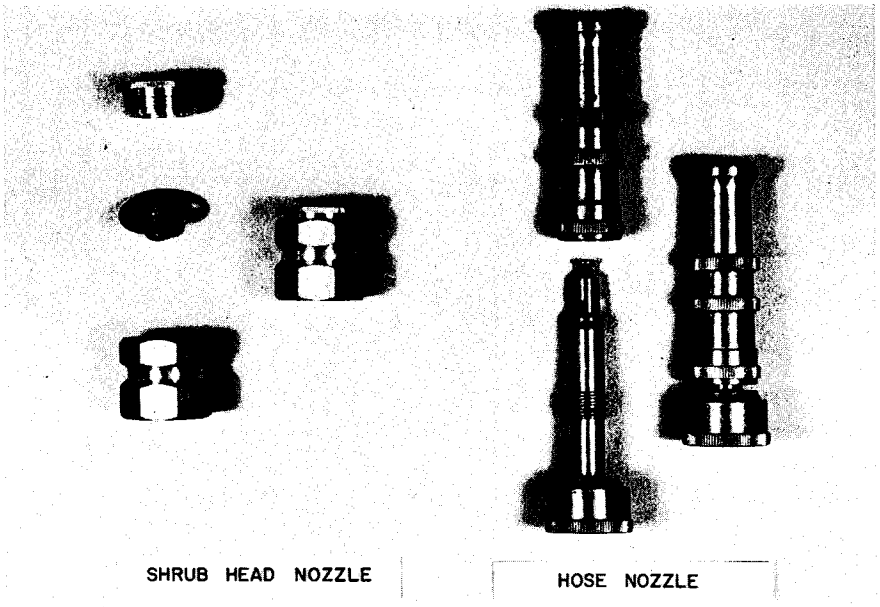

Figure 2-23. Nozzles used in the study.

trailer under test conditions. Friction measurements were taken at 20, 40, and 60 mph with both E-17 treaded and smooth tires. The internal watering system was used for only a portion of the measurements, as indicated.

Additional friction measurements were taken with the British Portable Skid Tester (60) in accordance with ASTM standard procedure (E303-69)*. Four locations were tested on each surface. Measurements were taken the same week that the trailer tests were made (Fig. 2-24).

Water depth measurements were taken with the Leopold and Stevens point gage (56) as shown in Fig. 2-25 and 2-27. A total of 15 measurements were

*Part 11, 1970 Annual Book of ASTM Standards, American Society for Testing and Materials, 1916 Race Street, Philadelphia, Pa.

TABLE 2-2

RAIN SIMULATOR CONTROLS

Nozzle Number and Type	Water Pressure psi	Resultant Approximate Rainfall Intensity, in/hr
128 shrub head nozzles (directed downward)	30	6
64 shrub head nozzles (directed downward)	30	3
32 shrub head nozzles (directed downward)	20	1½
32 hose nozzles* (directed upward)	15	1

*Use discontinued due to wind effects.

taken for a given reported average water depth.

Macrotexture measurements of the surfaces were taken by the putty impression method (53, 56) as shown in Fig. 2-26. Four measurements were taken on each surface and an average of these was reported.

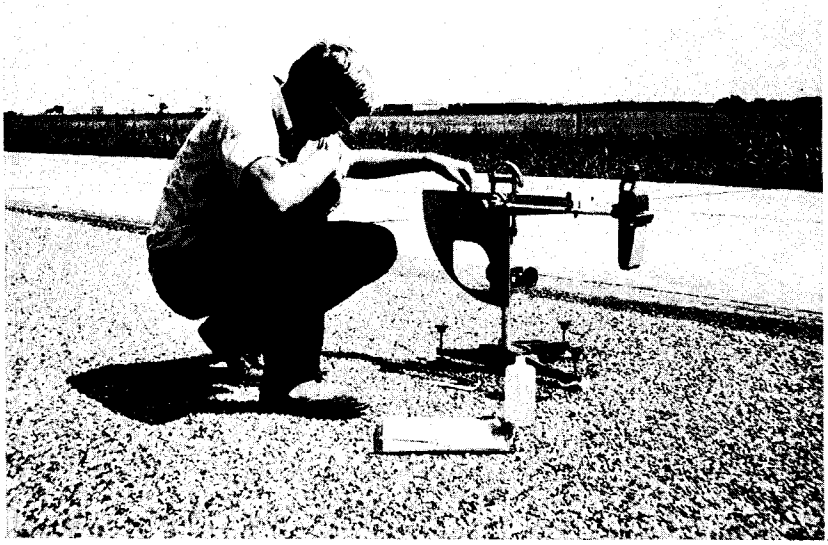

Figure 2-24. British portable skid tester used for skid-resistance measurements.

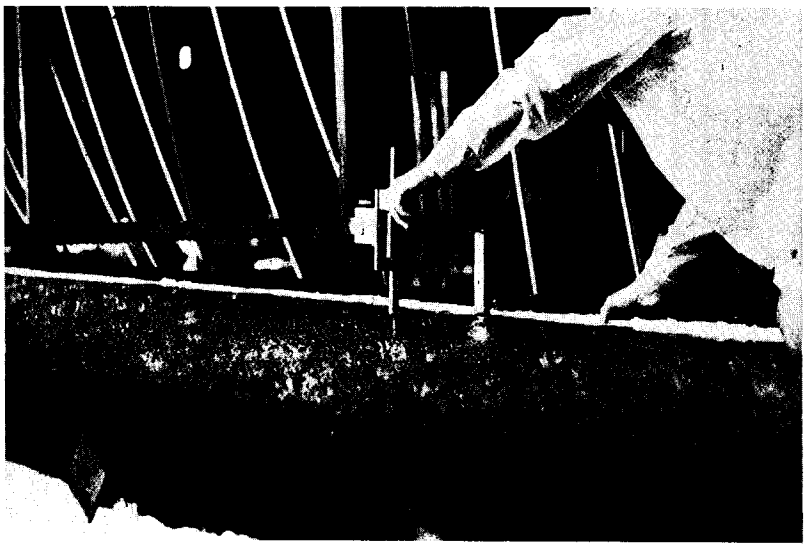

Figure 2-25. Point gage used for water-depth measurements.

Figure 2-26. Putty impression method used for texture measurements.

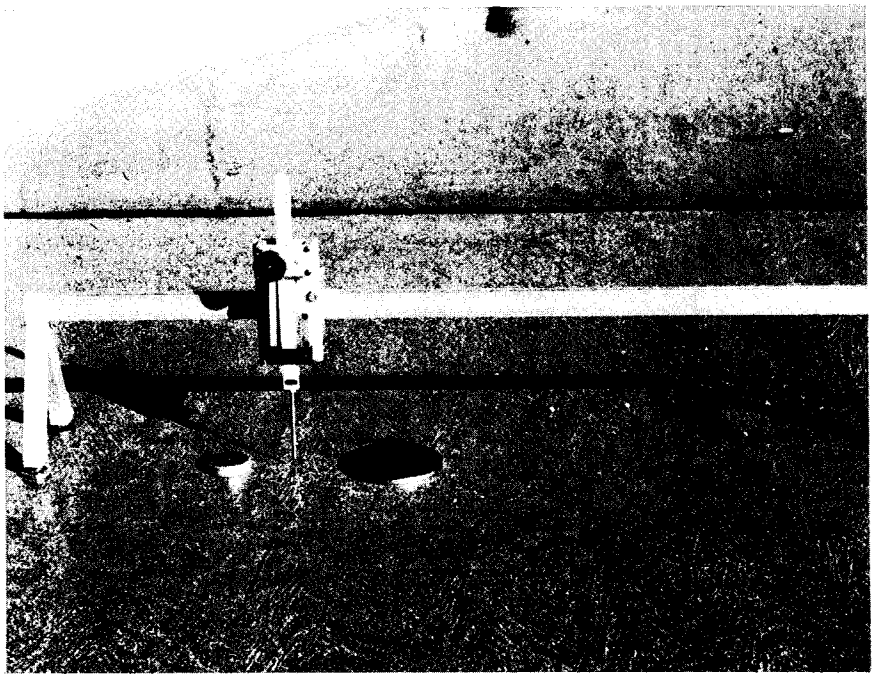

Figure 2-27. Leopold and Stevens point gage.

Testing Procedure

Two series of 20, 40, and 60 mph skid tests at various water depths using both ASTM E-17 treaded and smooth tires were conducted with the trailer. A total of four measurements were taken at each speed-tire-water depth combination. Each surface was tested at 5 or 6 different water depths and additionally with the trailer's internal watering system. Average skid numbers at 20, 40, and 60 mph were calculated for each surface-tire-water depth combination. The series was repeated for tire inflation pressures of 24 and 32 psi.

Gradients (denoted by G) of the skid number-speed curve between 20 and 60 mph were calculated. In addition, in order to reflect the relative position of the curve, percentage gradients were calculated. Curves of a given gradient positioned low on the graph would have higher percentage gradients than curves with the same gradient positioned high on the graph. Thus, percentage gradient is defined as the percentage of the gradient, obtained under test conditions, to a theoretical gradient if the skid number at the higher speed were zero. Calculations appear in Figure 2-28.

Water depth and rainfall intensity measurements were also taken during the skid testing sequence. The rain simulator controls were set to give three rates of rainfall. The following rain simulator adjustments were made to produce the desired range of rainfall.

a) For each rainfall intensity, a total of two water depths were tested (A pass in a south bound direction and a pass in a northerly direction).

b) Three rainfall intensities were used.
   1) 128 shrub head nozzles open with water pressure set at 20 psi - Approximately 6" per hour (called heavy water)

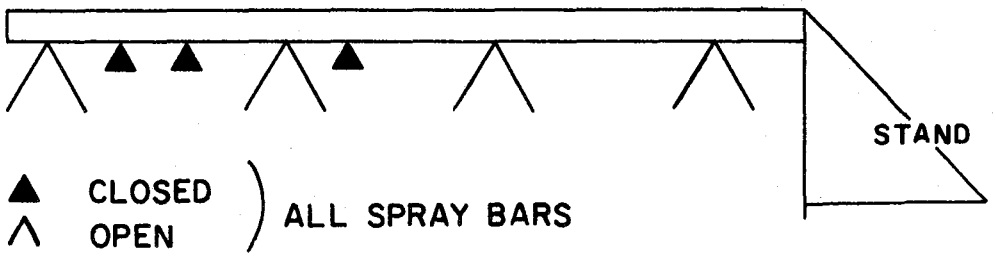

2) 64 shrub head nozzles open with water pressure set at 20 psi - Approximately 3.5" per hour

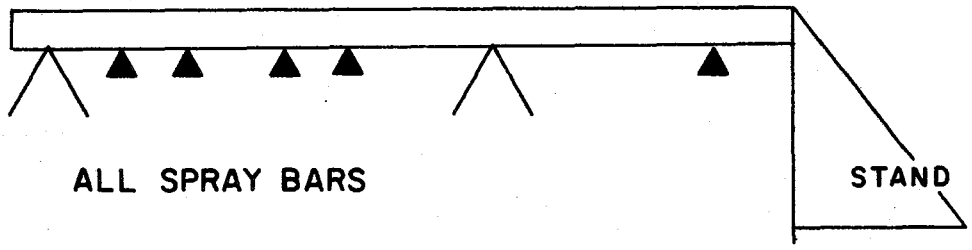

3) 32 plus 2 hose nozzles - 2 hose nozzles open an alternate bars and each end bar with 18 psi pressure rainfall intensity approximately 1" per hour

The water pressure given is the pressure measured at the manifold near the entry point of the water to the entire section of the simulator. Other combinations of numbers, sizes and types of nozzles would probably yield different rainfall intensities.

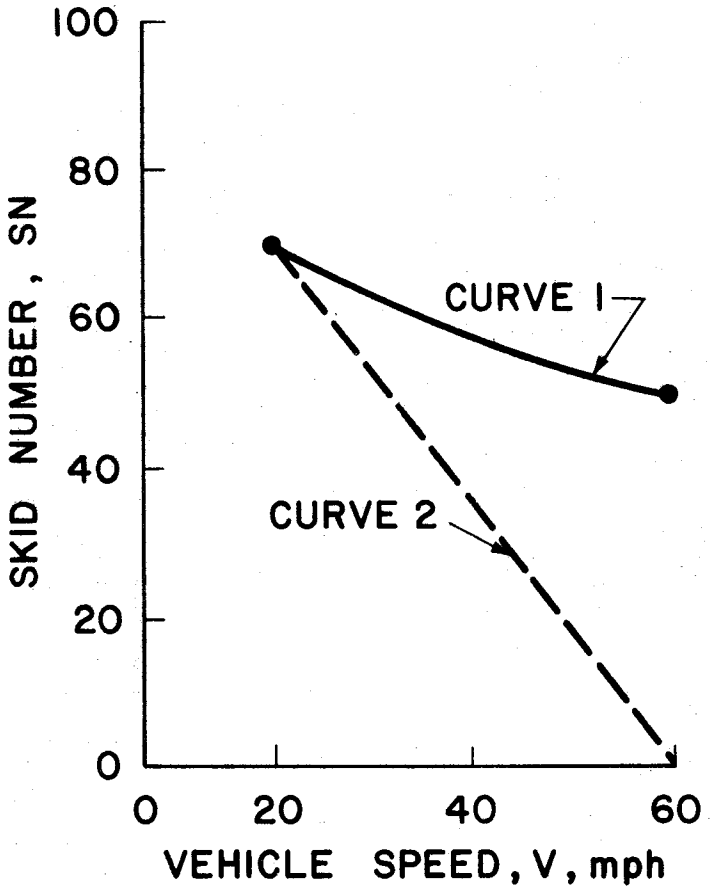

$$\text{GRADIENT } (G) = \frac{SN_{20} - SN_{60}}{40}$$

$$\text{GRADIENT } (G_2) = \frac{SN_{20} - 0}{40}$$

$$\text{PERCENTAGE GRADIENT (PG)} = \frac{G}{G_2} \times 100 = \frac{SN_{20} - SN_{60}}{SN_{20}} \times 100$$

Figure 2-28. Gradient and percentage gradient calculations.

Chapter III

ANALYSIS AND DISCUSSION OF TEST RESULTS

Friction data obtained on the Research Annex Test Pads are given in the eighteen tables that follow (Tables Nos. 3-1 thru 3-18). As discussed previously, skid trailer measurements were obtained on seven other surfaces and details on them are given in Tables 3-19 thru 3-25 in this report.

The skid trailer friction data for the combined surfaces were analyzed using a computerized multiple-regression program to obtain the best fit of the data. Equations relating the relative effects of speed, water depth, texture, and tire-tread depth to skid number were developed. Tire-tread depths were assumed as 0.25-inch for the E-17 treaded tire and 0.02-inch for the smooth tire. ASTM specifications permit E-17 tread depth between 0.15 and 0.35-inch. A value slightly greater than zero was used for the smooth tire. Water depths were referenced at the top of the texture. Equations relating the same variables, excluding speed, to gradient and percentage gradient were also developed and values are shown in the tables mentioned above. The selected equations are shown on page 83 of this report followed by a sensitivity analysis and stochastic considerations.

For ease of analysis of the data included, the following series of tables are similarly arranged. However, for purposes of interpretation, one should look at the data from both the overall and the specific viewpoints.

Collection of the data extended over a time period of many months with one series of tests conducted on full scale prototype pavement surfaces of nine types located at the Texas A&M Research Annex (Tables 3-1 thru 3-18) and another series carried out on a portland cement concrete controlled access highway at the east city limits of Bryan and College Station, Texas (Tables 4-1 thru 4-7). This latter series of tests included seven different textural types.

Actually, the tables are arranged in pairs with each pair representing a single surface tested under simulated rain at each of two tire inflation pressures, namely, 24 and 32 psi. The test surface or Pad No. and texture depth are given in the title of the table as is the tire pressure. The columnized data are arranged beginning from left to right with the water depth, the test tire type, the tread depth and the air temperature. Skid numbers at 20, 40 and 60 mph follow with the associated skid number-speed gradient and the percentage gradient.

Take, for example, Pad No. 1 data for which are shown in Table 3-1. Beginning at the top left of the table it may be observed that the ASTM E-249 standard skid resistance tire was tested at six different water depths and two different tread depths, specifically, no tread and 10/32-inch of tread.

The Jet 2 tire was tested at six different water depths, three different tread depths and three different speeds. The three tread depths included are 1/32, 5/32 and 9/32 inch, and the data are arranged in this order.

Similarly, throughout the series of tables the skid numbers are grouped with increasing water depth and increasing tread depth.

In Table 3-2 the series of tests documented in the aforementioned table are repeated at a tire inflation pressure of 32 psi.

In the second series of tests for which data appear in Tables 3-19 thru 3-25 results for both 24 and 32 psi tire inflation pressures are given together for ease of comparison and tabular space saving.

The reader should be aware of the fact that only two tires were used in this series of tests. Both carry an ASTM designation, but the tires were different in several respects. The ASTM 14 (14-inch rim) was the same tire used in the first series of tests conducted at the Texas A&M Research Annex; whereas, the ASTM 15 (15-inch rim) was an interim standard supplied on trial for calibration and correlation testing to a number of agencies across the country and later withdrawn by ASTM. The data for this tire are included for whatever insight they may supply toward a better understanding of the performance of different tread configurations on pavements of various textures tested at different water depths.

Any detailed analysis and comparison of the data listed in all of these tables inescapably involves a measure of speculation and, naturally, some considered opinions, since in many instances the pure numbers one may wish to compare do not necessarily convey the same meaning. One example of this where the meanings are similar is the texture of the various surfaces. Pad No. 1 (TTI Annex) had at the time of the tests a texture depth of about 0.036 inches and Test Section F-6 (data given in Table 3-24) had a texture depth of about 0.039. The difference in these numbers is of minor significance, and if one considers the water depths of 0.45 and 0.40 mm, respectively, for

these pavements, the performance as indicated by the respective SN values is quite similar. These pavements are both portland cement concrete. Pad No. 1 is more than 25 years old and has a belt finish whereas F6 was at the time of testing a new surface unexposed to traffic. Conflict appears if we compare Pads Nos. 6 and 7 at, for example, water depth of 0.66 and 0.50 and the ASTM tire with 10/32 inch of tread operated at 24 psi. The texture depth of Pad No. 6 is given as 0.159 whereas that of Pad No. 7 is listed as 0.136, a difference of about 18 percent if the reference is made to Pad No. 7. Now look at the SN values at 20, 40 and 60 mph. Although the textures are significantly different, Pad No. 7 exhibits much higher SN values; yet it has less texture and more water. From a simple analysis of the parameter values one might predict other than the values shown in the table.

One might consider the water depths listed for the tests on Pads Nos. 6 and 7. Comparison of these figures indicates a marked difference in the drainage characteristics of the two surfaces. The range of rainfall intensities for the two surfaces was about the same; however, in the case of Pad No. 6 water depths ranged from -2.21 to +0.77 mm, whereas the water depth on Pad No. 7 ranged from -0.50 to +1.60 mm. If one averages these depths, the result is -1.44 mm for Pad No. 6 and +1.10 mm for Pad No. 7. Yet, Pad No. 7 gave much higher SN values.

Particle shape and surface texture are suggested as the key factors explaining these observed differences. The gradings of the two aggregates used in these seal coats were essentially the same when they were constructed, but because the crushed synthetic or manufactured aggregate of Pad No. 7 degraded somewhat due to construction rolling and subsequent service, and since there was only limited degradation of the natural rounded siliceous gravel of Pad No. 6 was larger, hence a higher texture value. The drainage

of Pad No. 6 was better than that of No. 7 for these reasons, namely, larger and smoother drainage channels. The higher SN values for Pad No. 7 may very well have merit, but one may also wish to consider another performance characteristic of this type of surface; this being splatter and spray. Pad No. 6 would be capable of draining large amounts of water for normal cross slopes of 1/8 to 1/4 inch per foot without appreciable splatter or spray. This is particularly important for night driving on two-lane highways and should not be completely disregarded on multilane divided highways.

How then does one weigh the advantage of higher SN values? Strictly speaking, other factors must be taken into account, because it is the combined effect on the total accident picture that must be considered and the interactions are numerous and often rather difficult to separate for analysis; yet, there must be an answer. Indeed, there must be not one but several answers, each tailored for a particular but somewhat general set of conditions and service demands. The number of categories of pavement surface textural types desirable for a given area or region will probably vary, but most likely three or four will suffice.

It is evident from the data presented that levels of performance, as defined by SN values, may be produced via several different types of surfaces. This being the case, it would seem that ease of construction, durability, uniformity and long term cost would become determining factors in the selection of the surface to be built.

Since driver expectancy is a critical input to overall highway safety, one should examine the effect of the SN value on this factor and consider this in the selection of the surface to be built. Probably the most important input to the driver expectancy-accident related phenomena is uniformity, that

is, uniformity of tire-pavement interaction feedback to the driver. Knowledge of this fact is a strong input to the final answer one may arrive at when he decides how many general categories of surfaces will be made available to the driving public and what will be the range of SN values furnished in each category.

Ideally, the variation in tire-pavement interaction feedback to the driver should be as small as practical. Any sudden change in the SN value, although it may be relatively small, can be the key causative factor in an accident. The driver will be unable to adjust to the new hazard in the very short time between cause and effect, if he has only recently entered a section of road with a significantly different SN value. This could be true whether the newly entered section has a higher or lower SN value than the segment passed over and to which he has become acclimated. Admittedly, change from a higher SN to a lower SN offers greater probability for an accident.

This concept would most likely discourage the use of pavements with very high SN values in favor of a system of streets and highways with intermediate ranges of SN values and pavements with relatively flat SN-speed curves, and encourage the early elimination of surfaces with low SN values and/or steep SN-speed curves. Of course, speed zoning could eliminate the need to avoid the latter, but quite often a pavement that is very speed sensitive is also sensitive to the wet condition, and therefore such a pavement would not be desirable even if the facility were speed zoned.

Graphical analyses of the tabular data are given in Figures 3-1 through 3-48. These graphical analyses are summarized in Figures 3-49 through 3-60.

TABLE 3-1

SKID TRAILER DATA UNDER SIMULATED RAIN, TEXAS A&M RESEARCH ANNEX
PAD NO. 1, TEXTURE DEPTH = 0.036 INCHES, 32 PSI, PORTLAND CEMENT CONCRETE

WD MM	TEST TIRE	TD /32 IN.	AIR TEMP F	SN 20	SN 40	SN 60	GRAD	PCT GRAD	TD /32 IN.	AIR TEMP F	SN 20	SN 40	SN 60	GRAD	PCT GRAD
0.07	ASTM	0	90	48	30	23	0.63	52	10	78	51	42	33	0.45	35
0.45	ASTM	0	90	49	26	18	0.77	63	10	78	52	41	25	0.67	52
1.11	ASTM	0	66	41	27	17	0.60	59	10	83	52	42	26	0.65	50
1.64	ASTM	0	66	44	25	16	0.70	64	10	83	55	44	21	0.85	62
2.40	ASTM	0	85	48	26	15	0.82	69	10	65	55	39	17	0.95	69
3.00	ASTM	0	85	49	27	15	0.85	69	10	65	55	42	19	0.90	65
0.07	JET2	1	89	46	31	21	0.63	54	5	70	49	38	23	0.65	53
0.45	JET2	1	89	47	26	13	0.85	72	5	70	47	39	18	0.72	62
1.11	JET2	1	85	41	28	12	0.72	71	5	61	47	35	18	0.72	62
1.64	JET2	1	85	42	24	11	0.77	74	5	61	46	35	15	0.77	67
2.40	JET2	1	85	48	23	13	0.88	73	5	72	48	36	12	0.90	75
3.00	JET2	1	85	49	26	14	0.88	71	5	72	50	36	13	0.92	74
0.07	JET2								9	72	48	39	26	0.55	46
0.45	JET2								9	72	47	36	21	0.65	55
1.11	JET2								9	84	45	35	22	0.57	51
1.64	JET2								9	84	45	36	17	0.70	62
2.40	JET2								9	75	47	34	12	0.88	74
3.00	JET2								9	75	50	41	14	0.90	72
0.07	LARRT	1	73	49	38	20	0.72	59	5	72	53	50	32	0.52	40
0.45	LARRT	1	73	50	33	15	0.88	70	5	72	55	45	27	0.70	51
1.11	LARRT	1	84	49	29	15	0.85	69	5	85	49	41	24	0.63	51
1.64	LARRT	1	84	47	30	15	0.80	68	5	85	51	45	20	0.77	61
2.40	LARRT	1	77	46	25	11	0.88	76	5	78	51	39	11	1.00	78
3.00	LARRT	1	77	48	30	12	0.90	75	5	78	52	43	11	1.02	79
0.07	GODWO	0	74	37	21	14	0.57	62	7	74	50	42	30	0.50	40
0.45	GODWO	0	74	36	19	13	0.57	64	7	74	49	40	31	0.45	37
1.11	GODWO	0	84	31	17	10	0.52	68	7	83	43	37	25	0.45	42
1.64	GODWO	0	84	33	16	9	0.60	73	7	83	44	36	17	0.67	61
2.40	GODWO	0	80	35	15	10	0.63	71	7	76	46	31	12	0.85	74
3.00	GODWO	0	80	37	18	11	0.65	70	7	76	46	38	14	0.80	70

TABLE 3-2

SKID TRAILER DATA UNDER SIMULATED RAIN, TEXAS A&M RESEARCH ANNEX
PAD NO. 1, TEXTURE DEPTH = 0.036 INCHES, 24 PSI, PORTLAND CEMENT CONCRETE

WD MM	TEST TIRE	TD /32 IN.	AIR TEMP F	SN 20	SN 40	SN 60	GRAD	PCT GRAD	TD /32 IN.	AIR TEMP F	SN 20	SN 40	SN 60	GRAD	PCT GRAD
0.07	ASTM	0	90	45	29	24	0.52	47	10	78	54	44	31	0.57	43
0.45	ASTM	0	90	44	25	18	0.65	59	10	78	55	42	24	0.77	56
1.11	ASTM	0	66	41	24	18	0.57	56	10	83	53	42	25	0.70	53
1.64	ASTM	0	66	40	23	17	0.57	58	10	83	55	40	21	0.85	62
2.40	ASTM	0	85	44	23	14	0.75	68	10	65	54	37	13	1.02	76
3.00	ASTM	0	85	47	26	15	0.80	68	10	65	59	41	13	1.15	78
0.07	JET2	1	89	46	26	18	0.70	61	5	70	49	32	22	0.67	55
0.45	JET2	1	89	46	24	12	0.85	74	5	70	50	27	16	0.85	68
1.11	JET2	1	85	40	23	13	0.67	68	5	60	48	38	17	0.77	65
1.64	JET2	1	85	39	19	11	0.70	72	5	61	45	31	15	0.75	67
2.40	JET2	1	85	46	20	13	0.82	72	5	72	48	26	12	0.90	75
3.00	JET2	1	85	47	22	14	0.82	70	5	72	46	27	13	0.82	72
0.07	JET2								9	72	46	36	24	0.55	48
0.45	JET2								9	72	46	33	20	0.65	57
1.11	JET2								9	84	46	35	17	0.72	63
1.64	JET2								9	84	45	35	16	0.72	64
2.40	JET2								9	75	47	27	11	0.90	77
3.00	JET2								9	75	48	38	13	0.88	73
0.07	LARRT	1	73	47	32	19	0.70	60	5	72	52	43	29	0.57	44
0.45	LARRT	1	73	46	30	16	0.75	65	5	72	51	41	26	0.63	49
1.11	LARRT	1	84	41	24	14	0.67	66	5	85	48	38	21	0.67	56
1.64	LARRT	1	84	39	27	16	0.57	59	5	85	50	39	18	0.80	64
2.40	LARRT	1	77	48	21	15	0.82	69	5	78	49	35	12	0.92	76
3.00	LARRT	1	77	49	27	15	0.85	69	5	78	51	46	13	0.95	75
0.07	GODWO	0	74	35	24	16	0.47	54	7	74	44	41	27	0.42	39
0.45	GODWO	0	74	34	16	13	0.52	62	7	74	46	39	22	0.60	52
1.11	GODWO	0	84	32	19	12	0.50	63	7	83	42	37	24	0.45	43
1.64	GODWO	0	84	31	15	11	0.50	65	7	83	44	32	16	0.70	64
2.40	GODWO	0	80	32	15	11	0.52	66	7	76	46	36	12	0.85	74
3.00	GODWO	0	80	34	16	12	0.55	65	7	76	47	38	14	0.82	70

TABLE 3-3

SKID TRAILER DATA UNDER SIMULATED RAIN, TEXAS A&M RESEARCH ANNEX
PAD NO. 2, TEXTURE DEPTH = 0.002 INCHES, 24 PSI, JENNITE FLUSH SEAL

WD MM	TEST TIRE	TD /32 IN.	AIR TEMP F	SN 20	SN 40	SN 60	GRAD	PCT GRAD	TD /32 IN.	AIR TEMP F	SN 20	SN 40	SN 60	GRAD	PCT GRAD
0.80	ASTM	0	76	22	10	10	0.30	55	10	76	24	18	12	0.30	50
0.92	ASTM	0	76	22	9	8	0.35	64	10	76	24	19	10	0.35	58
1.50	ASTM	0	80	20	11	7	0.32	65	10	76	24	16	10	0.35	58
1.87	ASTM	0	76	24	11	9	0.38	63							
1.98	ASTM	0	80	18	10	7	0.27	61	10	76	25	18	9	0.40	64
2.50	ASTM	0	76	22	10	7	0.38	68							
0.80	JET2	1	78	25	13	10	0.28	60	5	79	26	19	16	0.25	38
0.92	JET2	1	78	23	13	9	0.38	65	5	79	23	18	10	0.32	57
1.50	JET2	1	79	23	11	6	0.42	74	5	88	23	13	7	0.40	70
1.87	JET2	1	84	21	11	6	0.38	71	5	84	26	14	7	0.47	73
1.98	JET2	1	89	23	10	6	0.42	74	5	88	24	14	8	0.40	67
2.50	JET2	1	84	21	10	6	0.38	71	5	84	26	16	8	0.45	69
0.80	JET2								9	82	22	17	11	0.27	50
0.92	JET2								9	82	22	13	9	0.32	59
1.50	JET2								9	82	24	15	8	0.40	67
1.87	JET2								9	84	23	14	7	0.40	70
1.98	JET2								9	82	22	13	7	0.38	68
2.50	JET2								9	84	21	13	6	0.38	71
0.80	LARRT	2	78	25	17	8	0.42	68	6	78	26	18	18	0.20	31
0.92	LARRT	2	78	24	13	8	0.40	67	6	80	23	17	10	0.32	57
1.50	LARRT	2	82	26	11	6	0.50	77	6	80	24	16	10	0.35	58
1.87	LARRT	2	92	28	11	7	0.52	75	6	78	29	20	7	0.55	76
1.98	LARRT	2	82	21	11	6	0.38	71	6	80	22	15	6	0.40	73
2.50	LARRT	2	92	22	12	5	0.42	77	6	78	24	17	7	0.42	71
0.80	GODWO	1	77	23	10	7	0.40	70	8	79	24	19	16	0.20	33
0.92	GODWO	1	77	20	9	8	0.30	60	8	79	23	17	18	0.13	22
1.50	GODWO	1	93	17	9	8	0.22	53	8	90	24	18	14	0.25	42
1.87	GODWO	1	80	20	7	6	0.35	70							
1.98	GODWO	1	93	19	9	9	0.25	53	8	90	23	17	9	0.35	61
2.50	GODWO	1	80	21	8	6	0.38	71							

TABLE 3-4

SKID TRAILER DATA UNDER SIMULATED RAIN, TEXAS A&M RESEARCH ANNEX
PAD NO. 2, TEXTURE DEPTH = 0.002 INCHES, 32 PSI, JENNITE FLUSH SEAL

WD MM	TEST TIRE	TD /32 IN.	AIR TEMP F	SN 20	SN 40	SN 60	GRAD	PCT GRAD	TD /32 IN.	AIR TEMP F	SN 20	SN 40	SN 60	GRAD	PCT GRAD
0.80	ASTM	0	76	23	12	10	0.32	57	10	76	28	18	15	0.32	46
0.92	ASTM	0	76	21	11	7	0.35	67	10	76	28	18	12	0.40	57
1.50	ASTM	0	80	21	12	7	0.35	67	10	76	26	17	14	0.30	46
1.87	ASTM	0	76	27	12	7	0.50	74							
1.98	ASTM	0	80	20	11	8	0.30	60	10	76	25	17	14	0.27	44
2.50	ASTM	0	76	24	12	8	0.40	67							
0.80	JET2	1	78	27	15	12	0.38	56	5	79	25	17	13	0.30	48
0.92	JET2	1	78	24	14	9	0.38	63	5	79	24	17	10	0.35	58
1.50	JET2	1	89	23	15	7	0.40	70	5	88	23	13	7	0.40	70
1.87	JET2	1	84	21	12	6	0.38	71	5	84	26	15	7	0.47	73
1.98	JET2	1	89	23	15	7	0.40	70	5	88	23	15	7	0.40	70
2.50	JET2	1	84	20	11	6	0.35	70	5	84	24	16	7	0.42	71
0.80	JET2								9	82	23	16	11	0.30	52
0.92	JET2								9	82	24	16	10	0.35	58
1.50	JET2								9	82	23	16	9	0.35	61
1.87	JET2								9	84	21	14	8	0.32	62
1.98	JET2								9	82	22	14	9	0.32	59
2.50	JET2								9	84	20	14	8	0.30	60
0.80	LARRT								2	78	27	18	12	0.38	56
0.80	LARRT								6	78	27	19	18	0.22	33
0.92	LARRT	2	78	24	16	8	0.40	67	6	78	27	19	14	0.32	48
1.50	LARRT	2	82	25	18	6	0.47	76	6	80	22	17	11	0.27	50
1.87	LARRT	2	92	29	18	7	0.55	76	6	78	29	21	14	0.38	52
1.98	LARRT	2	82	24	16	7	0.42	71	6	80	23	17	10	0.32	57
2.50	LARRT	2	92	23	14	5	0.45	78	6	78	25	18	8	0.42	68
0.80	GODWO	1	77	22	10	8	0.35	64	8	79	26	19	16	0.25	38
0.92	GODWO	1	77	22	10	6	0.40	73	8	79	23	19	14	0.22	39
1.50	GODWO	1	93	20	9	6	0.35	70	8	90	27	16	14	0.32	48
1.87	GODWO	1	80	21	12	6	0.38	71							
1.98	GODWO	1	93	20	10	8	0.30	60	8	90	22	16	12	0.25	45
2.50	GODWO	1	80	20	11	6	0.35	70							

TABLE 3-5

SKID TRAILER DATA UNDER SIMULATED RAIN, TEXAS A&M RESEARCH ANNEX
PAD NO. 3, TEXTURE DEPTH = 0.012 INCHES, 24 PSI, LIMESTONE HOT MIX TERAZZO

WD MM	TEST TIRE	TD /32 IN.	AIR TEMP F	SN 20	SN 40	SN 60	GRAD	PCT GRAD	TD /32 IN.	AIR TEMP F	SN 20	SN 40	SN 60	GRAD	PCT GRAD
0.00	ASTM	0	78	63	31	24	0.97	62	10	68	80	67	49	0.77	39
1.10	ASTM	0	83	58	22	18	1.00	69	10	80	68	53	35	0.82	49
1.40	ASTM	0	78	56	29	19	0.92	66	10	68	71	54	31	1.00	56
1.83	ASTM	0	83	51	25	19	0.80	63	10	80	66	58	30	0.90	55
2.47	ASTM	0	68	55	21	14	1.02	75	10	67	73	57	20	1.32	73
3.50	ASTM	0	68	53	23	16	0.92	70	10	67	65	55	30	0.88	54
0.00	JET2	1	77	52	35	17	0.88	67	4	76	56	45	28	0.70	50
1.10	JET2	1	82	43	21	14	0.72	67	4	88	45	32	15	0.75	67
1.40	JET2	1	77	47	36	15	0.80	68	4	76	52	39	16	0.90	69
1.83	JET2	1	82	47	24	13	0.85	72	4	88	51	32	13	0.95	75
2.47	JET2	1	79	50	16	12	0.95	76	4	83	55	38	10	1.13	82
3.50	JET2	1	79	48	12	16	0.80	67	4	83	49	35	8	1.02	84
0.00	LARRT	1	58	56	36	16	1.00	71	5	64	52	41	27	0.63	48
1.10	LARRT	1	85	42	26	14	0.70	67	5	87	52	38	18	0.85	65
1.40	LARRT	1	58	46	35	14	0.80	70	5	64	51	39	17	0.85	67
1.83	LARRT	1	85	47	32	14	0.82	70	5	87	49	36	16	0.82	67
2.47	LARRT	1	90	68	24	13	1.38	81	5	87	64	43	14	1.25	78
3.50	LARRT	1	90	61	21	12	1.22	80	5	87	65	49	13	1.30	80
0.00	JET2								7	78	58	53	27	0.77	53
1.10	JET2								7	83	47	36	19	0.70	60
1.40	JET2								7	78	56	47	24	0.80	57
1.83	JET2								7	83	55	41	19	0.90	65
2.47	JET2								7	75	53	41	12	1.02	77
3.50	JET2								7	75	51	34	17	0.85	67
0.00	GODWO	0	72	57	22	19	0.95	67	6	70	62	48	42	0.50	32
1.10	GODWO	0	88	49	16	12	0.92	76	6	88	48	37	19	0.72	60
1.40	GODWO	0	72	53	20	16	0.92	70	6	70	50	39	21	0.72	58
1.83	GODWO	0	88	45	16	13	0.80	71	6	88	58	37	15	1.07	74
2.47	GODWO	0	80	52	21	12	1.00	77	6	80	58	42	13	1.13	78
3.50	GODWO	0	80	48	14	11	0.92	77	6	80	52	33	10	1.05	81

TABLE 3-6

SKID TRAILER DATA UNDER SIMULATED RAIN, TEXAS A&M RESEARCH ANNEX
PAD NO. 3, TEXTURE DEPTH = 0.012 INCHES, 32 PSI, LIMESTONE HOT MIX TERAZZO

WD MM	TEST TIRE	TD /32 IN.	AIR TEMP F	SN 20	SN 40	SN 60	GRAD	PCT GRAD	TD /32 IN.	AIR TEMP F	SN 20	SN 40	SN 60	GRAD	PCT GRAD
0.00	ASTM	0	78	59	39	25	0.85	58	10	68	85	68	56	0.72	34
1.10	ASTM	0	83	51	25	16	0.88	69	10	80	73	59	38	0.88	48
1.40	ASTM	0	78	57	36	21	0.90	63	10	68	73	61	40	0.82	45
1.83	ASTM	0	83	50	27	18	0.80	64	10	80	74	58	39	0.88	47
2.47	ASTM	0	68	57	26	14	1.07	75	10	67	74	58	32	1.05	57
3.50	ASTM	0	68	61	25	18	1.07	70	10	67	68	56	45	0.57	34
0.00	JET2	1	77	52	38	16	0.90	69	4	76	59	44	35	0.60	41
1.10	JET2	1	82	46	29	13	0.82	72	4	88	47	34	16	0.77	66
1.40	JET2	1	77	58	38	15	1.07	74	4	76	49	37	17	0.80	65
1.83	JET2	1	82	48	34	13	0.88	73	4	88	53	41	17	0.90	68
2.47	JET2	1	79	46	28	10	0.90	78	4	83	59	45	10	1.22	83
3.50	JET2	1	79	49	22	11	0.95	78	4	83	52	41	9	1.07	83
0.00	JET2								7	78	66	59	30	0.90	55
1.10	JET2								7	83	50	40	21	0.72	58
1.40	JET2								7	78	53	53	22	0.77	58
1.83	JET2								7	83	51	42	19	0.80	63
2.47	JET2								7	75	61	41	15	1.15	75
3.50	JET2								7	75	60	41	12	1.20	80
0.00	LARRT	1	58	50	37	17	0.82	66	5	64	57	47	32	0.63	44
1.10	LARRT	1	85	53	30	15	0.95	72	5	87	51	39	22	0.72	57
1.40	LARRT	1	58	49	34	12	0.92	76	5	64	50	37	19	0.77	62
1.83	LARRT	1	85	51	37	14	0.92	73	5	87	49	44	25	0.60	49
2.47	LARRT	1	90	69	40	13	1.40	81	5	87	68	55	14	1.35	79
3.50	LARRT	1	90	62	37	12	1.25	81	5	87	66	45	11	1.38	83
0.00	GODWO	0	72	61	30	18	1.07	70	6	70	64	54	42	0.55	34
1.10	GODWO	0	88	44	17	10	0.85	77	6	70	48	38	20	0.70	58
1.40	GODWO	0	72	52	21	15	0.92	71	6	70	54	41	27	0.67	50
1.83	GODWO	0	88	52	24	11	1.02	79	6	88	59	38	21	0.95	64
2.47	GODWO	0	80	58	18	8	1.25	86	6	80	62	46	13	1.22	79
3.50	GODWO	0	80	54	23	7	1.17	87	6	80	58	37	11	1.17	81

TABLE 3-7

SKID TRAILER DATA UNDER SIMULATED RAIN, TEXAS A&M RESEARCH ANNEX
PAD NO. 4, TEXTURE DEPTH = 0.031 INCHES, 24 PSI, CRUSHED SILICEOUS GRAVEL HOT MIX

	WD MM	TEST TIRE	TD /32 IN.	AIR TEMP F	SN 20	SN 40	SN 60	GRAD	PCT GRAD	TD /32 IN.	AIR TEMP F	SN 20	SN 40	SN 60	GRAD	PCT GRAD
	0.08	ASTM	0	86	51	31	24	0.67	53	10	90	61	48	35	0.65	43
	0.84	ASTM	0	92	44	28	22	0.55	50	10	88	55	44	35	0.50	36
	0.97	ASTM	0	86	45	24	21	0.60	53	10	90	52	44	31	0.52	40
	1.36	ASTM	0	92	41	27	22	0.47	46	10	88	52	43	30	0.55	42
20	1.40	ASTM	0	83	49	21	18	0.77	63	10	79	59	48	32	0.67	46
19	2.15	ASTM	0	83	48	23	17	0.77	65	10	79	59	46	24	0.88	59
18	0.08	JET2	1	78	42	30	17	0.63	60	6	82	34	31	20	0.35	41
17	0.84	JET2	1	76	36	28	15	0.52	58	6	82	35	29	11	0.60	69
16	0.97	JET2	1	78	39	26	12	0.67	69	6	82	32	26	13	0.47	59
15	1.36	JET2	1	76	36	28	14	0.55	61	6	82	34	26	13	0.52	62
14	1.40	JET2	1	92	41	26	14	0.67	66	6	90	40	30	17	0.57	58
13	2.15	JET2	1	92	39	28	14	0.63	64	6	90	38	30	17	0.52	55
	0.08	JET2								9	82	48	37	27	0.52	44
	0.84	JET2								9	74	41	31	20	0.52	51
	0.97	JET2								9	82	42	35	19	0.57	55
	1.36	JET2								9	74	38	33	20	0.45	47
	1.40	JET2								9	80	44	29	16	0.70	64
	2.15	JET2								9	80	42	33	23	0.47	45
12	0.08	LARRT	1	84	45	37	28	0.42	38	6	77	49	41	28	0.52	43
11	0.84	LARRT	1	90	42	30	17	0.63	60	6	90	46	41	22	0.60	52
10	0.97	LARRT	1	84	39	29	16	0.57	59	6	77	41	34	22	0.47	46
9	1.36	LARRT	1	90	42	31	18	0.60	57	6	90	41	36	23	0.45	44
8	1.40	LARRT	1	85	42	30	15	0.67	64	6	90	44	37	16	0.70	64
7	2.15	LARRT	1	85	42	32	16	0.65	62	6	90	42	36	23	0.47	45
6	0.08	GODWO	1	86	40	28	15	0.63	63	9	86	48	38	32	0.40	33
5	0.84	GODWO	1	84	33	17	12	0.52	64	9	89	37	33	17	0.50	54
4	0.97	GODWO	1	86	36	17	13	0.57	64	9	86	43	34	20	0.57	53
	1.36	GODWO	1	84	33	17	13	0.50	61	9	89	37	30	19	0.45	49
	1.40	GODWO	1	100	39	16	14	0.63	64	9	95	40	37	17	0.57	58
	2.15	GODWO	1	100	36	20	16	0.50	56	9	95	39	30	18	0.52	54

TABLE 3-8

SKID TRAILER DATA UNDER SIMULATED RAIN, TEXAS A&M RESEARCH ANNEX
PAD NO. 4, TEXTURE DEPTH = 0.031 INCHES, 32 PSI, CRUSHED SILICEOUS GRAVEL HOT MIX

	WD MM	TEST TIRE	TD /32 IN.	AIR TEMP F	SN 20	SN 40	SN 60	GRAD	PCT GRAD	TD /32 IN.	AIR TEMP F	SN 20	SN 40	SN 60	GRAD	PCT GRAD
	0.08	ASTM	0	86	50	34	23	0.67	54	10	90	64	55	46	0.45	28
	0.84	ASTM	0	92	43	29	21	0.55	51	10	88	57	44	33	0.60	42
	0.97	ASTM	0	86	44	29	18	0.65	59	10	90	57	49	35	0.55	39
	1.36	ASTM	0	92	46	32	22	0.60	52	10	88	54	42	29	0.63	46
	1.40	ASTM	0	83	49	25	16	0.82	67	10	79	56	48	30	0.65	46
	2.15	ASTM	0	83	46	27	17	0.72	63	10	79	58	46	26	0.80	55
	0.08	JET2	1	78	42	31	20	0.55	52	6	82	41	34	23	0.45	44
	0.84	JET2	1	76	37	33	15	0.55	59	6	82	34	30	14	0.50	59
	0.97	JET2	1	78	37	31	15	0.55	59	6	82	38	30	15	0.57	61
	1.36	JET2	1	76	35	29	13	0.55	63	6	82	32	28	10	0.55	69
	1.40	JET2	1	92	41	32	15	0.65	63	6	90	42	35	17	0.63	60
	2.15	JET2	1	92	37	30	14	0.57	62	6	90	39	34	22	0.42	44
	0.08	JET2								9	82	43	34	24	0.47	44
	0.84	JET2								9	74	44	36	19	0.63	57
	0.97	JET2								9	82	39	32	16	0.57	59
	1.36	JET2								9	74	41	33	17	0.60	59
	1.40	JET2								9	80	46	36	16	0.75	65
	2.15	JET2								9	80	41	33	22	0.47	46
12	0.08	LARRT	1	84	48	39	28	0.50	42	6	77	49	42	31	0.45	37
11	0.84	LARRT	1	90	45	36	21	0.60	53	6	90	45	43	20	0.63	56
10	0.97	LARRT	1	84	42	34	17	0.63	60	6	77	41	36	27	0.35	34
9	1.36	LARRT	1	90	41	36	21	0.50	49	6	90	45	35	25	0.50	44
8	1.40	LARRT	1	85	45	36	14	0.77	69	6	90	48	41	20	0.70	58
7	2.15	LARRT	1	85	37	36	14	0.57	62	6	90	42	36	25	0.42	40
6	0.08	GODWO	1	86	40	26	15	0.63	63	9	86	46	42	32	0.35	30
5	0.84	GODWO	1	84	33	18	11	0.55	67	9	89	40	34	17	0.57	58
4	0.97	GODWO	1	86	41	20	12	0.72	71	9	86	43	32	28	0.38	35
	1.36	GODWO	1	84	32	17	12	0.50	63	9	89	36	31	21	0.38	42
	1.40	GODWO	1	100	38	18	11	0.67	71	9	95	43	33	19	0.60	56
	2.15	GODWO	1	100	41	21	13	0.70	68	9	95	40	24	18	0.55	55

TABLE 3-9

SKID TRAILER DATA UNDER SIMULATED RAIN, TEXAS A&M RESEARCH ANNEX
PAD NO. 5, TEXTURE DEPTH = 0.026 INCHES, 24 PSI, ROUNDED SILICEOUS GRAVEL HOT MIX

WD MM	TEST TIRE	TD /32 IN.	AIR TEMP F	SN 20	SN 40	SN 60	GRAD	PCT GRAD	TD /32 IN.	AIR TEMP F	SN 20	SN 40	SN 60	GRAD	PCT GRAD
0.25	ASTM	0	76	34	26	17	0.42	50	10	78	43	38	29	0.35	33
0.88	ASTM	0	76	34	24	14	0.50	59	10	78	47	37	22	0.63	53
1.11	ASTM	0	75	33	22	15	0.45	55	10	79	46	39	21	0.63	54
1.70	ASTM	0	75	42	24	14	0.70	67	10	79	58	37	18	1.00	69
1.85	ASTM	0	84	40	19	12	0.70	70	10	85	54	42	15	0.97	72
3.61	ASTM	0	84	36	18	14	0.55	61	10	85	42	35	16	0.65	62
0.25	JET2	0	82	32	24	13	0.47	59	3	84	34	29	15	0.47	56
0.88	JET2	0	82	32	23	12	0.50	63	3	84	31	26	13	0.45	58
1.11	JET2	0	84	27	21	12	0.38	56	3	77	31	26	13	0.45	58
1.70	JET2	0	84	33	22	9	0.60	73	3	77	35	26	11	0.60	69
1.85	JET2	0	72	37	18	12	0.63	68	3	74	34	25	10	0.60	71
3.61	JET2	0	72	31	20	14	0.42	55	3	74	30	24	12	0.45	60
0.25	JET2								7	82	37	29	21	0.40	43
0.88	JET2								7	82	34	30	18	0.40	47
1.11	JET2								7	82	32	25	16	0.40	50
1.70	JET2								7	82	39	30	12	0.67	69
3.61	JET2								7	72	32	25	14	0.45	56
0.25	LARRT	1	80	34	28	16	0.45	53	4	80	40	32	22	0.45	45
0.88	LARRT	1	80	34	25	14	0.50	59	4	80	38	32	16	0.55	58
1.11	LARRT	1	75	32	21	12	0.50	63	4	73	35	29	17	0.45	51
1.70	LARRT	1	75	36	25	10	0.65	72	4	73	43	34	14	0.72	67
1.85	LARRT	1	73	33	21	11	0.55	67	4	74	40	29	11	0.72	73
3.61	LARRT	1	73	32	20	12	0.50	63	4	74	32	26	14	0.45	56
0.25	GODWO	0	79	32	19	14	0.45	56	6	72	40	33	20	0.50	50
0.88	GODWO	0	79	33	19	14	0.47	58	6	72	39	33	18	0.52	54
1.11	GODWO	0	69	32	19	13	0.47	59	6	77	34	29	16	0.45	53
1.70	GODWO	0	69	37	18	12	0.63	68	6	77	40	30	13	0.67	68
1.85	GODWO	0	60	33	14	10	0.57	70	6	64	38	28	11	0.67	71
3.61	GODWO	0	60	29	14	14	0.38	52	6	64	33	26	17	0.40	48

TABLE 3-10

SKID TRAILER DATA UNDER SIMULATED RAIN, TEXAS A&M RESEARCH ANNEX
PAD NO. 5, TEXTURE DEPTH = 0.026 INCHES, 32 PSI, ROUNDED SILICEOUS GRAVEL HOT MIX

WD MM	TEST TIRE	TD /32 IN.	AIR TEMP F	SN 20	SN 40	SN 60	GRAD	PCT GRAD	TD /32 IN.	AIR TEMP F	SN 20	SN 40	SN 60	GRAD	PCT GRAD
0.25	ASTM	0	76	35	26	17	0.45	51	10	78	46	39	31	0.38	33
0.88	ASTM	0	76	35	26	14	0.52	60	10	78	47	40	28	0.47	40
1.11	ASTM	0	75	35	24	15	0.50	57	10	79	48	38	22	0.65	54
1.70	ASTM	0	75	43	27	14	0.72	67	10	79	57	39	24	0.82	58
1.85	ASTM	0	84	40	26	13	0.67	68	10	85	55	43	18	0.92	67
3.61	ASTM	0	84	36	23	14	0.55	61	10	85	46	36	20	0.65	57
0.25	JET2	0	82	34	27	15	0.47	56	3	84	34	30	17	0.42	50
0.88	JET2	0	82	31	25	13	0.45	58	3	84	37	28	16	0.52	57
1.11	JET2	0	84	29	23	12	0.42	59	3	77	34	21	14	0.50	59
1.70	JET2	0	84	34	26	10	0.60	71	3	77	39	28	11	0.70	72
1.85	JET2	0	72	34	23	10	0.60	71	3	74	35	30	10	0.63	71
3.61	JET2	0	72	33	26	12	0.52	64	3	74	33	29	12	0.52	64
0.25	JET2								7	82	37	31	21	0.40	43
0.88	JET2								7	82	37	30	19	0.45	49
1.11	JET2								7	82	34	29	16	0.45	53
1.70	JET2								7	82	39	32	13	0.65	67
3.61	JET2								7	72	34	29	15	0.47	56
0.25	LARRT	1	80	36	30	17	0.47	53	4	80	40	31	21	0.47	48
0.88	LARRT	1	80	36	27	15	0.52	58	4	80	38	34	20	0.45	47
1.11	LARRT	1	75	35	25	13	0.55	63	4	73	37	32	17	0.50	54
1.70	LARRT	1	75	42	27	11	0.77	74	4	73	47	37	14	0.82	70
1.85	LARRT	1	73	36	28	10	0.65	72	4	74	42	38	11	0.77	74
3.61	LARRT	1	73	31	29	12	0.47	61	4	74	35	32	16	0.47	54
0.25	GODWO	0	79	34	19	14	0.50	59	6	72	40	30	22	0.45	45
0.88	GODWO	0	79	33	21	13	0.50	61	6	72	42	32	21	0.52	50
1.11	GODWO	0	69	30	20	13	0.42	57	6	77	30	28	18	0.30	40
1.70	GODWO	0	69	39	21	10	0.72	74	6	77	43	31	14	0.72	67
1.85	GODWO	0	60	33	18	10	0.57	70	6	64	38	30	14	0.60	63
3.61	GODWO	0	60	29	19	14	0.38	52	6	64	35	27	16	0.47	54

TABLE 3-11

SKID TRAILER DATA UNDER SIMULATED RAIN, TEXAS A&M RESEARCH ANNEX
PAD NO. 6, TEXTURE DEPTH = 0.159 INCHES, 24 PSI, ROUNDED GRAVEL CHIP SEAL

WD MM	TEST TIRE	TD /32 IN.	AIR TEMP F	SN 20	SN 40	SN 60	GRAD	PCT GRAD	TD /32 IN.	AIR TEMP F	SN 20	SN 40	SN 60	GRAD	PCT GRAD
-2.21	ASTM	0	62	45	43	36	0.22	20	8	56	51	45	41	0.25	20
-1.20	ASTM	0	74	46	40	30	0.40	35	10	67	54	45	35	0.47	35
-0.66	ASTM	0	62	46	39	27	0.47	41	8	56	53	43	28	0.63	47
0.77	ASTM	0	74	43	38	22	0.52	49	10	67	54	44	27	0.67	50
-2.21	JET2								3	75	39	34	25	0.35	36
-1.20	JET2	0	73	42	40	30	0.30	29	2	50	41	36	29	0.30	29
-0.66	JET2								3	75	43	34	25	0.45	42
0.77	JET2	0	73	42	37	21	0.52	50	2	50	42	35	20	0.55	52
-2.21	JET2								7	74	44	37	31	0.32	30
-1.20	JET2								7	58	43	39	30	0.32	30
-0.66	JET2								7	74	48	37	25	0.57	48
0.77	JET2								7	58	46	38	23	0.57	50
-2.21	LARRT	1	75	40	36	29	0.27	28	3	75	43	38	29	0.35	33
-1.20	LARRT	1	75	42	38	33	0.22	21	3	76	43	39	31	0.30	28
-0.66	LARRT	1	75	46	39	23	0.57	50	3	75	46	40	25	0.52	46
0.77	LARRT	1	75	42	36	19	0.57	55	3	76	45	38	21	0.60	53
-2.21	GODWO	0	72	42	34	31	0.27	26	5	70	47	38	31	0.40	34
-1.20	GODWO	0	76	41	33	26	0.38	37	6	76	44	37	33	0.27	25
-0.66	GODWO	0	72	42	31	22	0.50	48	5	70	45	35	24	0.52	47
0.77	GODWO	0	76	39	29	17	0.55	56	6	76	44	34	19	0.63	57

TABLE 3-12

SKID TRAILER DATA UNDER SIMULATED RAIN, TEXAS A&M RESEARCH ANNEX
PAD NO. 6, TEXTURE DEPTH = 0.159 INCHES, 32 PSI, ROUNDED GRAVEL CHIP SEAL

WD MM	TEST TIRE	TD /32 IN.	AIR TEMP F	SN 20	SN 40	SN 60	GRAD	PCT GRAD	TD /32 IN.	AIR TEMP F	SN 20	SN 40	SN 60	GRAD	PCT GRAD
-2.21	ASTM	0	62	47	44	35	0.30	26	8	56	54	45	39	0.38	28
-1.20	ASTM	0	74	48	42	33	0.38	31	10	67	55	46	36	0.47	35
-0.66	ASTM	0	62	48	41	28	0.50	42	8	56	50	43	30	0.50	40
0.77	ASTM	0	74	48	43	26	0.55	46	10	67	56	45	29	0.67	48
-2.21	JET2								3	75	41	37	28	0.32	32
-1.20	JET2	0	73	45	40	33	0.30	27	2	50	41	37	30	0.27	27
-0.66	JET2								3	75	44	38	25	0.47	43
0.77	JET2	0	73	42	38	26	0.40	38	2	50	40	36	24	0.40	40
-2.21	JET2								7	74	46	39	33	0.32	28
-1.20	JET2								7	58	44	38	31	0.32	30
-0.66	JET2								7	74	48	38	29	0.47	40
0.77	JET2								7	58	42	37	26	0.40	38
-2.21	LARRT	1	75	42	37	32	0.25	24	3	75	44	38	32	0.30	27
-1.20	LARRT	1	75	41	38	33	0.20	20	3	76	42	40	31	0.27	26
-0.66	LARRT	1	75	42	41	27	0.38	36	3	75	46	40	29	0.42	37
0.77	LARRT	1	75	42	39	24	0.45	43	3	76	44	38	24	0.50	45
-2.21	GODWO	0	72	38	33	24	0.35	37	5	70	48	41	35	0.32	27
-1.20	GODWO	0	76	38	32	26	0.30	32	6	76	43	39	33	0.25	23
-0.66	GODWO	0	72	41	32	18	0.57	56	5	70	44	37	27	0.42	39
0.77	GODWO	0	76	39	30	16	0.57	59	6	76	42	36	20	0.55	52

TABLE 3-13

SKID TRAILER DATA UNDER SIMULATED RAIN, TEXAS A&M RESEARCH ANNEX
PAD NO. 7, TEXTURE DEPTH = 0.136 INCHES, 24 PSI, LIGHTWEIGHT AGGREGATE CHIP SEAL

WD MM	TEST TIRE	TD /32 IN.	AIR TEMP F	SN 20	SN 40	SN 60	GRAD	PCT GRAD	TD /32 IN.	AIR TEMP F	SN 20	SN 40	SN 60	GRAD	PCT GRAD
-0.50	ASTM	0	66	75	61	41	0.85	45	8	56	78	67	46	0.80	41
0.30	ASTM	0	66	74	50	25	1.22	66	8	56	76	58	33	1.07	57
1.40	ASTM	0	73	77	44	27	1.25	65	10	74	84	59	27	1.42	68
1.80	ASTM	0	73	74	52	29	1.13	61	10	74	81	60	39	1.05	52
-0.50	JET2								5	60	70	58	36	0.85	49
0.30	JET2								5	60	73	54	24	1.22	67
1.40	JET2	2	76	73	48	22	1.27	70	6	76	74	48	22	1.30	70
1.80	JET2	2	76	71	45	21	1.25	70	6	76	74	50	24	1.25	68
1.40	LARRT								3	77	76	54	23	1.32	70
1.80	LARRT								3	77	73	55	24	1.22	67
-0.50	GODWO								4	66	69	62	47	0.55	32
0.30	GODWO								4	66	68	45	22	1.15	68
1.80	GODWO								5	74	69	44	23	1.15	67

TABLE 3-14

SKID TRAILER DATA UNDER SIMULATED RAIN, TEXAS A&M RESEARCH ANNEX
PAD NO. 7, TEXTURE DEPTH = 0.136 INCHES, 32 PSI, LIGHTWEIGHT AGGREGATE CHIP SEAL

WD MM	TEST TIRE	TD /32 IN.	AIR TEMP F	SN 20	SN 40	SN 60	GRAD	PCT GRAD	TD /32 IN.	AIR TEMP F	SN 20	SN 40	SN 60	GRAD	PCT GRAD
-0.50	ASTM	0	66	74	64	39	0.88	47	8	56	76	67	49	0.67	36
0.30	ASTM	0	66	76	61	28	1.20	63	8	56	77	62	33	1.10	57
1.40	ASTM	0	73	76	47	23	1.32	70	10	74	79	60	34	1.13	57
1.80	ASTM	0	73	71	45	30	1.02	58	10	74	81	66	44	0.92	46
-0.50	JET2								5	60	72	59	39	0.82	46
0.30	JET2								5	60	72	59	27	1.13	63
1.40	JET2	2	76	71	54	23	1.20	68	6	76	76	50	29	1.17	62
1.80	JET2	2	76	69	54	27	1.05	61	6	76	75	54	29	1.15	61
1.40	LARRT								3	77	73	53	25	1.20	66
1.80	LARRT								3	77	72	58	24	1.20	67
-0.50	GODWO								4	66	67	60	50	0.42	25
0.30	GODWO								4	66	70	51	27	1.07	61
1.40	GODWO								5	74	72	47	24	1.20	67
1.80	GODWO								5	74	70	48	25	1.13	64

TABLE 3-15

SKID TRAILER DATA UNDER SIMULATED RAIN, TEXAS A&M RESEARCH ANNEX
PAD NO. 8, TEXTURE DEPTH = 0.032 INCHES, 24 PSI, LIGHTWEIGHT AGGREGATE HOT MIX

WD MM	TEST TIRE	TD /32 IN.	AIR TEMP F	SN 20	SN 40	SN 60	GRAD	PCT GRAD	TD /32 IN.	AIR TEMP F	SN 20	SN 40	SN 60	GRAD	PCT GRAD
0.41	ASTM	0	92	51	22	19	0.80	63	10	90	60	46	24	0.90	60
0.90	ASTM	0	92	50	25	20	0.75	60	10	90	59	45	25	0.85	58
1.32	ASTM	0	74	56	25	16	1.00	71	10	73	72	55	37	0.88	49
1.70	ASTM	0	74	51	21	17	0.85	67	10	73	72	50	16	1.40	78
2.55	ASTM	0	72	45	21	16	0.72	64	10	90	69	54	16	1.32	77
2.99	ASTM	0	72	44	18	15	0.72	66	10	90	68	55	25	1.07	63
0.41	JET2	1	83	50	34	20	0.75	60							
0.67	JET2	1	77	54	37	21	0.82	61							
0.83	JET2	1	77	54	42	15	0.97	72							
0.90	JET2	1	83	53	26	14	0.97	74							
2.55	JET2	1	74	51	17	9	1.05	82							
2.99	JET2	1	74	49	16	12	0.92	76							
0.41	JET2	6	90	48	37	19	0.72	60	10	89	52	40	23	0.72	56
0.90	JET2	6	90	56	39	13	1.07	77	10	89	56	40	19	0.92	66
1.32	JET2	6	73	53	24	14	0.97	74	10	76	60	38	24	0.90	60
1.70	JET2	6	73	51	27	11	1.00	78	10	76	54	36	16	0.95	70
2.55	JET2	6	74	53	31	11	1.05	79	10	77	59	35	14	1.13	76
2.99	JET2	6	74	52	30	14	0.95	73	10	77	56	31	15	1.02	73
0.41	LARRT	2	85	52	38	21	0.77	60	7	94	59	45	32	0.67	46
0.67	LARRT	2	73	56	44	18	0.95	68	7	72	61	48	28	0.82	54
0.83	LARRT	2	73	53	38	13	1.00	75	7	72	57	44	20	0.92	65
0.90	LARRT	2	85	55	39	9	1.15	84	7	94	61	48	25	0.90	59
2.55	LARRT	2	92	55	44	11	1.10	80	7	90	60	43	13	1.17	78
2.99	LARRT	2	92	53	32	14	0.97	74	7	90	56	46	22	0.85	61
0.41	GODWO	2	92	42	17	12	0.75	71	9	92	58	44	31	0.67	47
0.67	GODWO	2	87	50	19	16	0.85	68							
0.83	GODWO	2	87	43	16	12	0.77	72							
0.90	GODWO	2	92	44	18	13	0.77	70	9	92	57	46	30	0.67	47
2.55	GODWO	2	90	52	18	13	0.97	75	9	84	57	41	18	0.97	68
2.99	GODWO	2	90	48	18	16	0.80	67	9	84	54	43	20	0.85	63

TABLE 3-16

SKID TRAILER DATA UNDER SIMULATED RAIN, TEXAS A&M RESEARCH ANNEX
PAD NO. 8, TEXTURE DEPTH = 0.032 INCHES, 32 PSI, LIGHTWEIGHT AGGREGATE HOT MIX

WD MM	TEST TIRE	TD /32 IN.	AIR TEMP F	SN 20	SN 40	SN 60	GRAD	PCT GRAD	TD /32 IN.	AIR TEMP F	SN 20	SN 40	SN 60	GRAD	PCT GRAD
0.41	ASTM								10	90	62	50	33	0.72	47
0.90	ASTM	0	92	48	24	17	0.77	65	10	90	61	48	36	0.63	41
1.32	ASTM	0	74	56	26	16	1.00	71	10	73	68	54	38	0.75	44
1.70	ASTM	0	74	47	20	12	0.88	74	10	73	66	49	25	1.02	62
2.55	ASTM	0	72	45	21	11	0.85	76	10	90	66	50	29	0.92	56
2.99	ASTM	0	72	51	18	11	1.00	78	10	90	65	47	37	0.70	43
0.41	JET2	1	83	49	36	20	0.72	59							
0.67	JET2	1	77	59	42	18	1.02	69							
0.83	JET2	1	77	55	32	14	1.02	75							
0.90	JET2	1	83	50	28	16	0.85	68							
2.55	JET2	1	74	53	27	11	1.05	79							
2.99	JET2	1	74	51	32	14	0.92	73							
0.41	JET2	6	90	55	40	28	0.67	49	10	89	52	43	31	0.52	40
0.90	JET2	6	90	51	39	20	0.77	61	10	89	54	40	25	0.72	54
1.32	JET2	6	73	53	37	16	0.92	70	10	76	60	44	24	0.90	60
1.70	JET2	6	73	54	30	11	1.07	80	10	76	54	41	17	0.92	69
2.55	JET2	6	74	52	37	16	1.15	88	10	77	58	40	15	1.07	74
2.99	JET2	6	74	51	34	13	0.95	75	10	77	57	39	23	0.85	60
0.41	LARRT	2	85	55	47	32	0.57	42	7	94	59	46	39	0.50	34
0.67	LARRT	2	73	59	46	21	0.95	64	7	72	63	50	31	0.80	51
0.83	LARRT	2	73	58	44	13	1.13	78	7	72	57	46	21	0.90	63
0.90	LARRT	2	85	56	46	19	0.92	66	7	94	56	46	28	0.70	50
2.55	LARRT	2	92	57	37	11	1.15	81	7	90	56	49	15	1.02	73
2.99	LARRT	2	92	54	37	15	0.97	72	7	90	57	46	26	0.77	54
0.41	GODWO	2	92	50	16	11	0.97	78	9	92	54	48	42	0.30	22
0.67	GODWO	2	87	49	21	13	0.90	73							
0.83	GODWO	2	87	40	16	9	0.77	78							
0.90	GODWO	2	92	41	17	11	0.75	73	9	92	55	47	33	0.55	40
2.55	GODWO	2	90	40	16	11	0.72	73	9	84	55	42	21	0.85	62
2.99	GODWO	2	90	41	20	14	0.67	66	9	84	55	40	23	0.80	58

TABLE 3-17

SKID TRAILER DATA UNDER SIMULATED RAIN, TEXAS A&M RESEARCH ANNEX
PAD NO. 9, TEXTURE DEPTH = 0.033 INCHES, 24 PSI, PAINTED PORTLAND CEMENT CONCRETE

WD MM	TEST TIRE	TD /32 IN.	AIR TEMP F	SN 20	SN 40	SN 60	GRAD	PCT GRAD	TD /32 IN.	AIR TEMP F	SN 20	SN 40	SN 60	GRAD	PCT GRAD
0.58	ASTM	0	81	31	17	11	0.50	65	10	80	49	36	22	0.67	55
0.75	ASTM	0	80	29	15	9	0.50	69	10	74	42	31	16	0.65	62
1.00	ASTM	0	81	30	15	9	0.52	70	10	80	48	37	21	0.67	56
1.20	ASTM	0	80	30	15	7	0.57	77	10	74	44	30	15	0.72	66
2.20	ASTM	0	66	35	16	10	0.63	71	10	70	48	33	17	0.77	65
2.22	ASTM	0	66	38	18	9	0.72	76	10	70	45	33	14	0.77	69
0.58	JET2	2	89	38	18	11	0.67	71	5	84	40	26	13	0.67	68
0.75	JET2	2	80	34	14	8	0.65	76	5	78	39	22	10	0.72	74
1.00	JET2	2	89	36	17	9	0.67	75	5	84	41	28	9	0.80	78
1.20	JET2	2	80	38	14	8	0.75	79	5	78	44	31	10	0.85	77
2.20	JET2	2	63	41	16	9	0.80	78	5	70	41	28	10	0.77	76
2.22	JET2	2	63	41	15	8	0.82	80	5	70	49	28	10	0.97	80
0.58	JET2								9	88	37	27	14	0.57	62
0.75	JET2								9	78	38	25	12	0.65	68
1.00	JET2								9	88	37	28	11	0.65	70
1.20	JET2								9	78	40	26	10	0.75	75
2.20	JET2								9	63	44	30	11	0.82	75
2.22	JET2								9	63	50	30	9	1.02	82
0.58	LARRT	2	77	42	23	10	0.80	76	6	76	44	32	21	0.57	52
0.75	LARRT	2	80	37	22	10	0.67	73	6	80	36	27	12	0.60	67
1.00	LARRT	2	77	40	21	10	0.75	75	6	76	46	33	15	0.77	67
1.20	LARRT	2	80	41	20	8	0.82	80	6	80	40	30	9	0.77	78
2.20	LARRT	2	70	43	18	9	0.85	79	6	67	43	33	12	0.77	72
2.22	LARRT	2	70	42	21	9	0.82	79	6	67	49	32	11	0.95	78
0.58	GODWO	1	88	29	13	10	0.47	66	7	87	42	32	23	0.47	45
0.75	GODWO	1	76	28	12	9	0.47	68	7	76	40	29	14	0.65	65
1.00	GODWO	1	88	34	12	8	0.65	76	7	87	39	28	17	0.55	56
1.20	GODWO	1	76	33	12	9	0.60	73	7	76	42	30	11	0.77	74
2.20	GODWO	1	72	29	12	11	0.45	62	7	68	40	28	12	0.70	70
2.22	GODWO	1	72	33	12	7	0.65	79	7	68	45	30	12	0.82	73

TABLE 3-18

SKID TRAILER DATA UNDER SIMULATED RAIN, TEXAS A&M RESEARCH ANNEX
PAD NO. 9, TEXTURE DEPTH = 0.033 INCHES, 32 PSI, PAINTED PORTLAND CEMENT CONCRETE

WD MM	TEST TIRE	TD /32 IN.	AIR TEMP F	SN 20	SN 40	SN 60	GRAD	PCT GRAD	TD /32 IN.	AIR TEMP F	SN 20	SN 40	SN 60	GRAD	PCT GRAD
0.58	ASTM	0	81	34	17	11	0.57	68	10	80	51	37	28	0.57	45
0.75	ASTM	0	80	32	16	10	0.55	69	10	74	45	30	18	0.67	60
1.00	ASTM	0	81	34	17	10	0.60	71	10	80	48	33	25	0.57	48
1.20	ASTM	0	80	31	15	10	0.52	68	10	74	47	34	16	0.77	66
2.20	ASTM	0	66	31	17	10	0.52	68	10	70	47	27	15	0.80	68
2.22	ASTM	0	66	35	17	11	0.60	69	10	70	41	29	13	0.70	68
0.58	JET2	2	89	37	21	12	0.63	68	5	84	41	28	13	0.70	68
0.75	JET2	2	80	35	20	7	0.70	80	5	78	39	24	12	0.67	69
1.00	JET2	2	89	32	20	11	0.52	66	5	84	41	29	11	0.75	73
1.20	JET2	2	80	36	20	8	0.70	78	5	78	39	28	11	0.70	72
2.20	JET2	2	63	43	22	9	0.85	79	5	70	42	29	10	0.80	76
2.22	JET2	2	63	46	22	9	0.92	80	5	70	43	30	10	0.82	77
0.58	JET2								9	88	42	26	17	0.63	60
0.75	JET2								9	78	38	28	12	0.65	68
1.00	JET2								9	88	39	26	13	0.65	67
1.20	JET2								9	78	47	29	12	0.88	74
2.20	JET2								9	63	49	32	13	0.90	73
2.22	JET2								9	63	51	31	13	0.95	75
0.58	LARRT	2	77	42	23	13	0.72	69	6	76	45	31	25	0.50	44
0.75	LARRT	2	80	37	26	10	0.67	73	6	80	39	27	14	0.63	64
1.00	LARRT	2	77	43	27	11	0.80	74	6	76	49	35	21	0.70	57
1.20	LARRT	2	80	39	27	9	0.75	77	6	80	38	28	12	0.65	68
2.20	LARRT	2	70	40	28	8	0.80	80	6	67	44	35	11	0.82	75
2.22	LARRT	2	70	40	30	8	0.80	80	6	67	46	32	11	0.88	76
0.58	GODWO	1	88	29	16	11	0.45	62	7	87	41	29	27	0.35	34
0.75	GODWO	1	76	35	12	9	0.65	74	7	76	37	24	18	0.47	51
1.00	GODWO	1	88	29	18	10	0.47	66	7	87	41	29	21	0.50	49
1.20	GODWO	1	76	29	13	8	0.52	72	7	76	50	25	14	0.90	72
2.20	GODWO	1	72	33	13	9	0.60	73	7	68	44	27	16	0.70	64
2.22	GODWO	1	72	36	13	7	0.72	81	7	68	44	25	14	0.75	68

TABLE 3-19

SKID TRAILER DATA UNDER SIMULATED RAIN
STATE HWY. 6 EAST BYPASS BRYAN-COLLEGE STATION
TEST SECTION F1, PORTLAND CEMENT CONCRETE
TRANSVERSE BROOM FINISH, TEXTURE DEPTH = 0.064 INCHES
0.043

WD MM	TEST TIRE	TD /32 IN.	AIR TEMP F	SN 20	SN 40	SN 60	GRAD	PCT GRAD	TD /32 IN.	AIR TEMP F	SN 20	SN 40	SN 60	GRAD	PCT GRAD
TIRE PRESSURE = 24 PSI															
-0.50	ASTM14	0	79	64	40	28	0.90	56	11	89	69	56	41	0.70	41
0.10	ASTM14	0	79	67	36	23	1.10	66	11	89	75	54	37	0.95	51
0.62	ASTM14	0	96	57	39	24	0.82	58	11	92	67	51	33	0.85	51
1.28	ASTM14	0	96	58	28	16	1.05	72	11	92	74	55	25	1.22	66
-0.50	ASTM15								9	92	61	46	40	0.52	34
0.10	ASTM15								9	92	60	44	29	0.77	52
0.62	ASTM15								9	90	64	40	22	1.05	66
1.28	ASTM15								9	90	70	44	18	1.30	74
TIRE PRESSURE = 32 PSI															
-0.50	ASTM14	0	81	65	42	27	0.95	58	11	89	73	56	42	0.77	42
0.10	ASTM14	0	81	73	37	23	1.25	68	11	89	78	56	37	1.02	53
0.62	ASTM14	0	94	49	37	23	0.65	53	11	92	71	52	32	0.97	55
1.28	ASTM14	0	94	63	29	16	1.17	75	11	92	77	56	29	1.20	62
-0.50	ASTM15								9	93	62	46	36	0.65	42
0.10	ASTM15								9	93	62	45	30	0.80	52
0.62	ASTM15								9	102	62	44	27	0.88	56
1.28	ASTM15								9	102	69	48	22	1.17	68

TABLE 3-20

SKID TRAILER DATA UNDER SIMULATED RAIN
STATE HWY. 6 EAST BYPASS BRYAN-COLLEGE STATION
TEST SECTION F2, PORTLAND CEMENT CONCRETE
TRANSVERSE TINES FINISH, TEXTURE DEPTH = 0.070 INCHES
0.064

WD MM	TEST TIRE	TD /32 IN.	AIR TEMP F	SN 20	SN 40	SN 60	GRAD	PCT GRAD	TD /32 IN.	AIR TEMP F	SN 20	SN 40	SN 60	GRAD	PCT GRAD
TIRE PRESSURE = 24 PSI															
-1.50	ASTM14	0	80	72	48			50	8	75	77	59	45	0.80	42
-0.90	ASTM14	0	75	77	47	32	1.13	58	8	84	82	62	47	0.88	43
0.00	ASTM14	0	80	72	56	43	0.72	40	8	75	74	62	49	0.63	34
0.60	ASTM14	0	75	84	47	28	1.40	67	8	84	84	59	34	1.25	60
-1.50	ASTM15								11	75	71	57	44	0.67	38
-0.90	ASTM15								11	85	70	60	53	0.42	24
0.00	ASTM15								11	75	69	61	51	0.45	26
0.60	ASTM15								11	85	74	52	31	1.07	58
TIRE PRESSURE = 32 PSI															
-1.50	ASTM14	0	77	72	57	40	0.80	44	8	77	77	62	49	0.70	36
-0.90	ASTM14	0	80	83	56	34	1.22	59	8	75	79	61	50	0.72	37
0.00	ASTM14	0	80	70	52	42	0.70	40	8	75	72	61	52	0.50	28
0.60	ASTM14	0	77	88	51	27	1.52	69	8	77	81	63	43	0.95	47
-1.50	ASTM15								11	74	72	61	46	0.65	36
-0.90	ASTM15								11	78	70	60	50	0.50	29
0.00	ASTM15								11	78	73	60	53	0.50	27
0.60	ASTM15								11	74	78	58	32	1.15	59

TABLE 3-21

SKID TRAILER DATA UNDER SIMULATED RAIN
STATE HWY. 6 EAST BYPASS BRYAN-COLLEGE STATION
TEST SECTION F3, PORTLAND CEMENT CONCRETE
LONGITUDINAL BROOM FINISH, TEXTURE DEPTH = 0.046 INCHES
0.028

WD MM	TEST TIRE	TD /32 IN.	AIR TEMP F	SN 20	SN 40	SN 60	GRAD	PCT GRAD	TD /32 IN.	AIR TEMP F	SN 20	SN 40	SN 60	GRAD	PCT GRAD
TIRE PRESSURE = 24 PSI															
-0.20	ASTM14	0	95	53	32	19	0.85	64	11	94	71	49	33	0.95	54
0.50	ASTM14	0	73	61	29	22	0.97	64	11	77	75	53	28	1.17	63
0.80	ASTM14	0	95	54	29	19	0.88	65	11	94	71	51	33	0.95	54
1.20	ASTM14	0	89	55	26	19	0.90	65	11	87	75	53	36	0.97	52
1.30	ASTM14	0	73	66	28	21	1.13	68	11	77	74	51	27	1.17	64
1.55	ASTM14	0	89	58	25	19	0.97	67	11	87	75	62	29	1.15	61
-0.20	ASTM15								12	95	69	49	26	1.07	62
0.50	ASTM15								12	87	66	40	28	0.95	58
0.80	ASTM15								12	95	70	49	23	1.17	67
1.20	ASTM15								12	83	75	50	26	1.22	65
1.30	ASTM15								12	87	66	43	22	1.10	67
1.55	ASTM15								12	83	73	48	24	1.22	67
TIRE PRESSURE = 32 PSI															
-0.20	ASTM14	0	95	58	31	22	0.90	62	11	94	66	52	33	0.82	50
0.50	ASTM14	0	73	65	32	21	1.10	68	11	77	73	54	32	1.02	56
0.80	ASTM14	0	95	50	28	19	0.77	62	11	94	70	51	33	0.92	53
1.20	ASTM14	0	89	60	26	18	1.05	70	11	80	75	57	42	0.80	43
1.30	ASTM14	0	73	67	30	18	1.22	73	11	77	78	53	34	1.10	56
1.55	ASTM14	0	89	56	26	15	1.02	73	11	80	79	62	31	1.20	61
-0.20	ASTM15								12	95	70	50	35	0.88	50
0.50	ASTM15								12	87	67	45	32	0.88	52
0.80	ASTM15								12	95	66	45	29	0.92	56
1.20	ASTM15								12	88	76	50	20	1.40	74
1.30	ASTM15								12	87	66	45	24	1.05	64
1.55	ASTM15								12	88	77	56	22	1.38	71

TABLE 3-22

SKID TRAILER DATA UNDER SIMULATED RAIN
STATE HWY. 6 EAST BYPASS BRYAN-COLLEGE STATION
TEST SECTION F4, PORTLAND CEMENT CONCRETE
LONGITUDINAL TINES FINISH, TEXTURE DEPTH = 0.094 INCHES
0.062

WD MM	TEST TIRE	TD /32 IN.	AIR TEMP F	SN 20	SN 40	SN 60	GRAD	PCT GRAD	TD /32 IN.	AIR TEMP F	SN 20	SN 40	SN 60	GRAD	PCT GRAD
TIRE PRESSURE = 24 PSI															
-0.65	ASTM14	0	78	75	50	29	1.15	61	11	83	80	61	35	1.13	56
0.20	ASTM14	0	78	76	47	23	1.32	70	11	83	84	67	28	1.40	67
0.70	ASTM14	0	86	69	35	20	1.22	71	11	77	75	64	28	1.17	63
1.50	ASTM14	0	86	74	30	18	1.40	76	11	77	75	63	24	1.27	68
-0.65	ASTM15								12	89	67	54	30	0.92	55
0.20	ASTM15								12	89	74	52	21	1.32	72
0.70	ASTM15								12	96	76	55	20	1.40	74
1.50	ASTM15								12	96	71	45	15	1.40	79
TIRE PRESSURE = 32 PSI															
-0.65	ASTM14	0	78	77	51	27	1.25	65	11	83	83	68	38	1.13	54
0.20	ASTM14	0	78	79	48	26	1.32	67	11	83	87	66	37	1.25	57
0.70	ASTM14	0	86	70	41	19	1.27	73	11	77	75	63	30	1.13	60
1.50	ASTM14	0	86	68	38	17	1.27	75	11	77	77	58	27	1.25	65
-0.65	ASTM15								12	89	68	55	33	0.88	51
0.20	ASTM15								12	89	76	53	27	1.22	64
0.70	ASTM15								12	96	69	58	26	1.07	62
1.50	ASTM15								12	96	76	54	20	1.40	74

TABLE 3-23

SKID TRAILER DATA UNDER SIMULATED RAIN
STATE HWY. 6 EAST BYPASS BRYAN-COLLEGE STATION
TEST SECTION E5, PORTLAND CEMENT CONCRETE
BURLAP AND LONGITUDINAL TINES FINISH, TEXTURE DEPTH = 0.086 INCHES
0.065

WD MM	TEST TIRE	TD /32 IN.	AIR TEMP F	SN 20	SN 40	SN 60	GRAD	PCT GRAD	TD /32 IN.	AIR TEMP F	SN 20	SN 40	SN 60	GRAD	PCT GRAD
TIRE PRESSURE = 24 PSI															
-0.86	ASTM14								11	84	67	59	42	0.63	37
-0.49	ASTM14								11	84	72	58	34	0.95	53
1.30	ASTM14								11	86	73	56	23	1.25	68
1.80	ASTM14								11	86	76	55	18	1.45	76
-0.35	ASTM14	0	102	69	40	23	1.15	67							
0.30	ASTM14	0	102	68	42	20	1.20	71							
1.30	ASTM14	0	79	72	46	20	1.30	72							
1.80	ASTM14	0	79	74	46	18	1.40	76							
-0.35	ASTM15								9	96	60	44	22	0.95	62
0.30	ASTM15								9	96	65	45	18	1.17	72
1.30	ASTM15								9	92	62	44	18	1.10	71
1.80	ASTM15								9	92	64	42	15	1.22	77
TIRE PRESSURE = 32 PSI															
-0.86	ASTM14								11	85	66	56	45	0.52	32
-0.49	ASTM14								11	85	77	56	40	0.92	48
1.30	ASTM14								11	85	75	64	31	1.10	59
1.80	ASTM14								11	85	84	62	29	1.38	65
-0.35	ASTM14	0	95	62	45	23	0.97	63							
0.30	ASTM14	0	95	66	44	21	1.13	68							
1.30	ASTM14	0	78	73	52	22	1.27	70							
1.80	ASTM14	0	78	73	52	22	1.40	72							
-0.35	ASTM15								9	96	63	45	26	0.92	59
0.30	ASTM15								9	96	63	49	24	0.97	62
1.30	ASTM15								9	88	63	45	25	0.95	60
1.80	ASTM15								9	88	67	50	23	1.10	66

TABLE 3-24

SKID TRAILER DATA UNDER SIMULATED RAIN
STATE HWY. 6 EAST BYPASS BRYAN-COLLEGE STATION
TEST SECTION E6, PORTLAND CEMENT CONCRETE
CONTROL SECTION BURLAP DRAG FINISH, TEXTURE DEPTH = 0.039 INCHES
0.032

WD MM	TEST TIRE	TD /32 IN.	AIR TEMP F	SN 20	SN 40	SN 60	GRAD	PCT GRAD	TD /32 IN.	AIR TEMP F	SN 20	SN 40	SN 60	GRAD	PCT GRAD
TIRE PRESSURE = 24 PSI															
-0.25	ASTM14	0	94	46	26	16	0.75	65	10	93	57	41	26	0.77	54
0.10	ASTM14	0	94	50	28	16	0.85	68	10	93	61	45	21	1.00	66
0.40	ASTM14	0	78	54	26	16	0.95	70	10	91	62	41	26	0.90	58
1.40	ASTM14	0	78	60	31	16	1.10	73	10	91	64	47	20	1.10	69
-0.25	ASTM15								12	95	55	47	25	0.75	55
0.10	ASTM15								12	95	59	39	18	1.02	69
0.40	ASTM15								12	94	56	41	20	0.90	64
1.40	ASTM15								12	94	61	41	12	1.22	80
TIRE PRESSURE = 32 PSI															
-0.25	ASTM14	0	94	48	26	16	0.80	67	10	93	50	40	27	0.57	46
0.10	ASTM14	0	94	55	29	16	0.97	71	10	93	61	46	25	0.90	59
0.40	ASTM14	0	75	56	31	12	1.10	79	10	89	59	41	26	0.82	56
1.40	ASTM14	0	75	69	38	13	1.40	81	10	89	66	48	21	1.13	68
-0.25	ASTM15								12	96	60	40	29	0.77	52
0.10	ASTM15								12	96	60	43	27	0.82	55
0.40	ASTM15								12	90	62	36	25	0.92	60
1.40	ASTM15								12	90	57	44	18	0.97	68

Table 3-25

SKID TRAILER DATA UNDER SIMULATED RAIN
STATE HWY. 6 EAST BYPASS BRYAN-COLLEGE STATION
TEST SECTION E7, PORTLAND CEMENT CONCRETE
TRANSVERSE BRUSH FINISH, TEXTURE DEPTH = 0.042 INCHES
0.033

WD MM	TEST TIRE	TD /32 IN.	AIR TEMP F	SN 20	SN 40	SN 60	GRAD	PCT GRAD	TD /32 IN.	AIR TEMP F	SN 20	SN 40	SN 60	GRAD	PCT GRAD
TIRE PRESSURE = 24 PSI															
0.00	ASTM14	0	78	64	35	25	0.97	61	10	75	83	63	43	1.00	48
0.50	ASTM14	0	89	56	30	25	0.77	55	10	92	78	55	38	1.00	51
0.80	ASTM14	0	78	66	32	22	1.07	65	10	75	85	65	36	1.22	58
1.26	ASTM14	0	89	49	29	23	0.65	53	10	92	70	56	26	1.10	63
0.00	ASTM15								12	78	68	53	36	0.80	47
0.50	ASTM15								12	89	67	50	27	1.00	60
0.80	ASTM15								12	78	75	54	25	1.25	67
1.26	ASTM15								12	89	72	43	21	1.27	71
TIRE PRESSURE = 32 PSI															
0.00	ASTM14	0	78	67	35	25	1.05	63	10	75	90	68	43	1.17	52
0.50	ASTM14	0	92	61	33	22	0.97	64	10	92	71	61	33	0.95	54
0.80	ASTM14	0	78	73	33	22	1.27	70	10	75	94	68	35	1.47	63
1.26	ASTM14	0	92	57	29	18	0.97	68	10	92	73	57	29	1.10	60
0.00	ASTM15								12	78	71	54	38	0.82	46
0.50	ASTM15								12	89	68	51	41	0.67	40
0.80	ASTM15								12	78	71	54	31	1.00	56
1.26	ASTM15								12	89	75	51	26	1.22	65

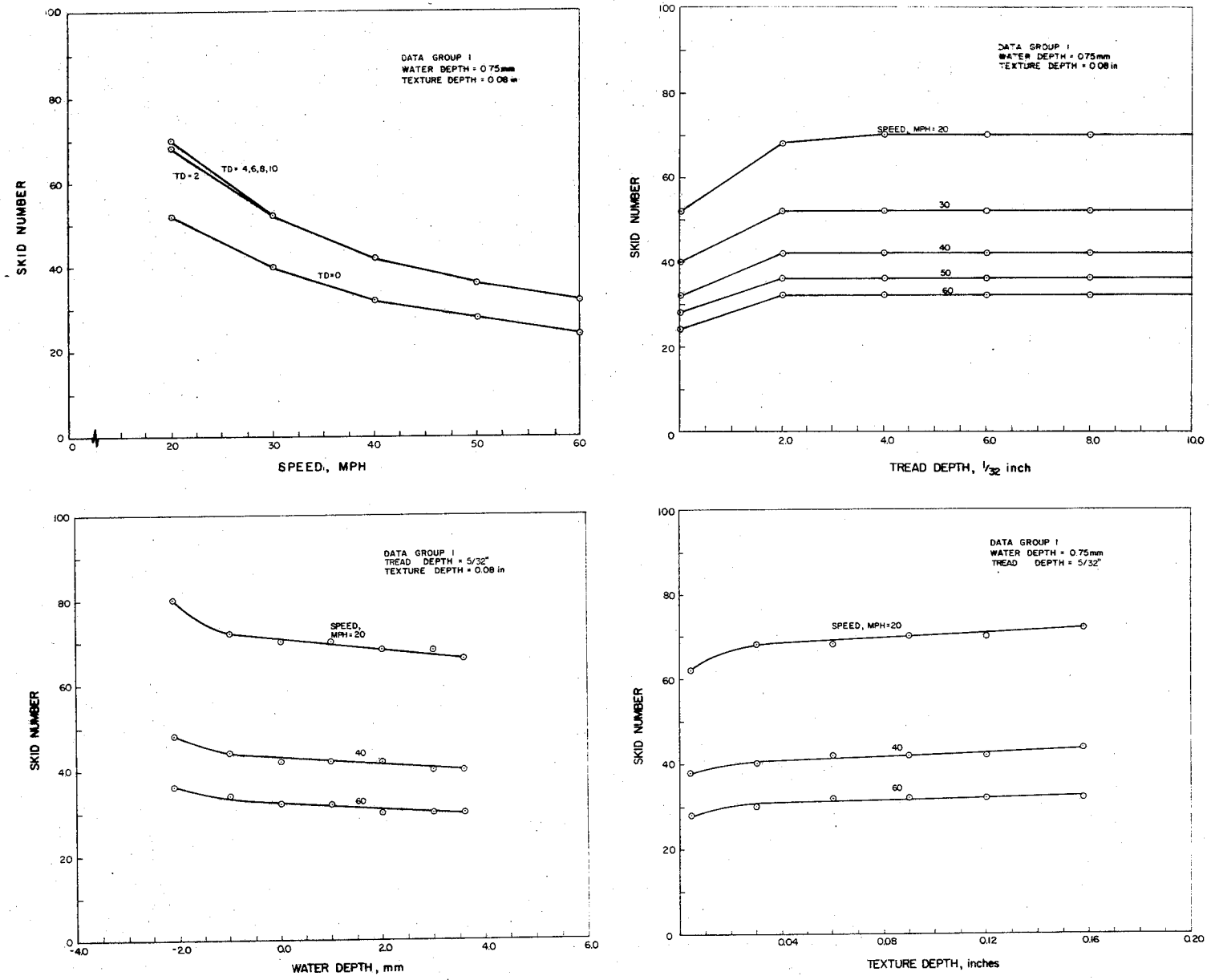

Figures 3-1 thru 3-4.

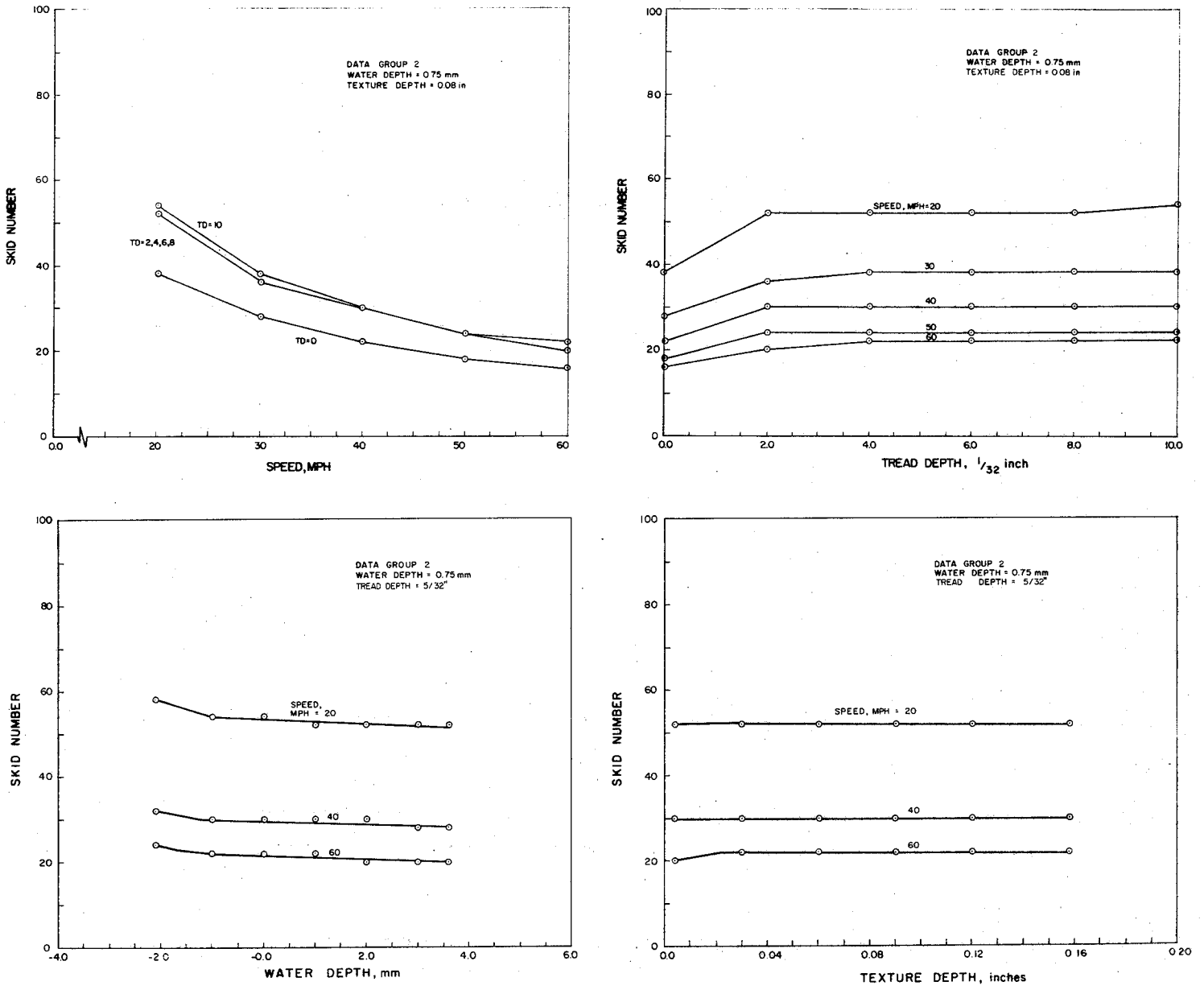

Figures 3-5 thru 3-8.

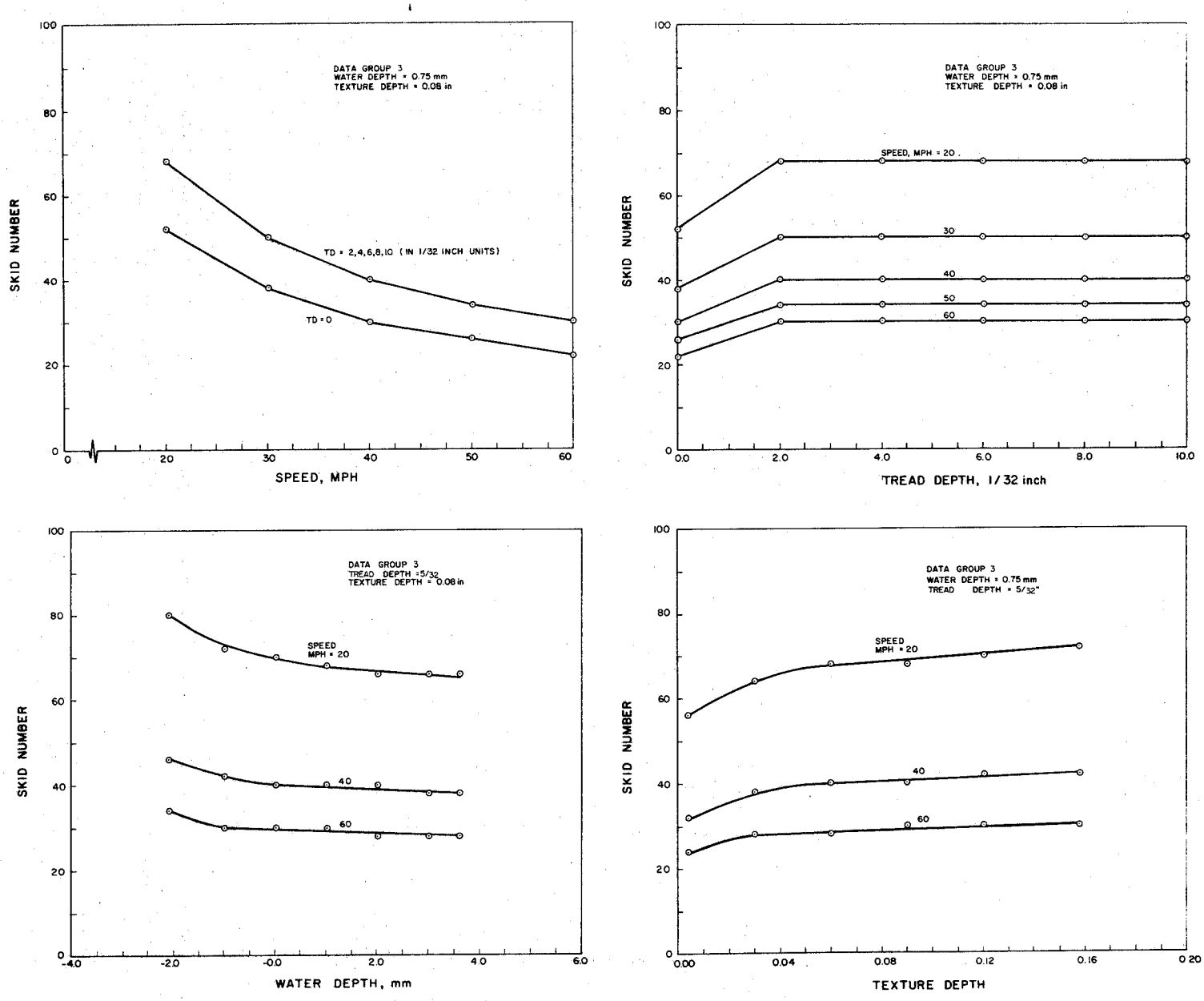

Figures 3-9 thru 3-12.

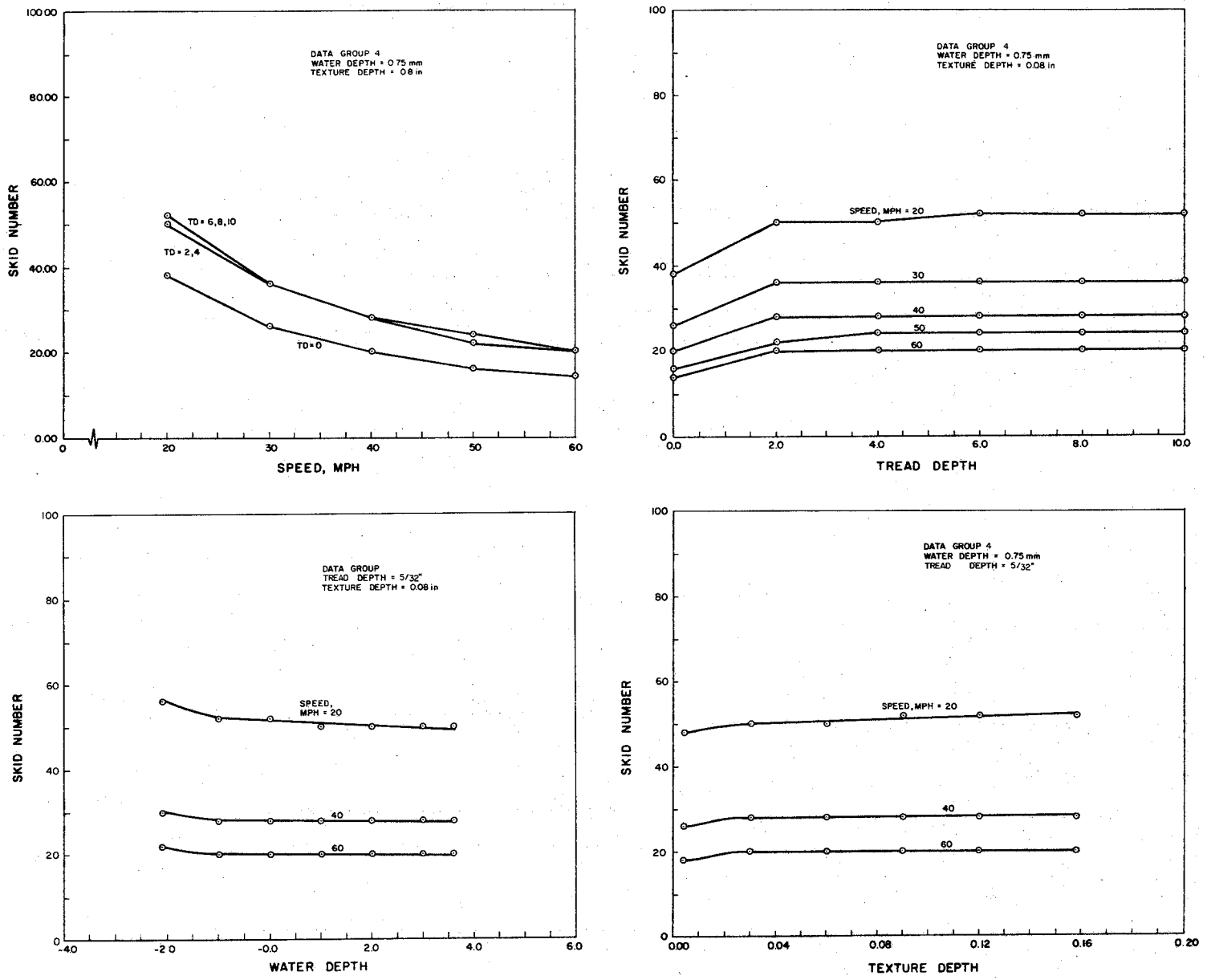

Figures 3-13 thru 3-16.

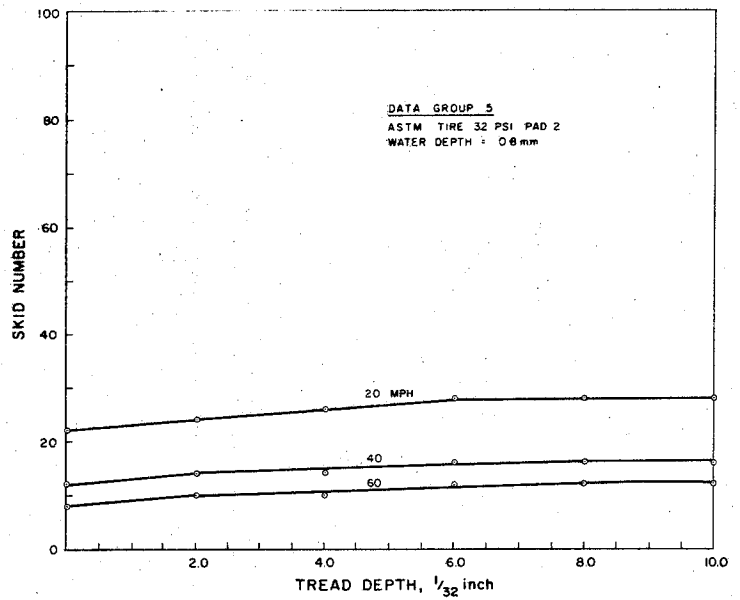

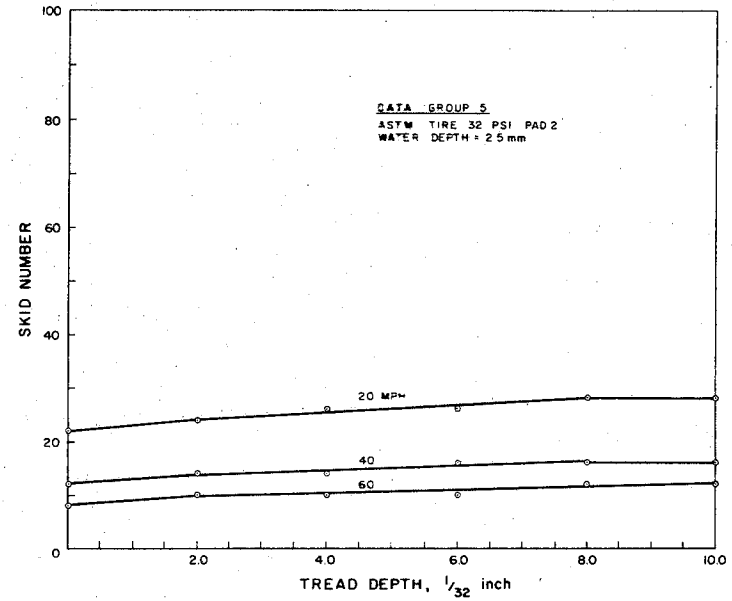

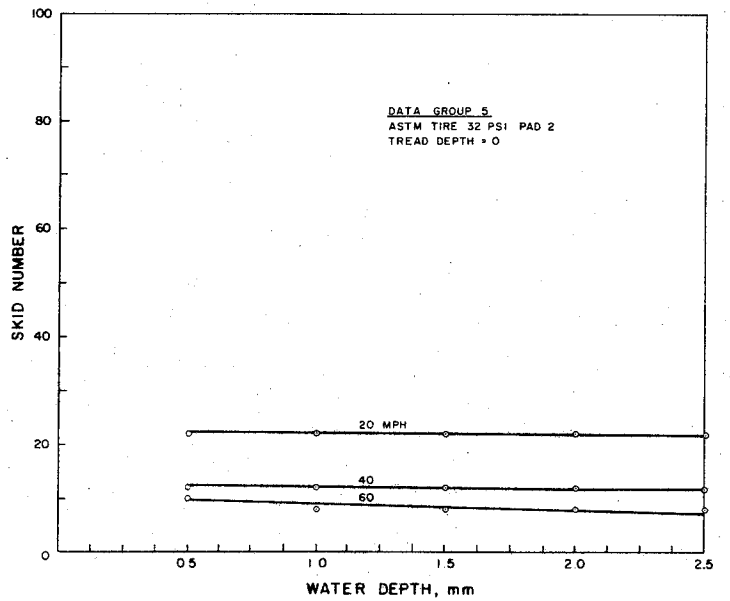

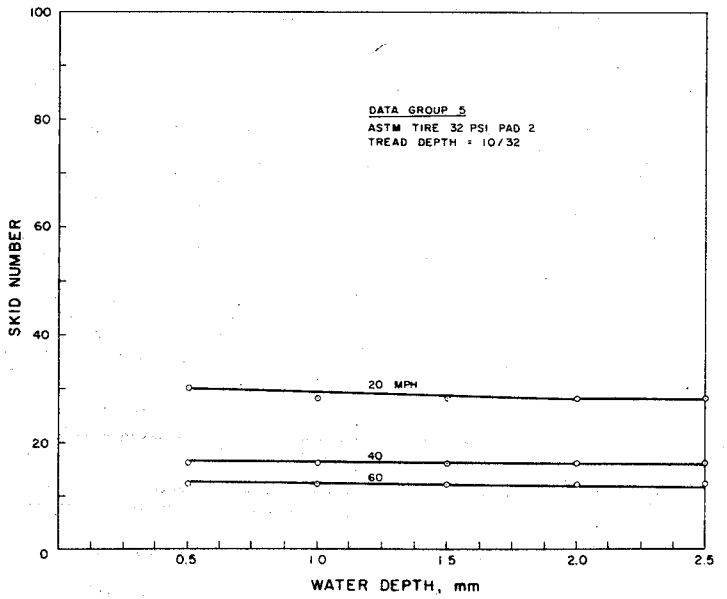

Figures 3-17 thru 3-20.

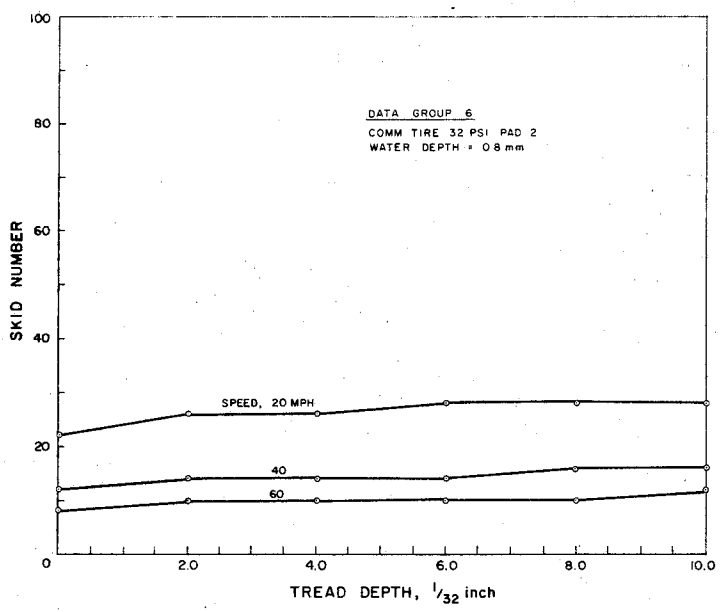

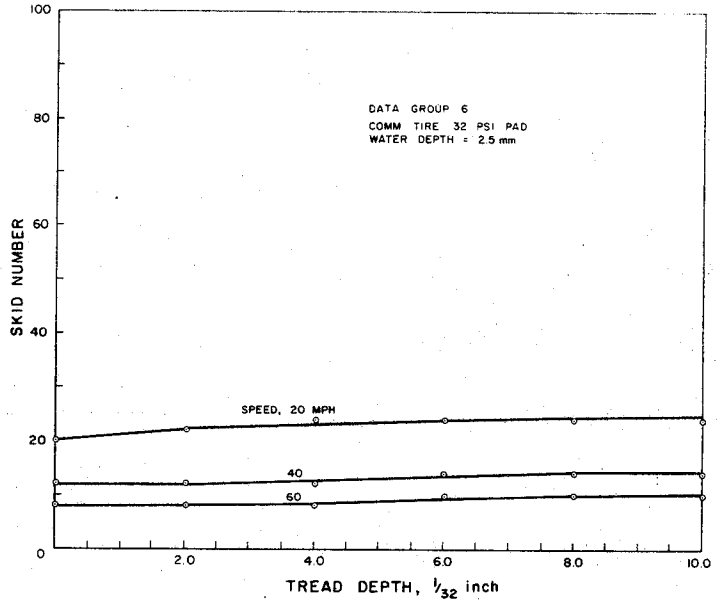

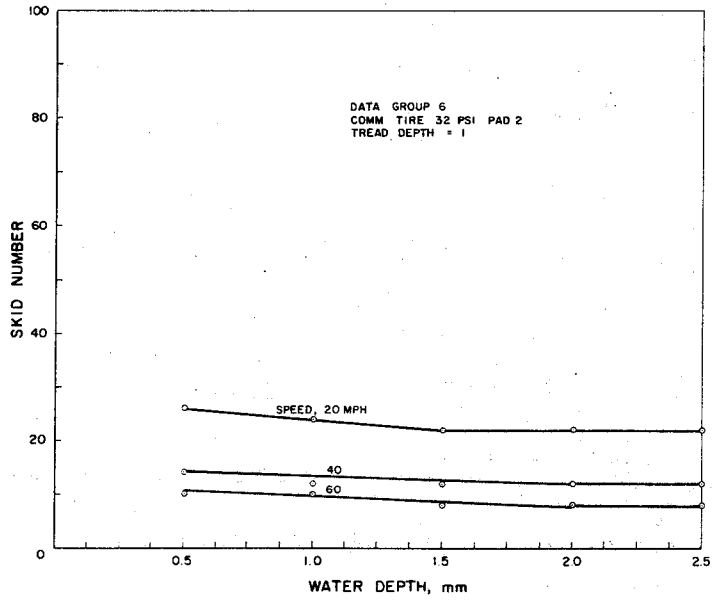

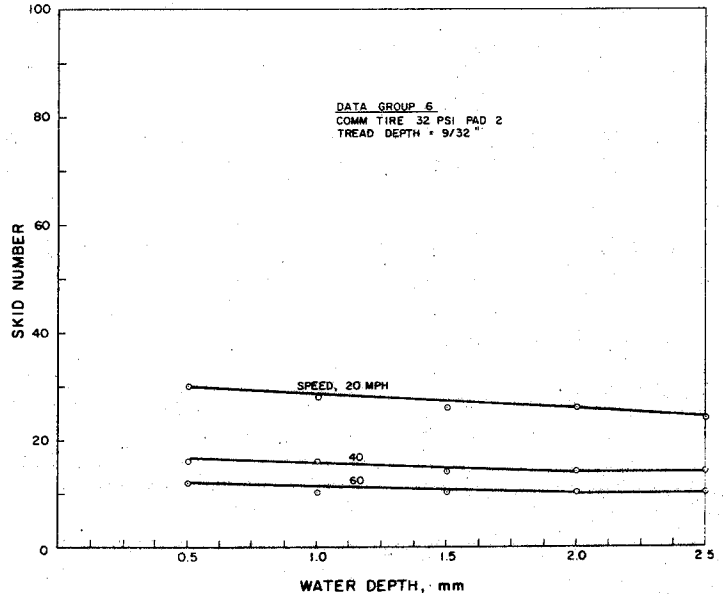

Figures 3-21 thru 3-24.

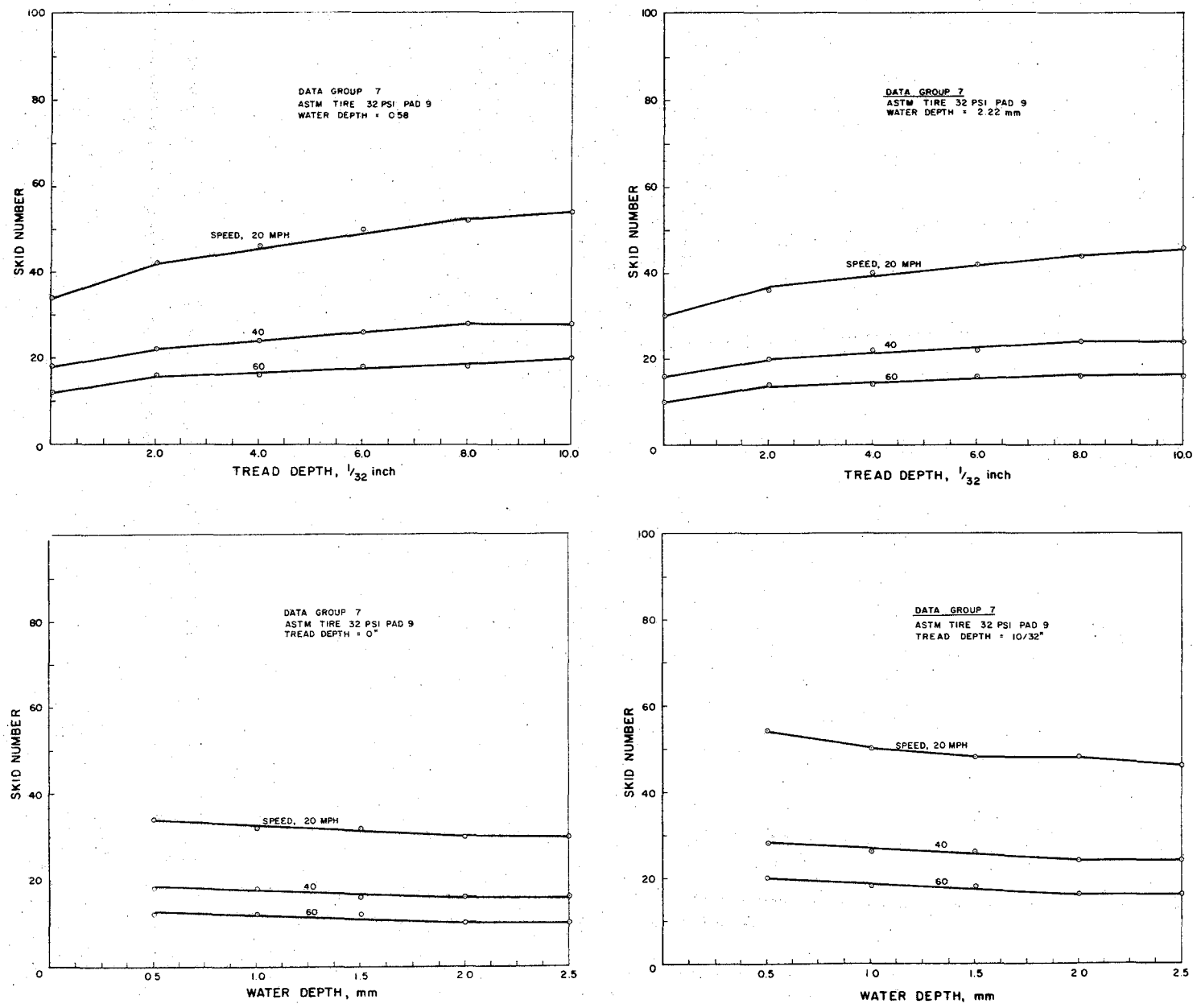

Figures 3-25 thru 3-28.

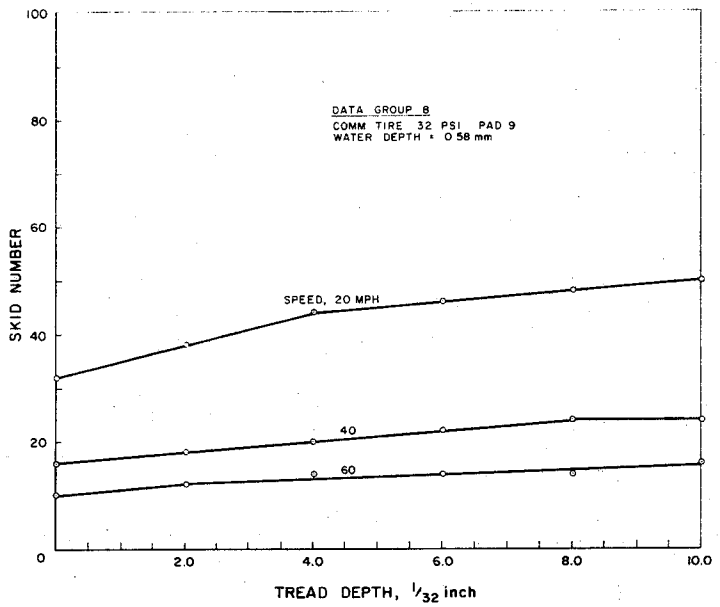

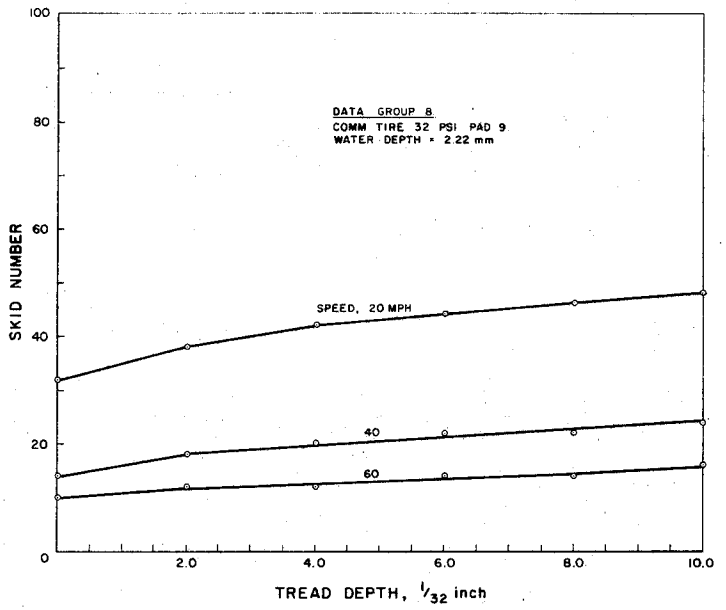

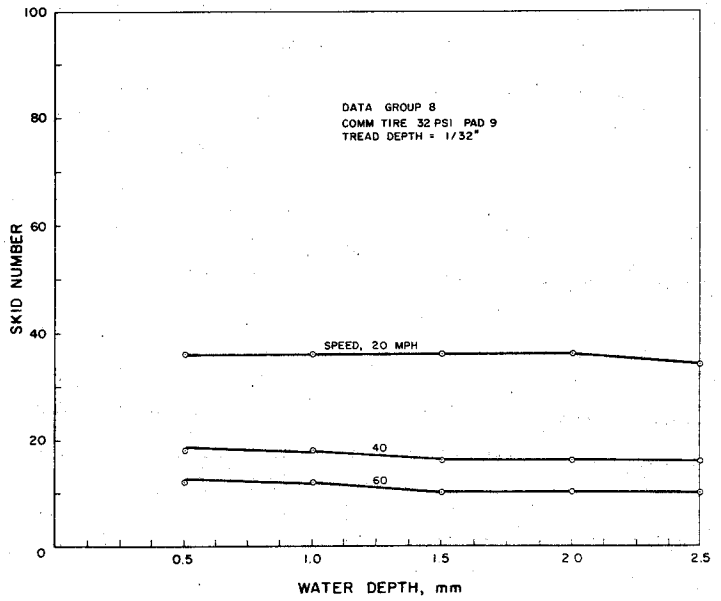

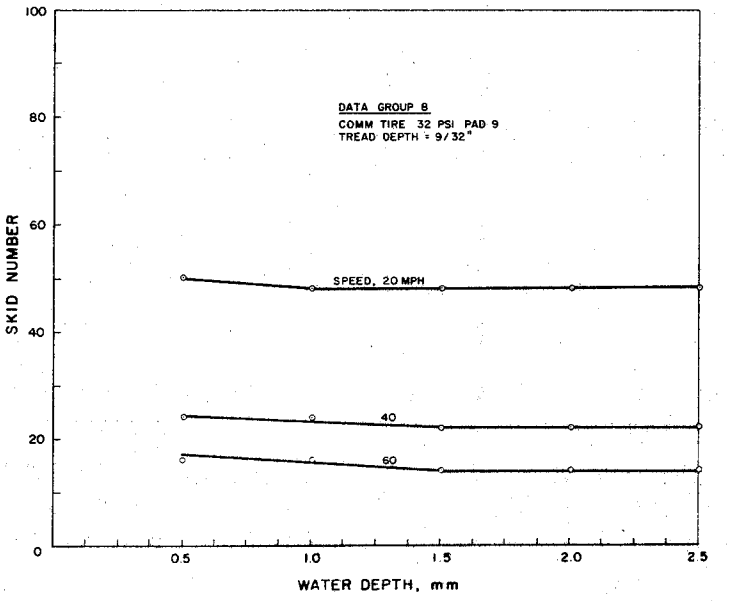

Figures 3-29 thru 3-32.

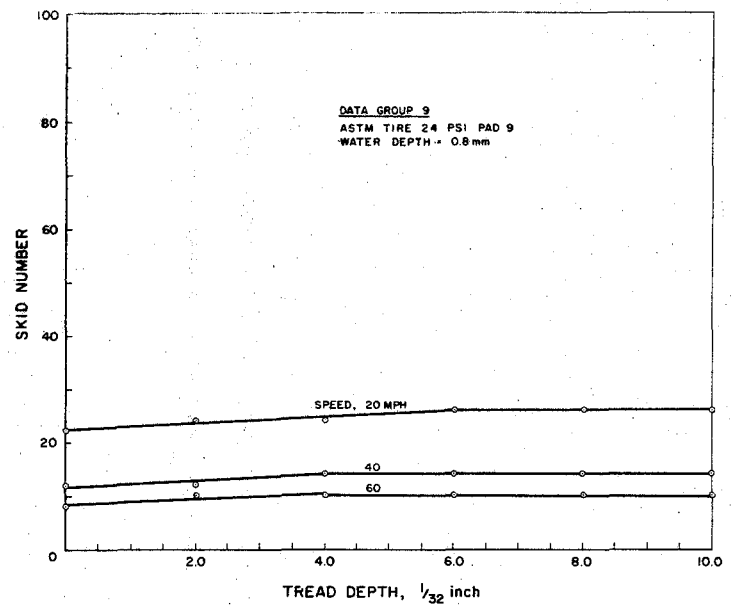

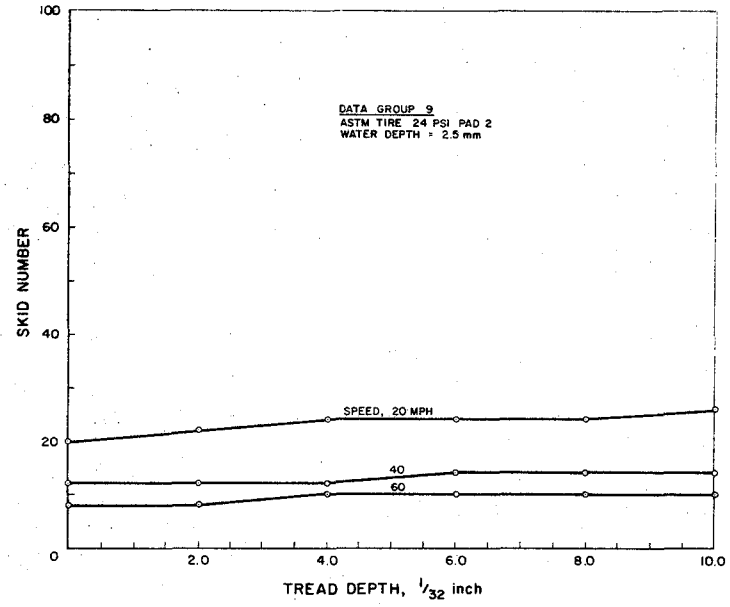

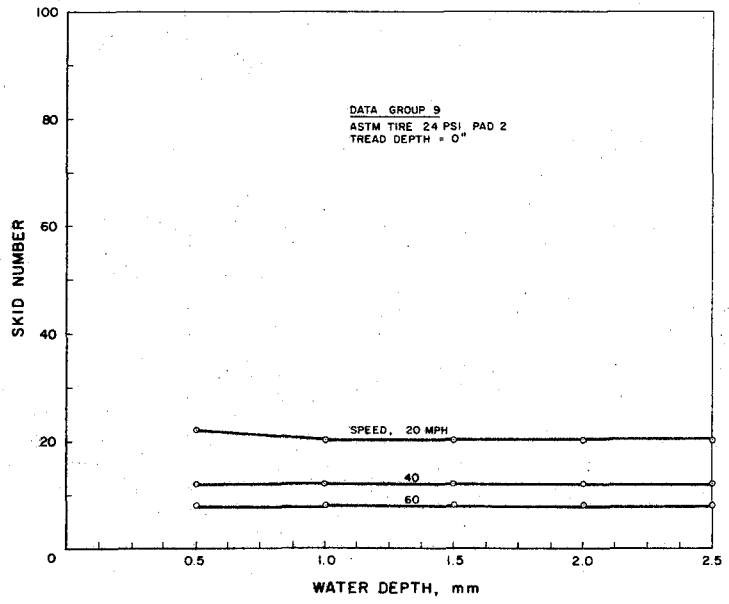

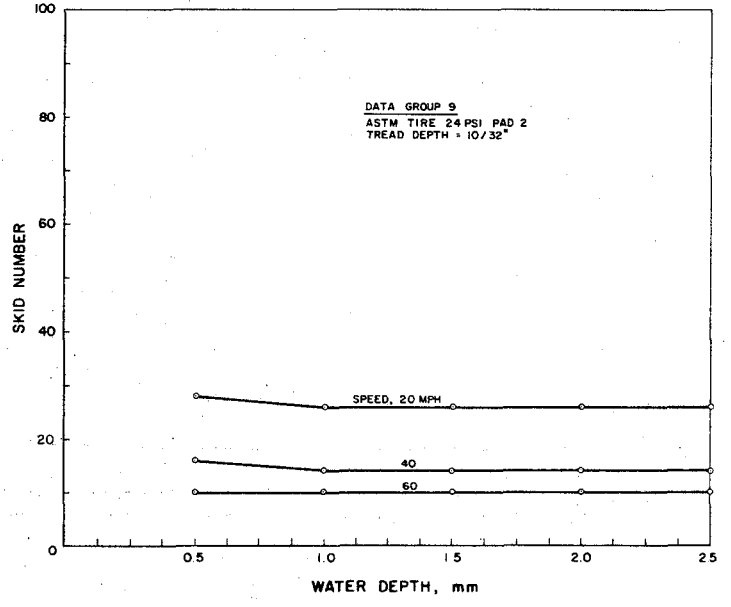

Figures 3-33 thru 3-36.

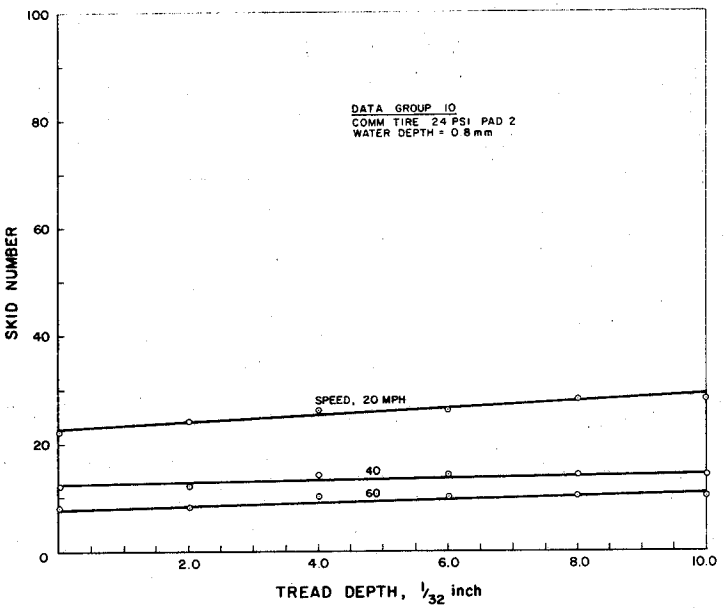

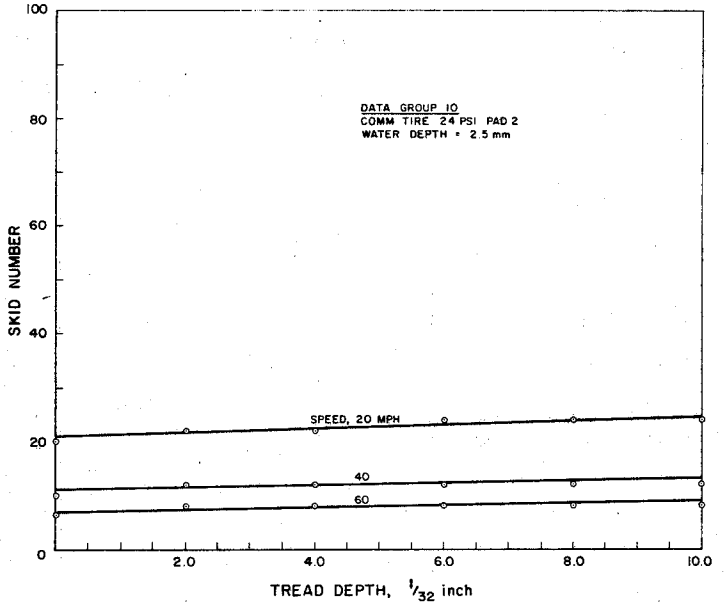

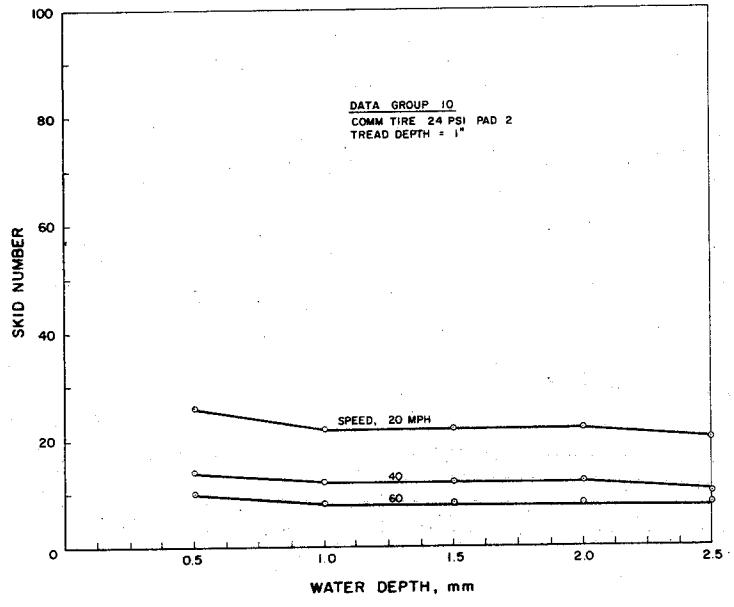

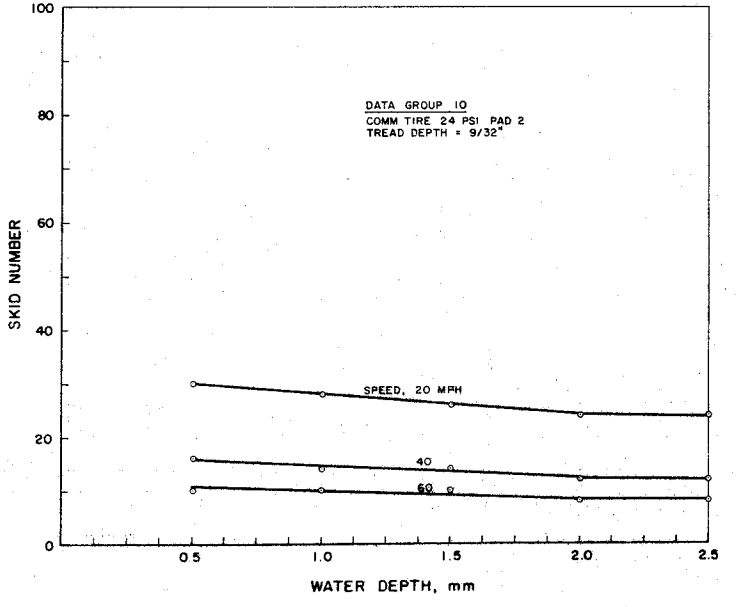

Figures 3-37 thru 3-40.

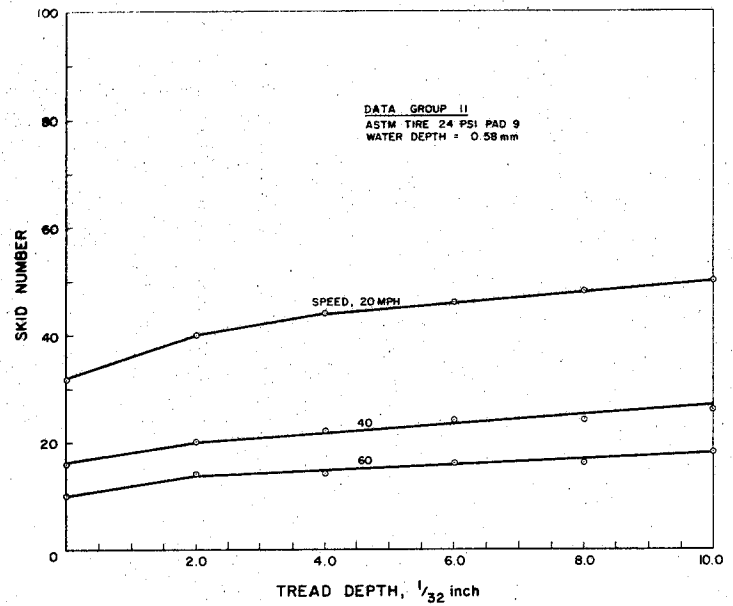

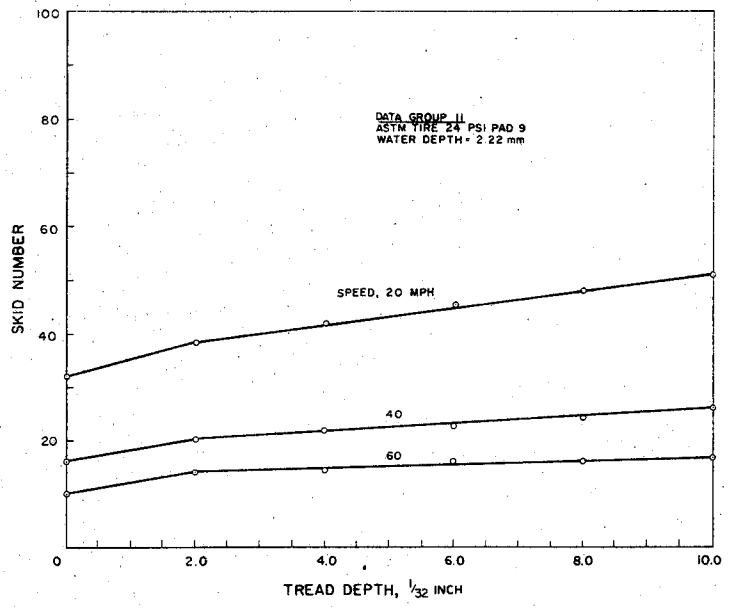

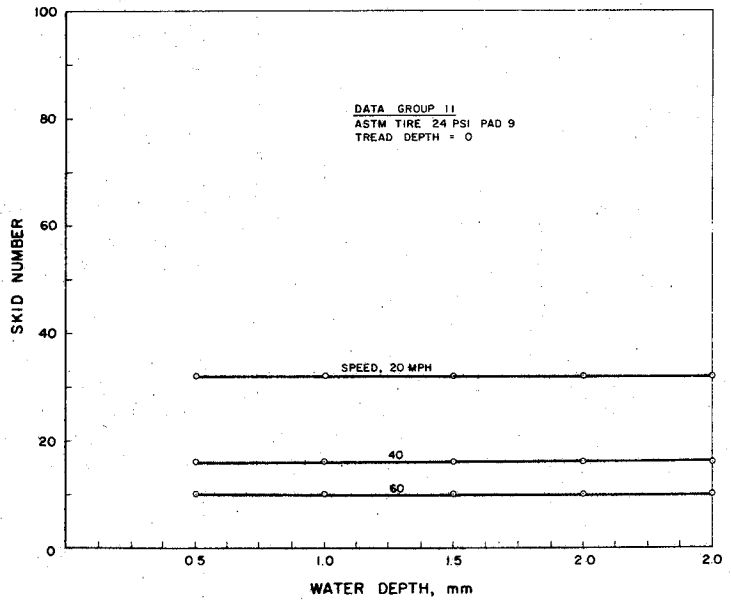

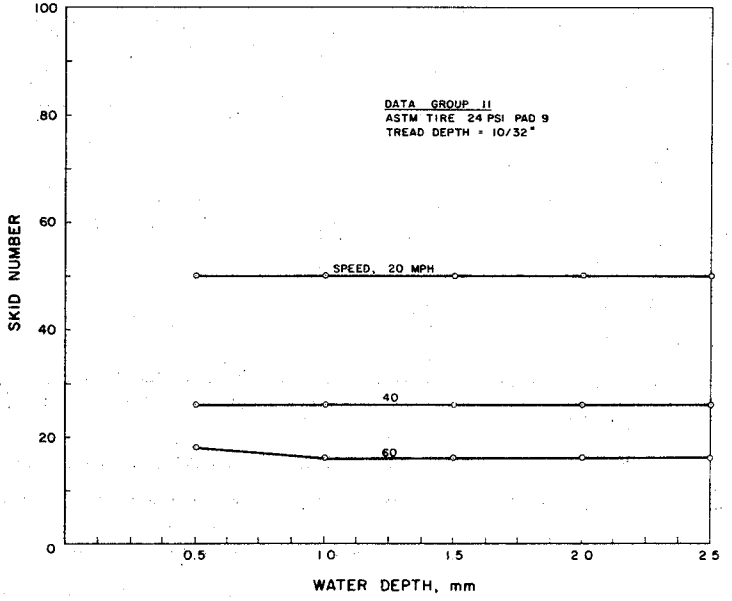

Figures 3-41 thru 3-44.

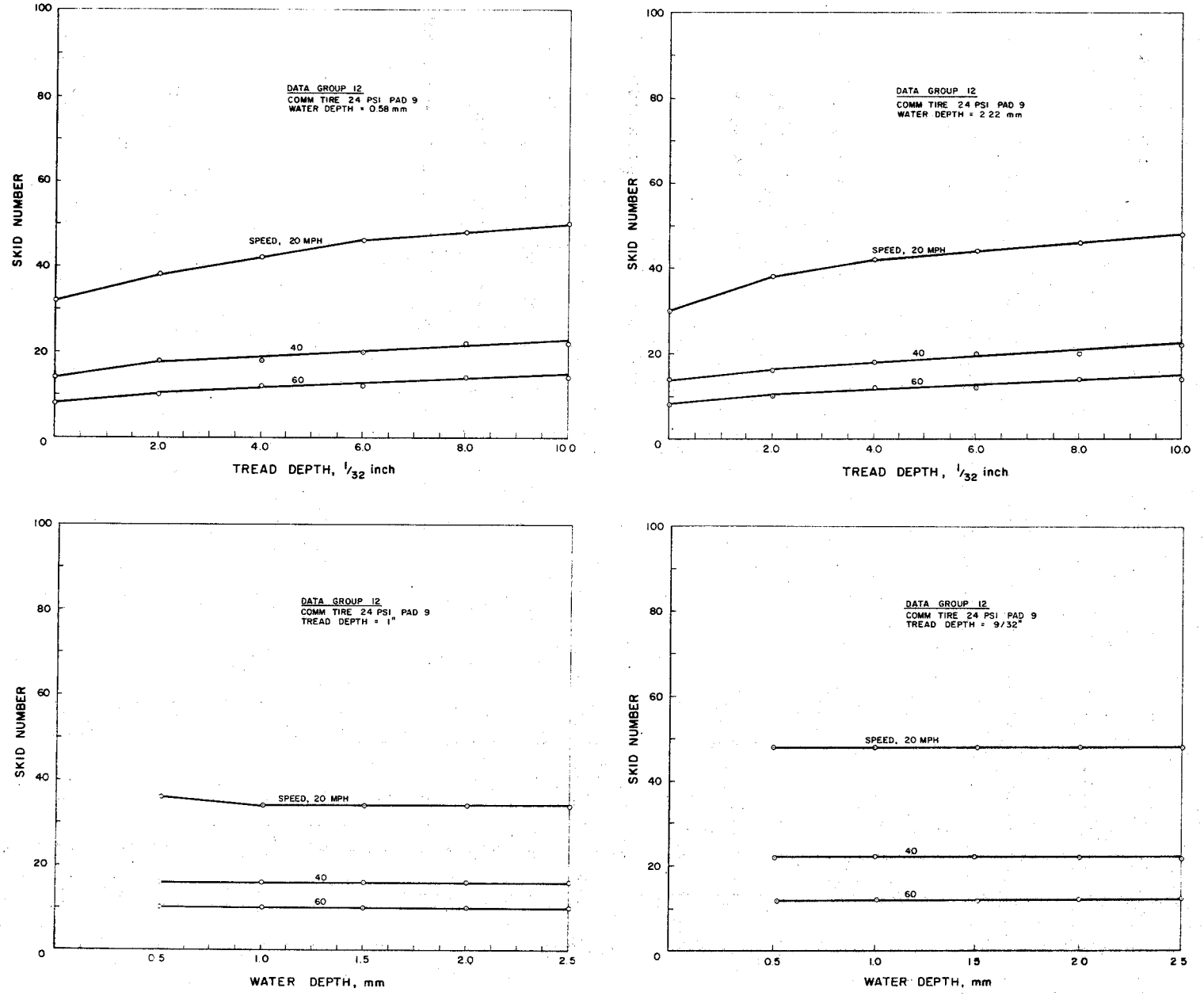

Figures 3-45 thru 3-48.

Regression Analysis of Test Data

The data from Pads 1, 3, 4, 5, 6, 7 and 8 at the Research Annex were divided into four groups for regression analysis:

1. ASTM tire at 32 psi.
2. Commercial tires at 32 psi.
3. ASTM tire at 24 psi.
4. Commercial tires at 24 psi.

Pads 2 and 9 are analyzed separately from the above pads because the friction potential of these two surfaces is rather low. They do, however, represent real world surfaces such as flushed bituminous surfaces or polished surfaces of the flexible or rigid type.

Several constraints were placed upon the results of the regression analysis. The equations derived must

1. Be simple expressions which include all of the variables,
2. Include the most significant interactions between variables, usually with such interactions expressed as the product or quotient of variables,
3. Have as high a correlation coefficient (R^2) as possible, while maintaining the other constraints, and
4. Be physically realistic.

The requirement of physical realism is imposed by specifying that only those statistical models which have the right kinds of relations among the variables are acceptable. In these cases, the signs of four "slopes" were specified.

1. $\frac{d(SN)}{d(MPH)} < 0$. The skid number (SN) decreases as the speed (MPH) increases.

2. $\frac{d(SN)}{d(TD)} > 0$. The skid number (SN) increases as the tread depth (TD) increases.

3. $\frac{d(SN)}{d(WD)} < 0$. The skid number (SN) decreases as the water depth (WD) increases.

4. $\frac{d(SN)}{d(TXD)} > 0$. The skid number (SN) increases as the texture depth (TXD) increases.

Regression Procedure

A select regression program (61) which implements the Hocking-Lamotte-Leslie's variable selection procedure (62, 63) was utilized. Based on the experience obtained in implementing this computer program, the decision was made to use a two-step regression analysis procedure.

Step 1: Log Model

The following log-model is assumed for each data group.

$$\ln(SN) = \ln(a_o) + a_1 \ln(MPH) + a_2 \ln(TD) + a_3 \ln(25.4WD + 2.5) + a_4 \ln(TXD).$$

This equation is equivalent to

$$SN = a_o \, MPH^{a_1} \, TD^{a_2} \, (25.4WD + 2.5)^{a_3} \, TXD^{a_4}$$

TABLE 3-26 Coefficients of Log Model

Data Group 1: ASTM, 32 psi

Model	a_1	a_2	a_3	a_4	R^2
1	-0.72	0.06	-0.08	0.05	0.719
2	-0.72	0.06	0	0.07	0.712
3	-0.72	0.06	-0.15	0	0.703
4	-0.72	0.06	0	0	0.676
5	-0.72	0	-0.08	0.05	0.533
6	-0.72	0	0	0.07	0.525
7	-0.72	0	-0.15	0	0.520
8	-0.72	0	0	0	0.493

Data Group 2: Com. 32 psi

Model	a_1	a_2	a_3	a_4	R^2
1	-0.83	0.07	-0.16	0.01	0.660
2	-0.83	0.07	0	0.04	0.660
3	-0.83	0.07	-0.16	0	0.640
4	-0.83	0.07	0	0	0.630
5	-	-	-	-	-
6	-0.83	0	0	0.04	0.589
7	-0.83	0	-0.16	0	0.568
8	-0.83	0	0	0	0.563

TABLE 3-26 (Cont'd)

Data Group 3: ASTM, 24 psi

Model	a_1	a_2	a_3	a_4	R^2
1	-0.77	0.05	-0.09	0.09	0.687
2	-0.77	0.05	0	0.12	0.681
3	-0.77	0.05	-0.16	0	0.673
4	-0.77	0.05	0	0	0.644
5	-0.77	0	-0.09	0.09	0.564
6	-0.71	0	0	0.02	0.557
7	-0.71	0	-0.16	0	0.549
8	-0.77	0	0	0	0.521

Data Group 4: Com. 24 psi

Model	a_1	a_2	a_3	a_4	R^2
1	-0.86	0.06	-0.13	0.07	0.712
2	-0.86	0.06	0	0.12	0.705
3	-0.86	0.06	-0.18	0	0.699
4	-0.86	0.06	0	0	0.669
5	-0.86	0	-0.13	0.07	0.653
6	-0.86	0	0	0.12	0.645
7	-0.86	0	-0.18	0	0.643
8	-0.86	0	0	0	0.613

The term, WD + 2.5, is assumed to obtain a positive value. The program output provides 14 models for each of the four data groups. Eight models (except data group 2 with 7 models) were selected for linear combination in Step 2 of this study. Selections are based on squared coefficient at correlation, R^2, and the constraints mentioned previously. These models are summarized in Table 3-26. Since linear combination is desired in Step 2, the constant term, a_o, is not important and is not shown in the table. This first step is important in determining the prime interactions and the powers the variables should have to best fit the data.

Step 2: Linear Combination Model

The following linear combination model was assumed for each data group.

$$SN = b_1 X_1 + b_2 X_2 + b_3 X_3 + 6_4 X_4 + b_5 X_5 + b_6 X_6 + b_7 X_7 + b_8 X_8.$$

For Data Group 1 (ASTM tire at 32 psi),

$$X_1 = \frac{TD^{0.06} \quad TXD^{0.05}}{MPH^{0.72} \quad (25.4WD + 2.5)^{0.08}} \qquad X_2 = \frac{TD^{0.06} \quad TXD^{0.07}}{MPH^{0.72}}$$

$$X_3 = \frac{TD^{0.06}}{MPH^{0.72} \quad (25.4WD + 2.5)^{0.15}} \qquad X_4 = \frac{TD^{0.06}}{MPH^{0.72}}$$

$$X_5 = \frac{TXD^{0.05}}{MPH^{0.72} \quad (25.4WD + 2.5)^{0.08}} \qquad X_6 = \frac{TXD^{0.07}}{MPH^{0.72}}$$

$$X_7 = \frac{1}{MPH^{0.72} \quad (25.4WD + 2.5)^{0.15}} \qquad X_8 = \frac{1}{MPH^{0.72}}$$

The following equation is selected as the final model, based on R^2, the physical constraints, simplicity of expression and inclusion of all four independent variables, namely, MPH, TD, WD, and TXD.

$$SN = 135.121 \quad X_4 + 563.655 \quad X_5$$

$$= 135.121 \quad \frac{TD^{0.06}}{MPH^{0.72}} + 563.655 \quad \frac{TXD^{0.05}}{MPH^{0.72} \quad (25.4WD + 2.5)^{0.08}}$$

$$= \frac{135}{MPH^{0.72}} \left[TD^{0.06} + \frac{4.18 \quad TXD^{0.05}}{(25.4WD + 2.5)^{0.08}} \right]$$

Data groups 2, 3, and 4 are regressed using the same procedures. Final models for each data group are shown below. Plots of these models are included in Fig. 3-49 thru 3-60.

Select Regression (Pads 1, 3, 4, 5, 6, 7, 8)

#1 ASTM 32 psi

$$SN = \frac{135}{MPH^{0.72}} \left[TD^{0.06} + \frac{4.18\ TXD^{0.05}}{(25.4WD + 2.5)^{0.08}} \right] \qquad \text{Equation 1.}$$

($N = 225$, $R^2 = 0.947$, SE = 10.22, DF = 2/223, F = 1978)

#2 Comm. 32 psi

$$SN = \frac{186}{MPH^{0.83}} \left[\frac{TD^{0.07}\ TXD^{0.01}}{(25.4WD + 2.5)^{0.16}} + 2.49 \right] \qquad \text{Equation 2.}$$

($N = 735$, $R^2 = 0.933$, SE = 9.47, DF = 2/733, F = 5131)

#3 ASTM 24 psi

$$SN = \frac{154}{MPH^{0.77}} \left[TD^{0.05} + \frac{4.71\ TXD^{0.09}}{(25.4WD + 2.5)^{0.09}} \right] \qquad \text{Equation 3.}$$

($N = 228$, $R^2 = 0.942$, SE = 10.32, DF = 2/226, F = 1825)

#4 Comm. 24 psi

$$SN = \frac{234}{MPH^{0.86}} \left[\frac{TD^{0.06}\ TXD^{0.07}}{(25.4WD + 2.5)^{0.13}} + 2.08 \right] \qquad \text{Equation 4.}$$

($N = 732$, $R^2 = 0.937$, SE = 8.79, DF = 2/730, F = 5441)

Sensitivity Analysis

Sensitivity of each variable can be obtained by applying the following differential analysis.

$$\Delta SN = \left(\frac{\partial SN}{\partial MPH}\right) \Delta MPH + \left(\frac{\partial SN}{\partial TD}\right) \Delta TD + \left(\frac{\partial SN}{\partial WD}\right) \Delta WD + \left(\frac{\partial SN}{\partial TXD}\right) \Delta TXD$$

ASTM Tire at 32 psi

$$\Delta SN = \frac{-97.2}{MPH^{1.72}} \left[TD^{0.06} + \frac{4.18\ TXD^{0.05}}{(25.4WD + 2.5)^{0.08}} \right] \Delta MPH + \frac{8.1}{MPH^{0.72}\ TD^{0.94}} \Delta TD - \frac{45.144\ TXD^{0.05}}{MPH^{0.72}\ (25.4WD + 2.5)^{1.08}} \Delta WD + \frac{28.215}{MPH^{0.72}\ (25.4WD + 2.5)^{0.08}\ TXD^{0.95}} \Delta TXD$$

Commercial Tire at 32 psi

$$\Delta SN = \frac{-154.38}{MPH^{1.83}} \left[\frac{TD^{0.07}\ TXD^{0.01}}{(25.4WD + 2.5)^{0.16}} + 2.49 \right] \Delta MPH + \frac{13.02\ TXD^{0.01}}{MPH^{0.83}\ (25.4WD + 2.5)^{0.16}\ TD^{0.93}} \Delta TD$$

$$- \frac{29.76\ TD^{0.07}\ TXD^{0.01}}{MPH^{0.83}\ (25.4WD + 2.5)^{1.16}} \quad \Delta\ WD$$

$$+ \frac{1.86\ TD^{0.07}}{MPH^{0.83}\ (25.4WD + 2.5)^{0.16}\ TXD^{0.99}} \quad \Delta\ TXD$$

ASTM tire at 24 psi

$$\Delta\ SN = \frac{-\ 118.58}{MPH^{1.77}} \left[\frac{TD^{0.05} + 4.71\ TXD^{0.09}}{(25.4WD + 2.5)^{0.09}} \right] \Delta\ MPH$$

$$+ \frac{7.7}{MPH^{0.77}\ TD^{0.95}} \quad \Delta TD$$

$$- \frac{65.28\ TXD^{0.09}}{MPH^{0.77}\ (25.4WD + 2.5)^{1.09}} \quad \Delta\ WD$$

$$+ \frac{65.28}{MPH^{0.77}\ (25.4WD + 2.5)^{0.09}\ TXD^{0.91}} \quad \Delta\ TXD$$

Commercial tire at 24 psi

$$\Delta\ SN = \frac{-\ 201.24}{MPH^{1.86}} \left[\frac{TD^{0.06}\ TXD^{0.07}}{(25.4WD + 2.5)^{0.13}} + 2.08 \right] \Delta\ MPH$$

$$+ \frac{14.04\ TXD^{0.07}}{MPH^{0.86}\ TD^{0.94}\ (25.4WD + 2.5)^{0.13}} \quad \Delta\ TD$$

$$- \frac{30.42\ TD^{0.06}\ TXD^{0.07}}{MPH^{0.86}\ (25.4WD + 2.5)^{1.13}} \quad \Delta\ WD$$

$$+ \frac{16.38\ TD^{0.06}}{MPH^{0.86}\ (25.4WD + 2.5)^{0.13}\ TXD^{0.93}} \quad \Delta\ TXD$$

Application of Sensitivity Analysis

The sensitivity equation for each data group can be represented in the following general form.

$$\Delta SN = -c_1 \Delta MPH + c_2 \Delta TD - c_3 \Delta WD + c_4 \Delta TXD$$

The sensitivity of any variable can be estimated by the changes of the other four variables. For instance, in order to obtain the same SN ($\Delta SN = 0$), when $\Delta WD = \Delta TXD = 0$, ΔMPH can be estimated by

$$\Delta MPH = \frac{c_2}{c_1} \Delta TD$$

This implies that if TD decreases one unit, then MPH must decrease $\frac{c_2}{c_1}$ unit to obtain the same SN. Also, let $\Delta SN = \Delta TD = \Delta TXD = 0$, then

$$\Delta MPH = -\frac{c_3}{c_1} \Delta WD$$

This implies that if WD increases one unit, then MPH must decrease $\frac{c_3}{c_1}$ unit to obtain the same SN.

Stochastic Considerations

Because these equations have been derived by regression, there will always be values of skid number that will differ on a random basis from those predicted by the equation. As a consequence, it is important to know how reliably these equations predict that a skid number will be above a minimum acceptable level. The reliability of skid-resistance prediction is the degree of confidence (say 95 percent) one has that the predicted value of SN is above the minimum level. This reliability can be calculated

from the statistical properties of the MPH, TD, WD, and TXD frequency distributions. The fact that it is not always 100 percent certain is because of the inherent uncertainty and variability of these variables. The regression equations shown in page 84 are all deterministic models. Stochastic models which include the variability of the variables can be composed based on the expected value and variance of SN. Let $\overline{X}$ and σ_x^2 represent the expected value and variance of variable x.

ASTM 32 psi Model

$$SN = \frac{135\ TD^{0.06}}{MPH^{0.72}} + \frac{564\ TXD^{0.05}}{MPH^{0.72}\ (25.4WD + 2.5)^{0.08}} = X_1 + X_2$$

then

$$\overline{SN} = \overline{X_1} + \overline{X_2}$$

$$\log \overline{X_1} - \frac{0.4343}{2}\left(\frac{\sigma_{X_1}^2}{X_1}\right) = \log 135 + 0.06 \log \overline{TD} \qquad (1)$$

$$- 0.72 \log \overline{MPH} - \frac{0.4343}{2}\left[0.06\left(\frac{\sigma_{TD}}{TD}\right)^2 - 0.72\left(\frac{\sigma_{MPH}}{MPH}\right)^2\right] \qquad (2)$$

$$\sigma_{X_1}^2 = \left(\frac{135\ \overline{TD}^{0.06}}{\overline{MPH}^{0.72}}\right)^2 \left[\left(0.06\ \frac{\sigma_{TD}}{\overline{TD}}\right)^2 + \left(0.72\ \frac{\sigma_{MPH}}{\overline{MPH}}\right)^2\right] \qquad (3)$$

$$\log \overline{X_2} - \frac{0.4343}{2}\left(\frac{\sigma_{X_2}}{X_2}\right)^2 = \log 564 + 0.05 \log \overline{TXD}$$

$$- 0.72 \log \overline{MPH} - 0.08 \log (25.4\overline{WD} + 2.5)$$

$$- \frac{0.4343}{2}\left[0.05\left(\frac{\sigma_{TXD}}{\overline{TXD}}\right)^2 - 0.72\left(\frac{\sigma_{MPH}}{\overline{MPH}}\right)^2 - 0.08\left(\frac{\sigma_{WD}}{25.4\,\overline{WD} + 2.5}\right)^2\right] \quad (4)$$

$$\sigma_{X_2}^2 = \left(\frac{564\ \overline{TXD}^{0.05}}{\overline{MPH}^{0.72}\ (25.4WD + 2.5)^{0.08}}\right)^2\left[\left(0.05\ \frac{\sigma_{TXD}}{\overline{TXD}}\right)^2 + \left(0.72\ \frac{\sigma_{MPH}}{\overline{MPH}}\right)^2\right.$$

$$\left. + \left(0.08\ \frac{\sigma_{WD}}{25.4WD + 2.5}\right)^2\right] \quad (5)$$

$$\sigma_{SN}^2 = \sigma_{X_1}^2 + \sigma_{X_2}^2 + \left(\frac{135}{\overline{MPH}^{0.72}}\right)^2\left[2\ \overline{TD}^{0.06}\left(\frac{4.18\ \overline{TXD}^{0.05}}{(25.4WD + 2.5)^{0.08}}\right)\right]$$

$$X \left(0.72\ \frac{\sigma_{MPH}}{\overline{MPH}}\right)^2 \quad (6)$$

Given $(\overline{MPH}, \sigma^2_{MPH})$, $(\overline{TD}, \sigma^2_{TD})$, $(\overline{WD}, \sigma^2_{WD})$, and $(\overline{TXD}, \sigma^2_{TXD})$, $\sigma^2_{X_1}$ and $\sigma^2_{X_2}$ can be calculated by equations (3) and (5). Substitute these values into equations (2) and (4), then

$$\log \overline{X_1} - \frac{C_1}{\overline{x_1}^2} = C_2$$

$$\log \overline{X_2} - \frac{C_3}{\overline{X_2}^2} = C_4$$

Where C_1, C_2, C_3, and C_4 are constants $\overline{X_1}$ and $\overline{X_2}$ can be calculated by interaction method. $\overline{SN}$ and σ^2_{SN} can thus be estimated by equations (1) and (6).

Similarly $\overline{SN}$ and σ^2_{SN} can be derived for the other regression models.

Application of Stochastic Concepts

Given distribution of SN, together with $\overline{SN}$ and σ^2_{SN}, a reliability model can be written as follows:

$P(\overline{SN} \geq SN_{min}) \geq$ minimum reliability level. The model is described as follows: the probability of SN exceeding a specified minimum SN must be greater than a specified reliability level. For instance, let $SN_{min} = 35$ with a minimum reliability = 0.95. This model means that the probability of SN, being greater than 35, should have more than 95% reliability. This is shown in the following figure

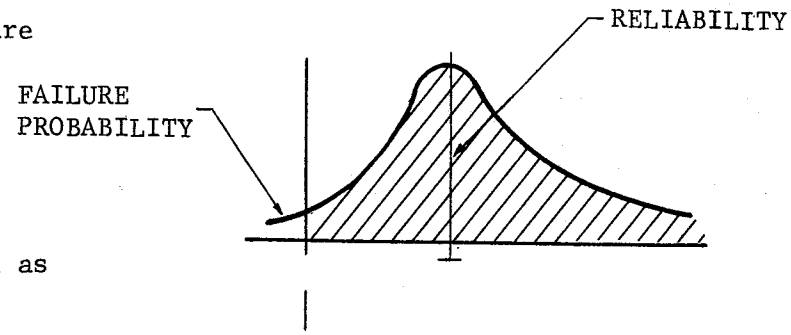

This model can be rewritten as

$$\overline{SN} - K\,\sigma_{SN} \geq SN_{min}$$

Where K is a reliability factor which determines the desired reliability of the predicted skid number.

$K \leq \dfrac{\overline{SN} + SN_{min}}{\sigma_{SN}}$. Typical values of K and the associated reliability, assuming a normal distribution of the variables is as follows:

K	Reliability %
0	50%
0.50	69%
1.00	84%
1.50	93%
2.00	98%

Replace ($\overline{SN}$, σ_{SN} by ($\overline{MPH}$, σ_{MPH}), ($\overline{TD}$, σ_{TD}), ($\overline{WD}$, σ_{WD}), ($\overline{WD}$, σ_{TD}), and ($\overline{TXD}$, σ_{TXD}), then restrictions on MPH and TD can be obtained to keep SN greater than SN_{min} at the desired reliability, subject to given WD and TXD.

Discussion

(1) The regression models (page 83) should satisfy the physical constraints, $\frac{d\ SN}{d\ MPH} < 0$, $\frac{d\ SN}{d\ TD} > 0$ $\frac{d\ SN}{d\ WD} < 0$ $\frac{d\ SN}{d\ TXD} > 0$

However, when TD = 0, Models #2 and #3 become

$$SN = \frac{463}{MPH^{0.83}} \quad \text{and} \quad SN = \frac{487}{MPH^{0.86}}$$

where SN is independent of WD and TXD, WD and TXD have very small effect on SN when TD = 0. The two models may be improved by:

(A) Dividing the commercial tire data into three subgroups: (JET2, UARRT, and GODWO) and finding a regression model for each type of tires or

(B) Replacing the TD variable by (TD + 1) and repeating the same regression analysis.

(2) Experimental data should be within the following ranges:

$20 \leq MPH \leq 60$, $0 \leq TD \leq 10$, $-2.1 \leq WD \leq 3.61$, and

$0.0032 \leq TXD \leq 0.1590$. The regression models may not be used to predict SN outside these ranges. Some plots of the four models are shown in the figures to follow later in the report.

(3) The sensitivity analysis and stochastic considerations may be utilized to establish criterion for skidding accident reduction.

Regression Analysis of Test Data on Pads Nos. 2 and 9

The regression analysis of data taken on Skid Pads Nos. 2 and 9 have, as previously mentioned, been separated from that of the remaining pads at the Annex. This decision came about as a result of a discussion centered around the difference in the surface characteristics of these pads. Both Pads No. 2 and 9 are low friction surfaces and would not be considered suitable for performance in the average traffic stream. They do, however, represent surface types that may be found in selected segments of almost any state highway system.

Pad No. 2 is generally representative of a flushed or bleeding bituminous pavement; whereas Pad No. 9 may be considered representative of a polished surface with moderate macrotexture.

The analyses were made by further sub-dividing the data into groups and treating these groups in selected and convenient manners. Groups 5 through 12 are described in Table 3-27 and the analysis follows in logical steps with a multiplicative model assumed for the first examination. Step 2 involves the assumption of a linear combination model and it is apparent from the value of R^2 that this model fits the data quite well, but admittedly the model is more complex and therefore not as easy to apply.

Table 3-27. Description of Data Groups

DATA GROUP	TRE	PRESSURE	PAD	NO. OF DATA PT.	TD MIN	TD MAX	WD MIN	WD MAX	MPH MAX	MPH MAX	TXD
5	ASTM	32	2	30	0	10	0.031	0.098	20	60	0.0020
6	COMM	32	2	120	1	9	0.031	0.098	20	60	0.0020
7	ASTM	32	9	36	0	10	0.023	0.088	20	60	0.0332
8	COMM	32	9	126	1	9	0.023	0.088	20	60	0.0332
9	ASTM	24	2	30	0	10	0.031	0.098	20	60	0.0030
10	COMM	24	2	120	1	9	0.031	0.098	20	60	0.0030
11	ASTM	24	9	36	0	10	0.023	0.088	20	60	0.0332
12	COMM	24	9	126	1	9	0.023	0.088	20	60	0.0332

(1) $20 \leq MPH \leq 60$

(2) $0 \leq TD \leq 10$

(3) $0.50 \leq WD \leq 2.50$

(4) $\frac{d\ SN}{d\ MPH} < 0$

(5) $\frac{d\ SN}{d\ TD} > 0$

(6) $\frac{d\ SN}{d\ WD} < 0$

TD, Tread Depth, 1/32's of an inch

WD, Water Depth, inches

TXD, Texture Depth, inches

STEP 1 TABLE 3-28. ASSUME A MULTIPLICATIVE MODEL

$$SN = a_o \, MPH^{a_1} \, WD^{a_2} \, (TD + 1)^{a_3}$$

Data #5* (ASTM 32 psi Pad 2)					Data #6 (COMM 32 psi Pad 2)				
Variable	R^2	a_1	a_2	a_3	Variable	R^2	a_1	a_2	a_3
1	0.9296	-0.82	-0.03	0.16	1	0.823	-0.87	-0.21	0.17
2	0.9288	-0.82	0	0.16	2	0.7869	-0.87	0	0.17
3	0.7588	-0.82	-0.13	0	3	0.7680	-0.87	-0.22	0
4	0.7433	-0.82	0	0	4	0.7302	-0.87	0	0
Data #7 (ASTM 32 psi Pad 9)					Data #8 (COMM 32 psi Pad 9)				
Variable	R^2	a_1	a_2	a_3	Variable	R^2	a_1	a_2	a_3
1	0.9257	-0.93	-0.12	0.22	1	0.8374	-1.07	-0.04	0.30
2	0.9130	-0.93	0	0.22	2	0.8363	-1.07	0	0.30
3	0.6701	-0.93	-0.12	0	3	0.7470	-1.07	-0.04	3
4	0.6574	-0.93	0	0	4	0.7459	-1.07	0	0
Data #9 (ASTM 24 psi Pad 2)					Data #10 (COMM 24 psi Pad 2)				
Variable	R^2	a_1	a_2	a_3	Variable	R^2	a_1	a_2	a_3
1	0.9180	-0.85	-0.07	0.13	1	0.8451	-0.93	-0.24	0.19
2	0.9138	-0.85	0	0.13	2	0.8046	-0.93	0	0.19
3	0.8096	-0.85	-0.16	0	3	0.7852	-0.93	-0.26	0
4	0.7885	-0.85	0	0	4	0.7394	-0.93	0	0
Data #11 (ASTM 24 psi Pad 9)					Data #12 (COMM 24 psi Pad 9)				
Variable	R^2	a_1	a_2	a_3	Variable	R^2	a_1	a_2	a_3
1	0.9156	-0.99	-0.01	0.24	1	0.8645	-1.15	-0.03	0.31
2	0.9154	-0.99	0	0.24	2	0.8637	-1.15	0	0.31
3	0.6463	-0.99	-0.01	0	3	0.7772	-1.15	-0.03	0
4	0.6461	-0.99	0	0	4	0.7765	-1.15	0	0

*Equations for data groups 1-4 are given on page 84 of this report.

BEST MULTIPLICATIVE MODEL

ASTM 32 psi Pad 2 (TXD = 0.0020) Equation 5.

$$SN = \frac{248\ (TD + 1)^{0.157}}{MPH^{0.824}\ 25.4WD^{0.028}}$$

(N = 30, R^2 = 0.9294. SE = 0.1238, Df = 3/26, F = 114)

COMM 32 psi Pad 2 (TXD = 0.0020) Equation 6.

$$SN = \frac{281\ (TD + 1)^{0.166}}{MPH^{0.873}\ 25.4WD^{0.206}}$$

(N = 120, R^2 = 0.8203, SE = 0.1998, Df = 3/116, F = 176)

ASTM 32 psi Pad 9 (TXD = 0.0332) Equation 7.

$$SN = \frac{506\ (TD + 1)^{0.219}}{MPH^{0.928}\ 25.4WD^{0.116}}$$

(N = 36, R^2 = 0.9257, SE = 0.1501, Df = 3/32, F = 133)

COMM 32 psi Pad 9 (TXD = 0.0332) Equation 8.

$$SN = \frac{657\ (TD + 1)^{0.301}}{MPH^{1.069}\ 25.4WD^{0.037}}$$

(N = 126, R^2 = 0.8374, SE = 0.2301, Df = 3/122, F = 209)

ASTM 24 psi Pad 2 (TXD = 0.0030) Equation 9

$$SN = \frac{261 \ (TD + 1)^{0.125}}{MPH^{0.851} \ 25.4WD^{0.072}}$$

(N = 30, R^2 = 0.9180, SE = 0.1337, Df = 3/26, F = 97)

COMM 24 psi Pad 2 (TXD = 0.0030) Equation 10

$$SN = \frac{316 \ (TD + 1)^{0.189}}{MPH^{0.930} \ 25.4WD^{0.240}}$$

(N = 120, R^2 = 0.8451, SE = 0.1964, Df = 3/116, F = 211)

ASTM 24 psi Pad 9 (TXD = 0.0332) Equation 11

$$SN = \frac{583 \ (TD + 1)^{0.241}}{MPH^{0.988} \ 25.4WD^{0.015}}$$

(N = 36, R^2 = 0.9156, SE = 0.1719, Df = 3/32, F = 116)

COMM 24 psi Pad 9 (TXD = 0.0332) Equation 12

$$SN = \frac{811 \ (TD + 1)^{0.312}}{MPH^{1.152} \ 25.4WD^{0.031}}$$

(N = 126, R^2 = 0.8645, SE = 0.2219, Df = 3/122, F = 259)

STEP 2 ASSUME A LINEAR COMBINATION MODEL

$$SN = \sum_{i=1}^{4} bi\ xi$$

$$= \sum_{i=1}^{4} bi\ MPH^{a_{1i}}\ WD^{a_{2i}}\ (TD + 1)^{a_{3i}}$$

ASTM 32 psi Pad 2 Equation 5a

$$SN = \frac{93}{MPH^{0.82}}\left[\frac{1.76\ (TD + 1)^{0.16}}{25.4WD^{0.03}} + 1\right]$$

(N = 30, R^2 = 0.9886, SE = 1.9350, Df = 2/28, F = 1209.90)

COMM 32 psi Pad 2 Equation 6a

$$SN = \frac{150}{MPH^{0-87}}\left[\frac{1.01\ (TD + 1)^{0.17}}{25.4WD^{0.21}} + 1\right]$$

(N = 120, R^2 = 0.9745, SE = 2.7844, Df = 2/112, F = 2255.51)

ASTM 32 psi Pad 9 Equation 7a

$$SN = \frac{109}{MPH^{0.93}}\left[\frac{3.85\ (TD + 1)^{0.22}}{25.4WD^{0.12}} + 1\right]$$

(N = 36, R^2 = 0.9830, SE = 3.8889, Df = 2/34, F = 983.348)

COMM 32 psi Pad 9 Equation 8a

$$SN = \frac{359}{MPH^{1.07}}\left[\frac{1.18\ (TD + 1)^{0.30}}{25.4WD^{0.04}} + 1\right]$$

(N = 126, R^2 = 0.9661, SE = 5.3443, Df = 2/124, F = 1768.15)

ASTM 24 psi Pad 2 Equation 9a

$$SN = \frac{83}{MPH^{0.85}}\left[\frac{2.22\ (TD + 1)^{0.13}}{25.4WD^{0.07}} + 1\right]$$

(N = 30, R^2 = 0.9857, SE = 1.9943, Df = 2/28, F = 967.795)

Comm 24 psi Pad 2 Equation 10a

$$SN = \frac{175}{MPH^{0.93}} \left[\frac{0.98 \ (TD + 1)^{0.19}}{25.4WD^{0.24}} + 1 \right]$$

(N = 120, R^2 = 0.9716, SE = 2.8195, Df = 2/118, F = 2018.30)

ASTM 24 psi Pad 9 Equation 11a

$$SN = \frac{153}{MPH^{0.99}} \left[\frac{3.03 \ (TD + 1)^{0.24}}{25.4WD^{0.01}} + 1 \right]$$

(N = 36, R^2 = 0.9756, SE = 4.6117, Df = 2/34, F = 680.235)

Comm 24 psi Pad 9 Equation 12a

$$SN = \frac{459}{MPH^{1.15}} \left[\frac{1.12 \ (TD + 1)^{0.31}}{25.4WD^{0.03}} + 1 \right]$$

(N = 126, R^2 = 0.9639, SE = 5.3297, Df = 2/124, F = 1657.68

THE GENERAL FORM IS

$$SN = \frac{c_o}{MPH^{c_1}} \left[\frac{c_2 \ (TD + 1)^{c_3}}{WD^{c_4}} + 1 \right]$$

In summary two alternative sets of regression models have been derived. Comparisons are as follows:

	Multiplicative Model	Combination Model
R^2	good	excellent
Simple expression	excellent	good

There are three alternatives in applying these models:

(1) Use multiplicative models

(2) Use combination models

(3) ASTM tire use multiplicative models

COMM tire use combination models

Data plots based on linear combination models are presented in figures 3-59 and 3-60 for Pads 2 and 9 respectively.

Analysis of SH6 Data

Shown in Figures 3-54 through 3-58 are graphical representations of data collected on several experimental portland cement concrete surfaces constructed as trial sections on the East ByPass of SH6 in Bryan, Texas. Complete descriptive information on these surfaces is contained in Research Report 141-4F by Ledbetter, Meyer and Ballard (64).

The regression analyses of the data yielded the equations shown in Table 3-29 and from these equations were plotted the figures mentioned above.

Because these data form a major part of the presentation in reference (64) only limited details are given here and these details should be assumed to serve only to amplify and extend the data previously given on the Annex Pads. As was the case with the nine surfaces at the Annex, these surfaces are highly sensitive to speed at all positive water depths irrespective of the values of the other variables. Values of skid resistance at speeds in excess of 40 to 50 mph are quite low indicating that for most rainy weather these quality surfaces may be hazardous. It is also evident that deep transverse texturing is superior to longitudinal texturing, all other factors being equal.

Skid values can be predicted from the equations given and the values so obtained may be considered reliable for wet weather conditions wherein sufficient water is present to create positive water depths.

TABLE 3-29. Regression Models for Experimentally Textured Portland Cement Concrete Pavements

Texture Direction	Regression Model	No. of Data Points	R^2[a]	SE[b]
Transverse	$SN = \frac{205}{MPH^{1.15}} \left[17.92\ (TD + 1)^{0.18}\ TXD^{0.29} + \frac{1}{(WD + 0.1)^{0.53}} \right]$	168	0.79	11.88
Longitudinal	$SN = \frac{910}{MPH^{1.37}} \left[3.06\ (TD + 1)^{0.14}\ TXD^{0.04} + \frac{1}{(WD + 0.1)^{0.31}} \right]$	252	0.76	13.56

[a]Correlation coefficient squared.

[b]Standard error in terms of skid number.

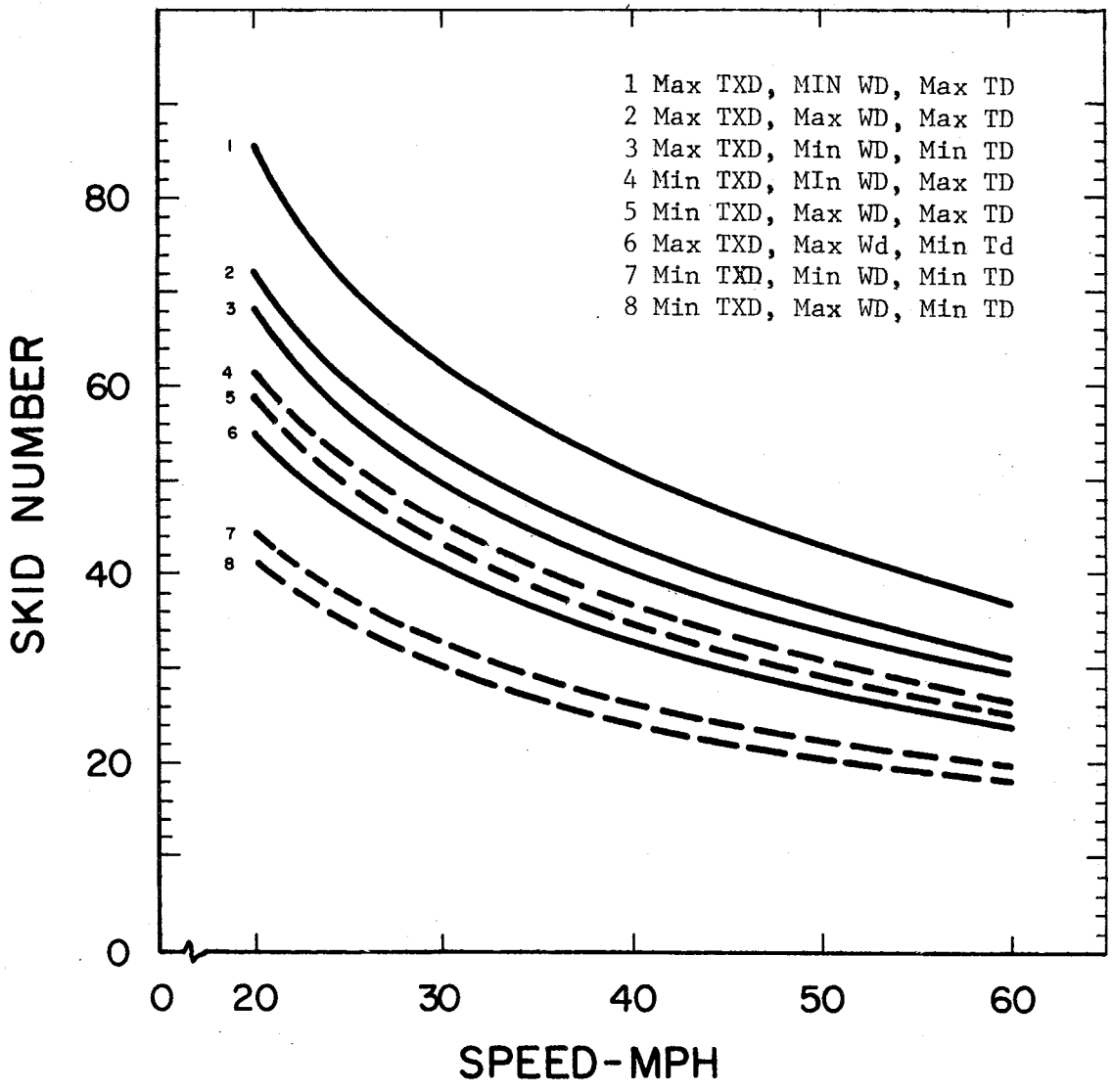

Fig. 3-49. Effects of pavement texture depths (TXD), tire tread depths (TD), and water film depths (WD) on the skid number at various speeds for the ASTM-14" tire at 24 psi tire inflation pressure, TAMU Annex data.

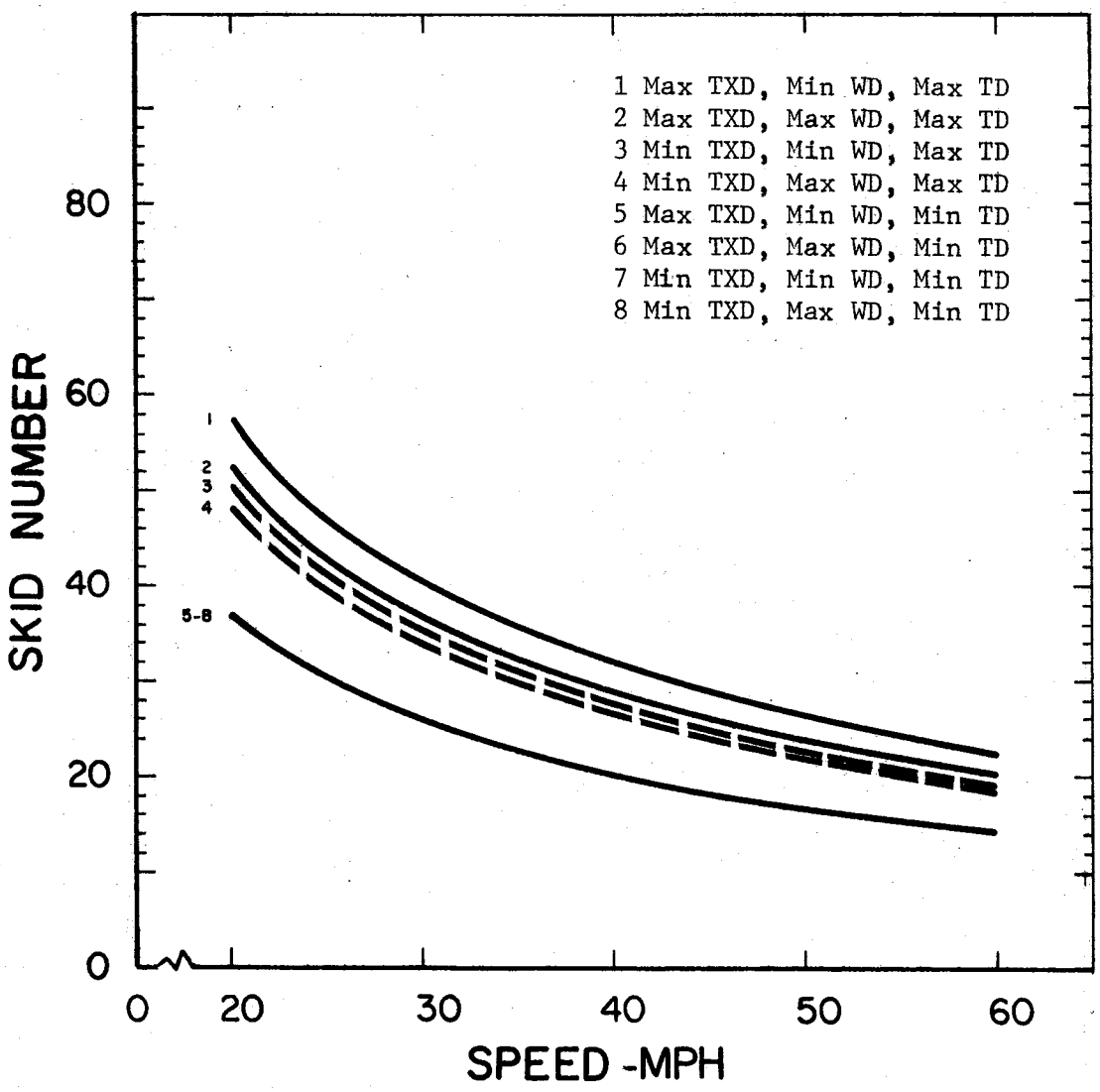

Fig. 3-50. Effects of pavement texture depth (TXD), tire tread depth (TD), and water depth (WD) on the skid numbers of commercial tires at 24 psi tire inflation pressure, TAMU Annex data.

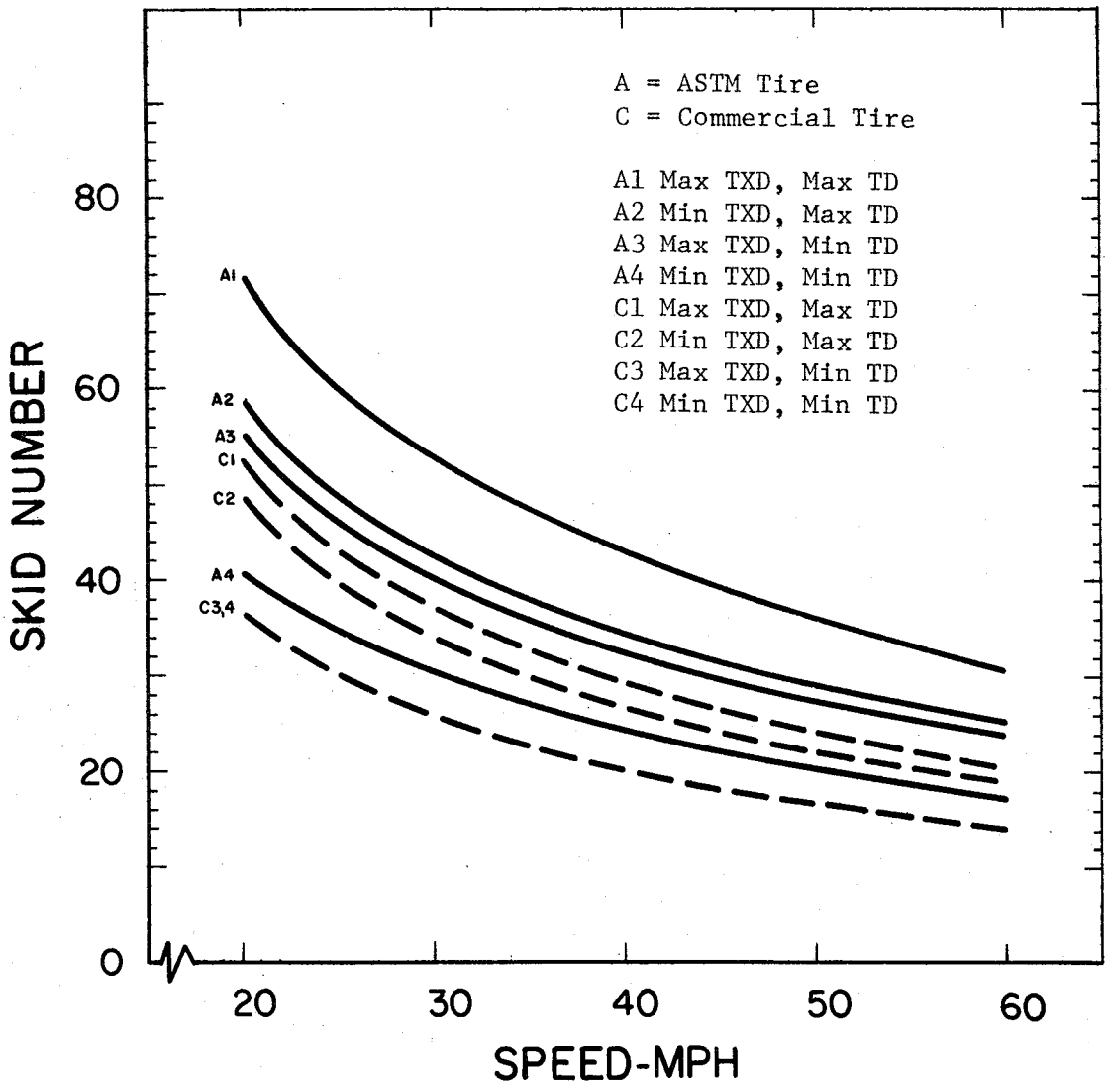

Fig. 3-51. Comparison of skid numbers for the ASTM tire and for the commercial tires at maximum water eepths (WD), minimum and maximum texture depths (TXD) and tire tread depths (TD), at 24 psi tire inflation pressure, TAMU Annex data.

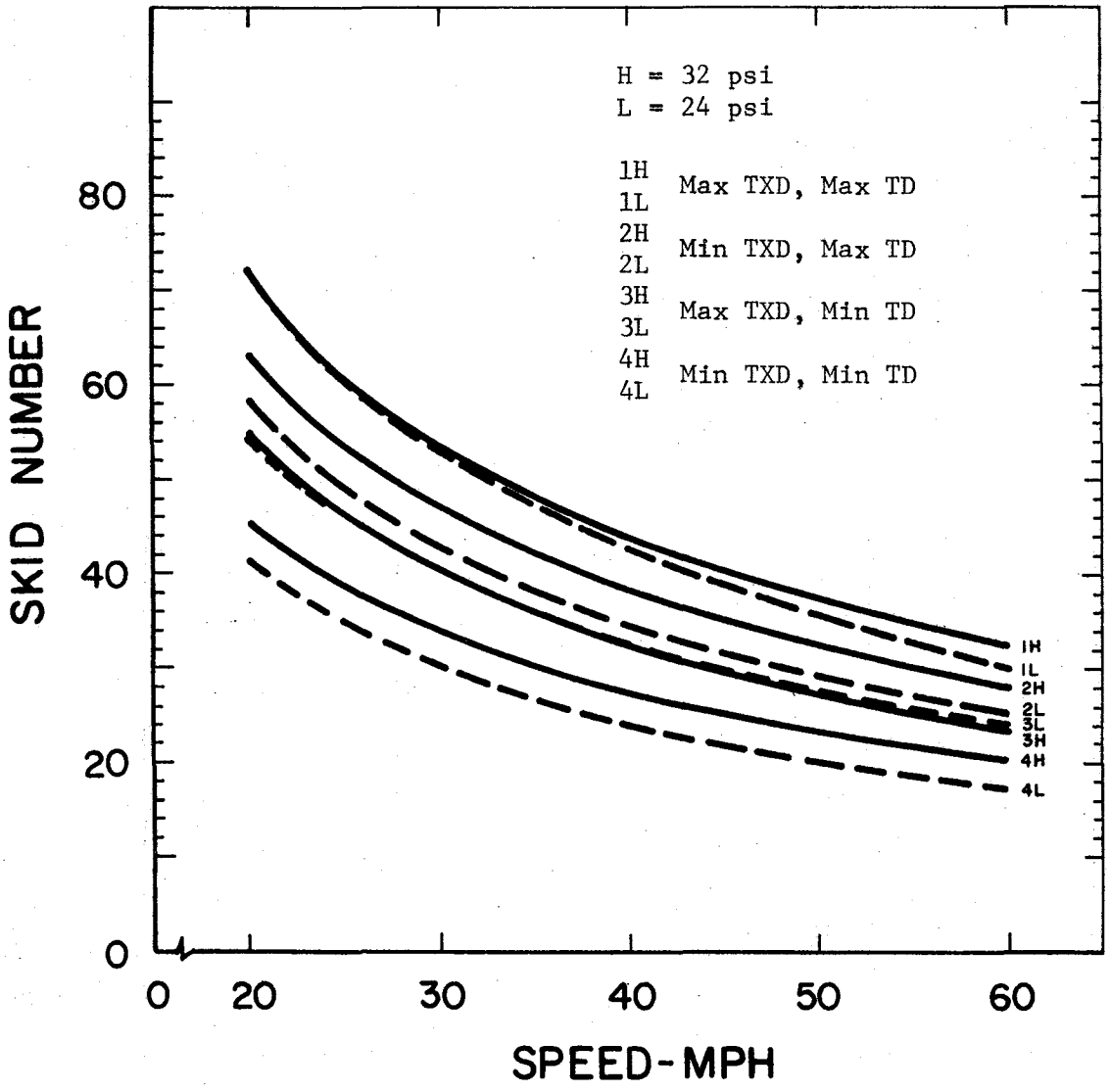

Fig. 3-52. Effects of tire inflation pressure on skid numbers for the ASTM tire at maximum water depth, minimum and maximum pavement texture depths (TXD) and tire tread depths (TD), TAMU Annex data.

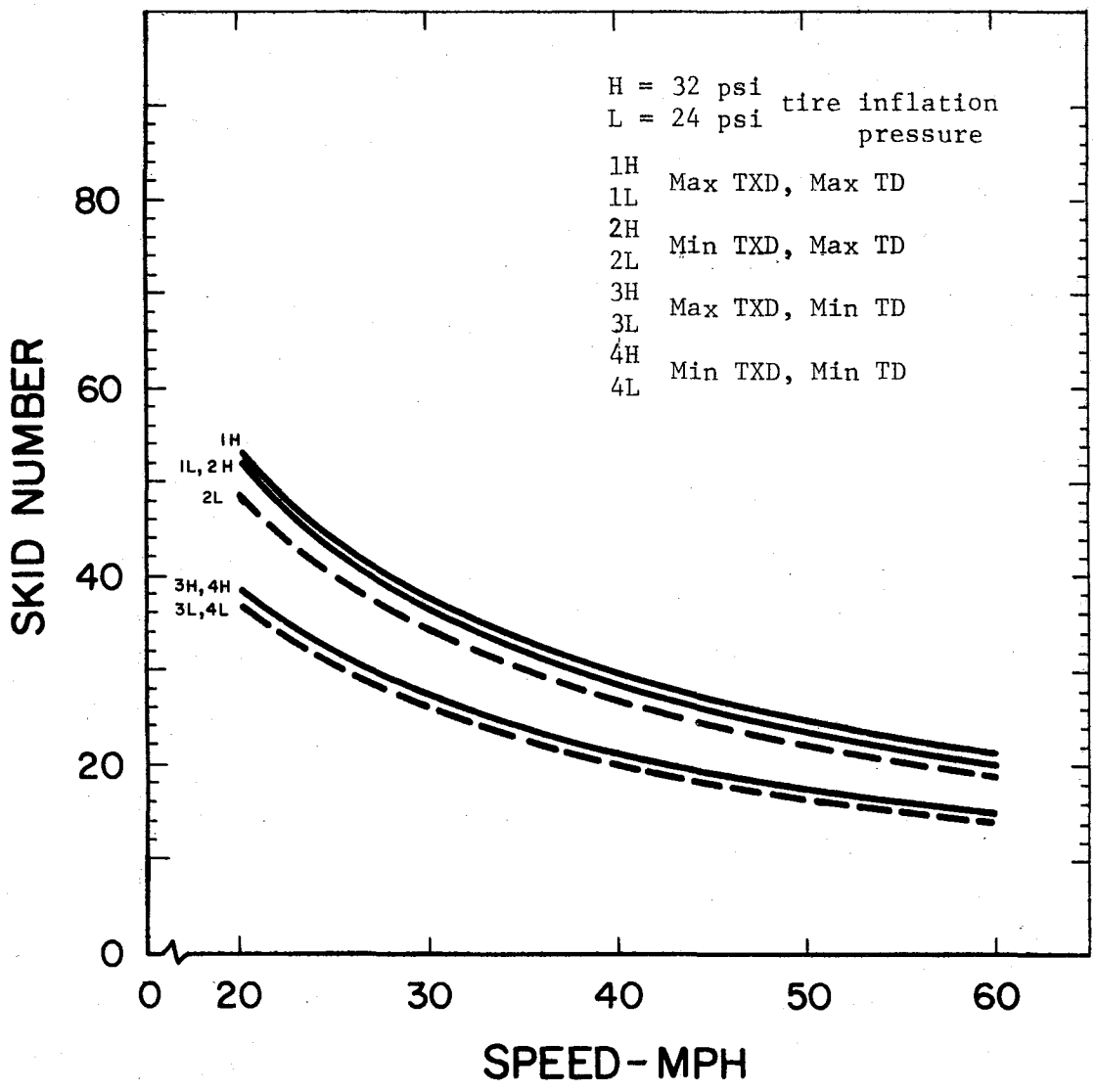

Fig.3-53. Effects of tire inflation pressure on skid numbers for the commercial tires tested at maximum water depth, minimum and maximum pavement texture depths (TXD) and tire tread depths (TD), TAMU Annex data.

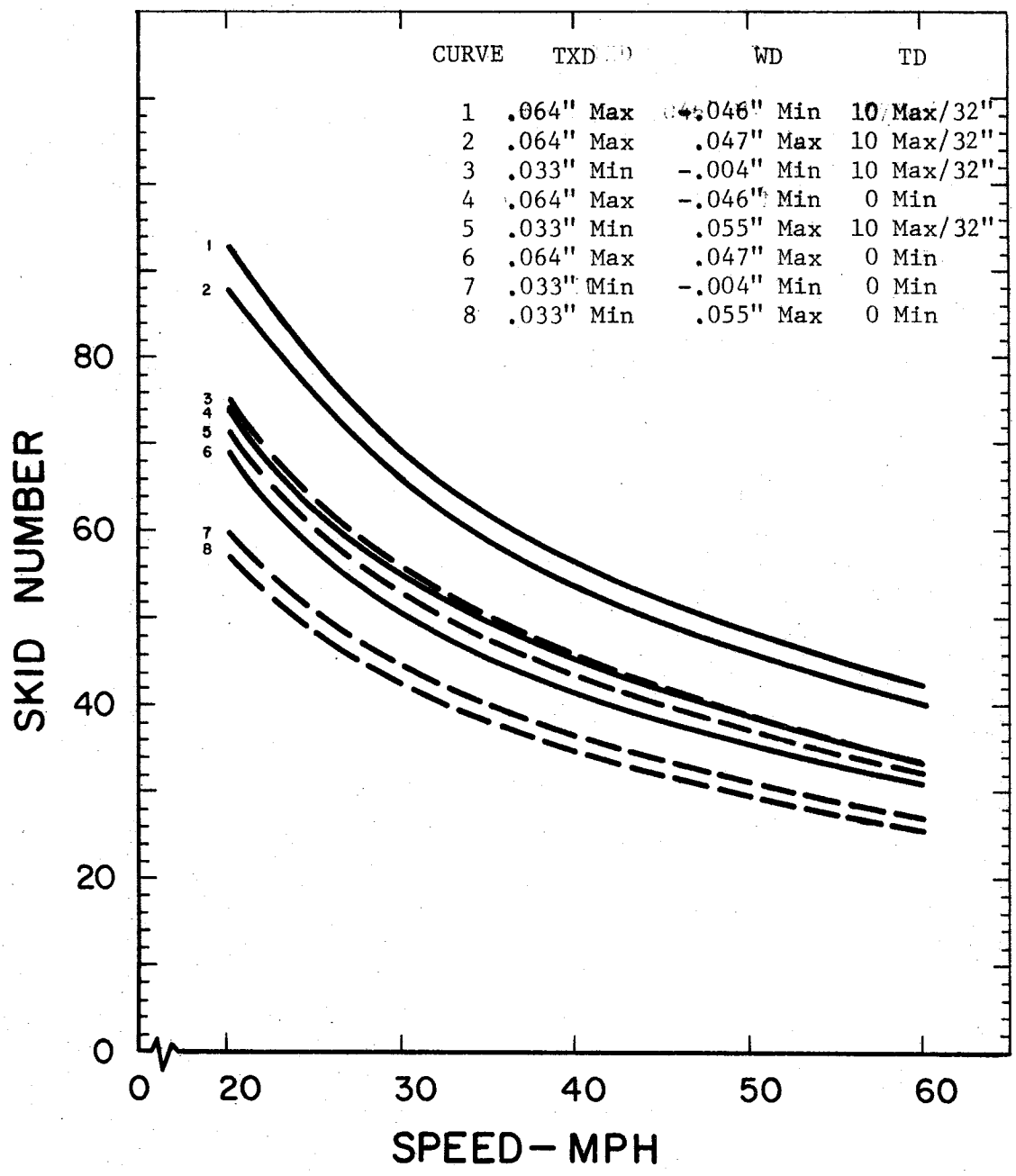

Fig. 3-54. Effects of concrete pavement transverse texture depths (TXD), tire tread depths (TD) and water film depths (WD) on the skid number at speeds of 20 to 60 MPH, ASTM-14" tire, tire pressure 24 psi, East Bypass data.

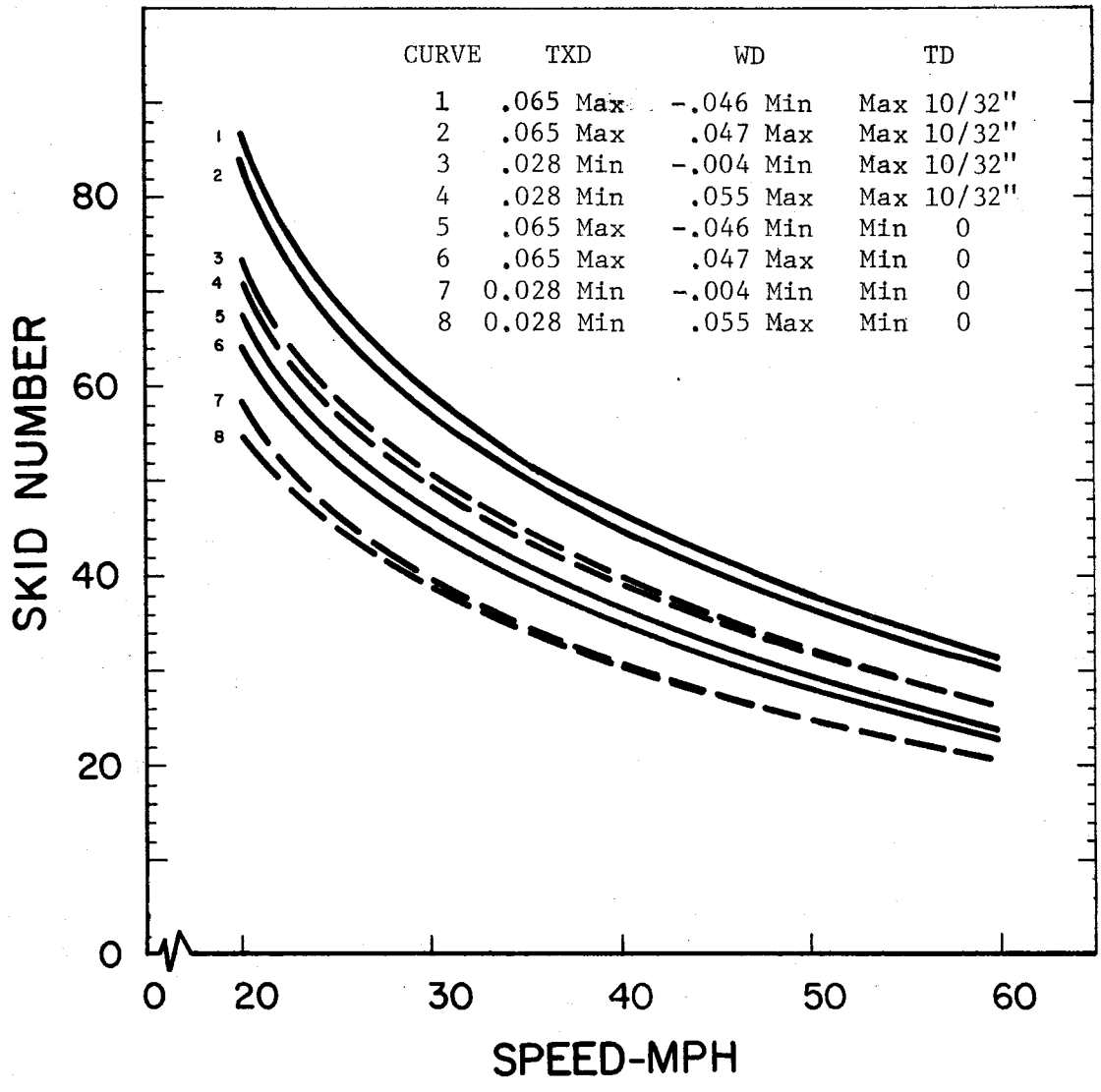

Fig. 3-55. Effects of concrete pavement longitudinal texture depths (TXD), tire tread depths (TD) and water film depths (WD) on the skid number at speeds of 20 to 60 MPH, ASTM-14" tire, tire pressure 24 psi, East Bypass data.

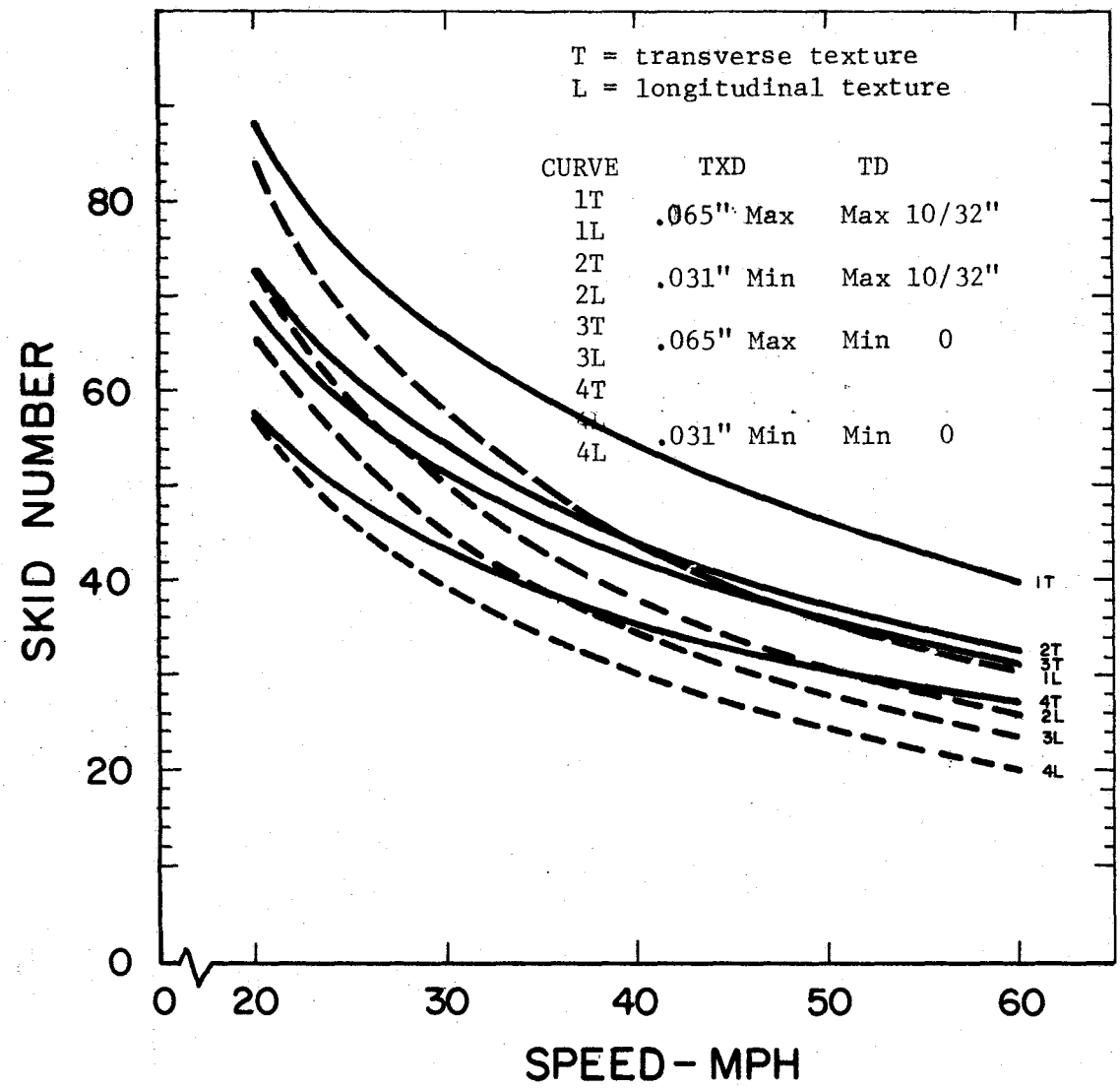

Fig. 3-56. Skid number comparison between transverse pavement texture (T) and longitudinal pavement texture (L) for the ASTM-14" tire 24 psi tire pressure and maximum water depths (WD), minimum and maximum tread depths (TD), and minumum and maximum texture depths (TXD), East Bypass data.

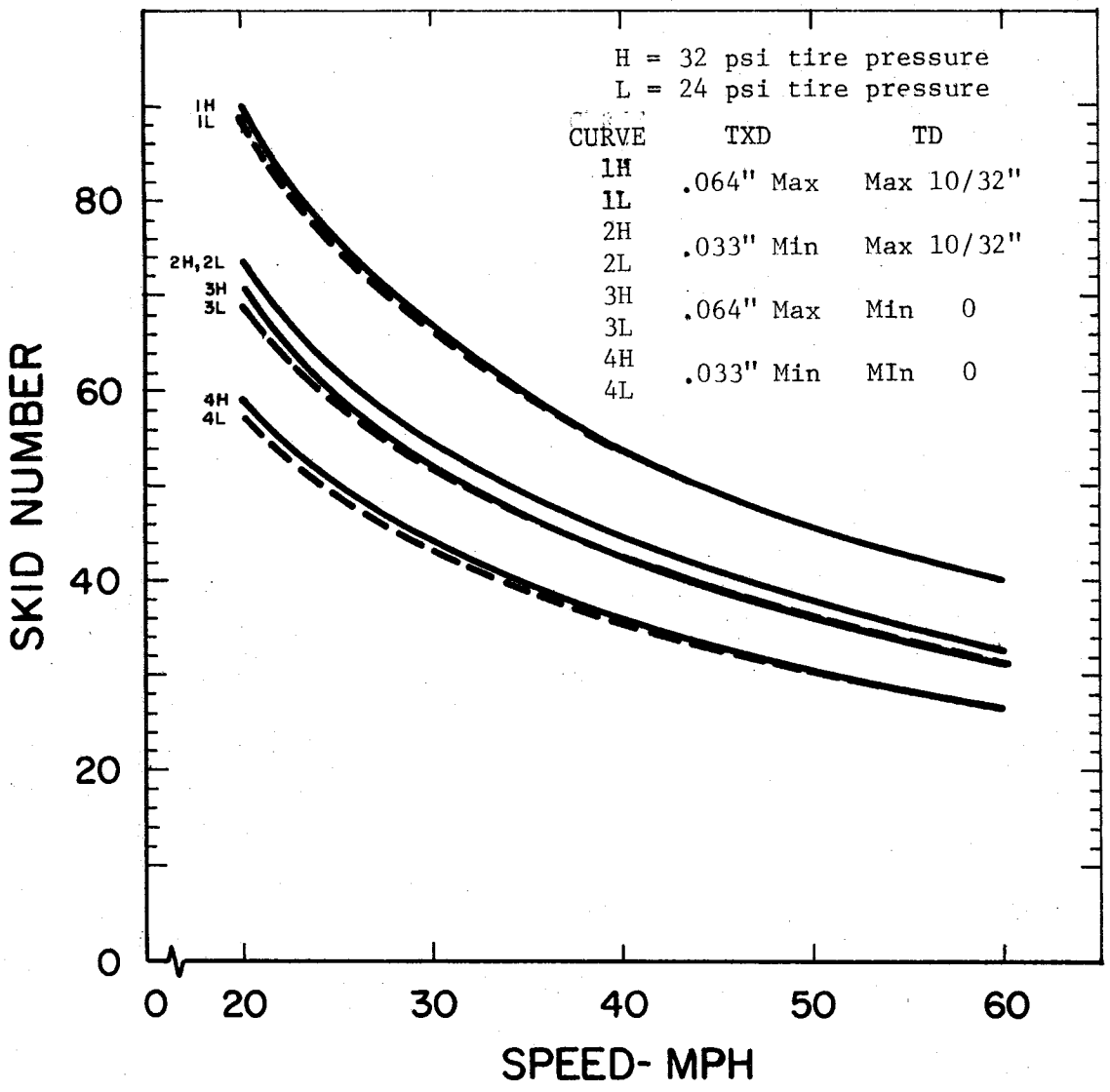

Fig. 3-57. Effects of tire inflation pressure on skid numbers for the ASTM-14" tire at maximum water depth, on transversely textured concrete pavement (TXD) and tire tread depaths (TD), East Bypass data.

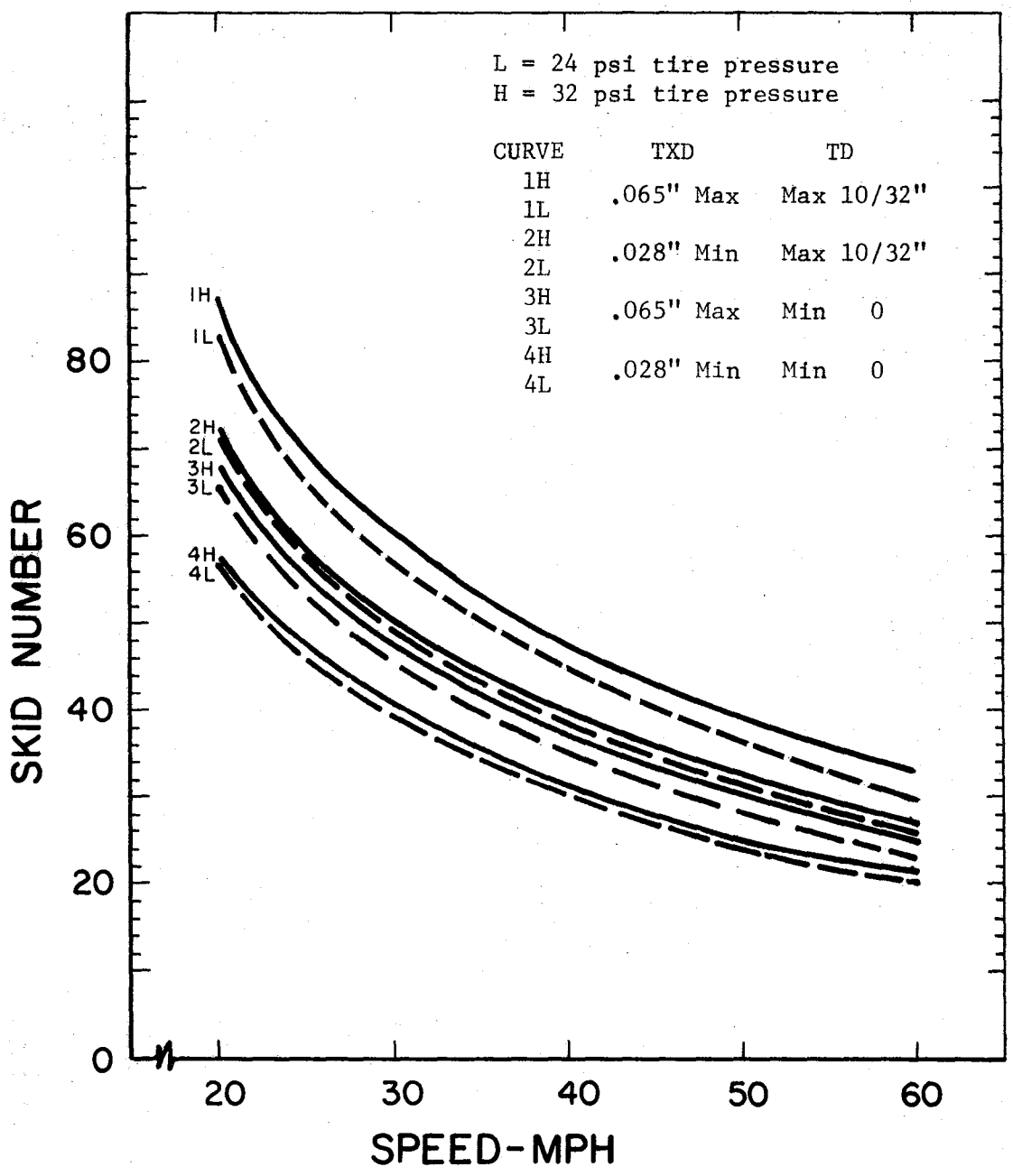

Fig.3-58. Effects of tire inflation pressure on skid numbers for the ASTM-14" tire at maximum water depth on longitudinally textured concrete pavements (TXD) and minimum and maximum tread depths (TD), East Bypass data.

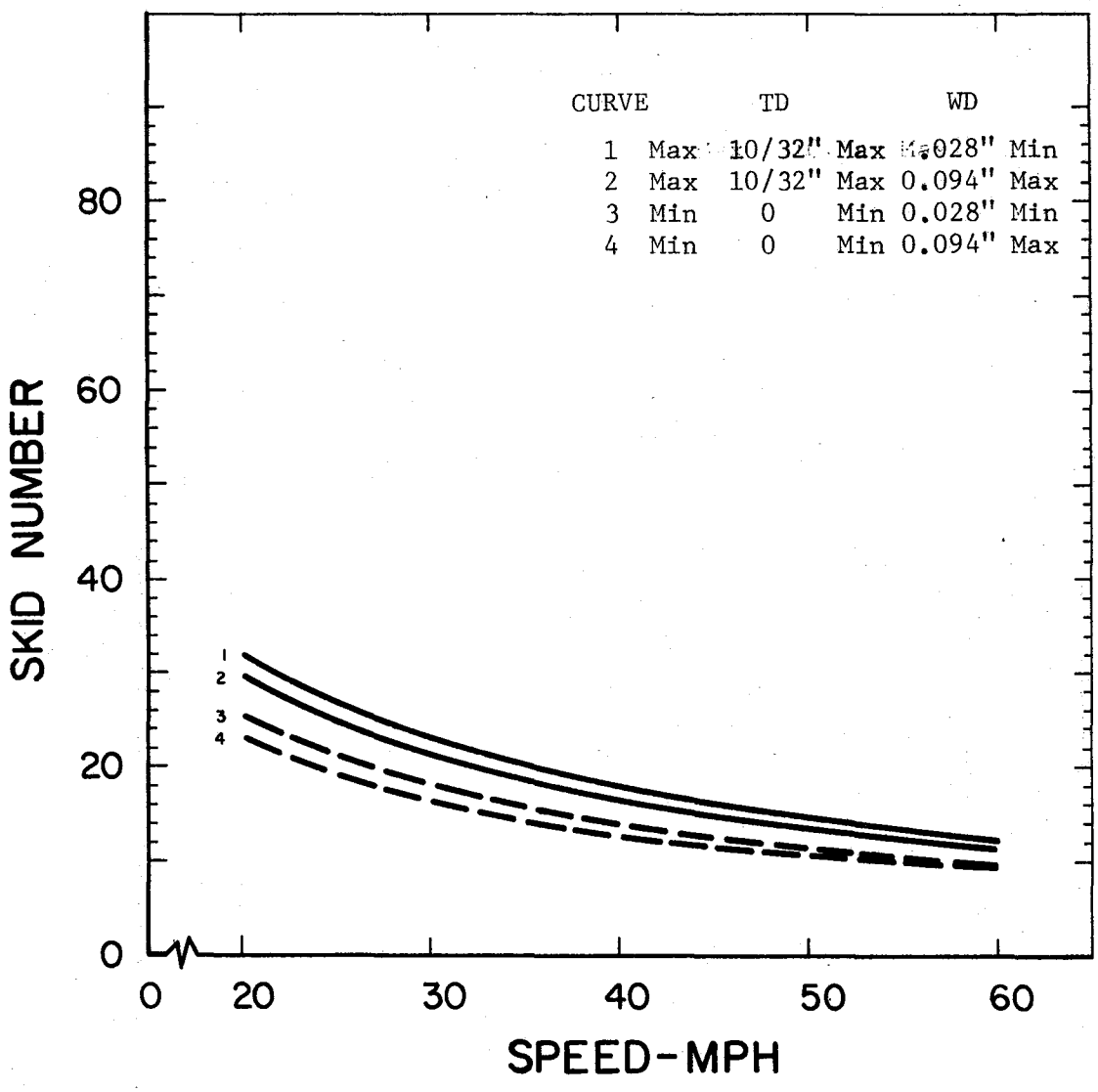

Fig. 3-59. Effects of tire tread depths (TD) and water depths (WD) on the skid number at various speeds for the ASTM-14" tire at 24 psi tire inflation pressure, Pad No. 2, Jennite surface, TAMU Annex data.

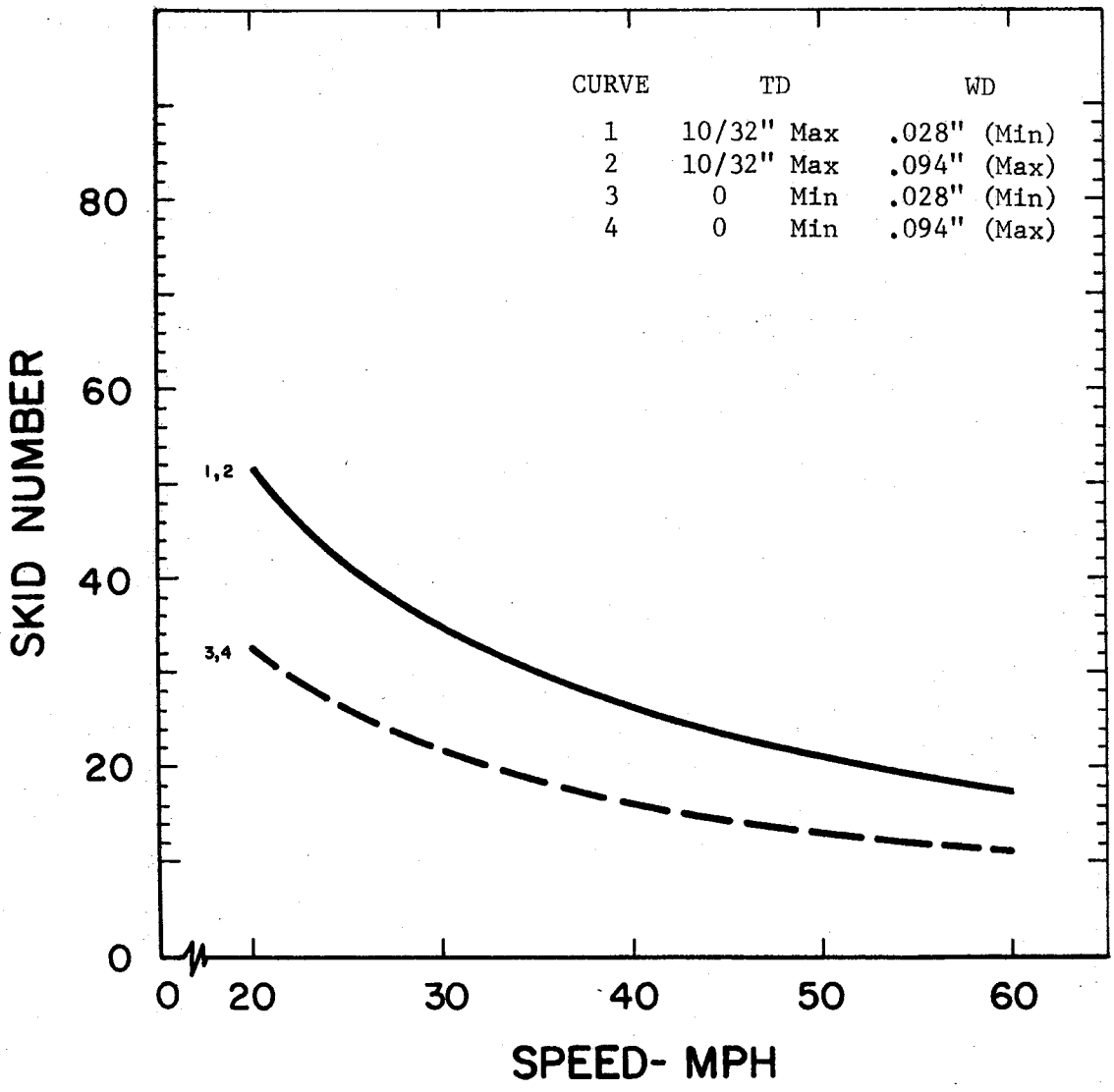

Fig. 3-60. Effect of tire tread depths (TD) and water depths (WD) on the skid number at various speeds for the ASTM-14" tire at 24 psi tire inflation pressure, Pad No. 9, painted concrete surface, TAMU Annex data.

Chapter IV

CONCLUSIONS AND RECOMMENDATIONS

A minimum tread-depth requirement should be included in vehicle inspection requirements. The minimum should not be less than about 0.06-inch.

The driving public should be advised of the intense dangers associated with high vehicle speeds and minimal tread depth during wet-pavement driving. This does not imply that the dangers exist only during periods of precipitation, but they exist in all instances when the surface is covered with a complete moisture film and/or loose debris.

Implicit procedures for adequately assessing the microtexture level of pavement surfaces need to be developed. This parameter, which is apparently an inherent property of the aggregate, is believed to affect the friction properties of surfaces to a greater extent than any other parameter. To date, however, only very crude methods (such as rubbing the aggregate surface with one's finger) have been found to be acceptable for assessment. Although not shown by hard data in this study, it appears that as the parameter characterizing the size of microtexture is increased from zero, the wet friction will first increase, reach a maximum value and then decrease. Optimizing this factor is therefore important.

The skid numbers and speed gradients of pavement surfaces tested by ASTM E-274-70 were found to be governed primarily by micro- and macrotexture parameters including size, spacing and shape. These determine the adhesion and hysteresis components of wet tire-pavement friction. Any rational pavement surface textural design technique must consider the interrelated effects of all of these texture parameters and a minimum average macrotexture depth should be included in highway design requirements. At high speeds

drainage at the tire-pavement interface is critically important and to effect this drainage macrotexture values in the 0.04 to 0.05 and above range are necessary for high speed traffic.

The skid number speed gradient is dependent on micro- and macrotexture parameters and both influence surface drainage; however, smooth surfaces have much lower speed gradients than those with microtexture only.

A minimum cross slope should be included in highway design requirements particularly for high speed pavements subject to frequent application of moisture. A minimum cross slope of 1.5% will reduce water depths and minimize the effects of unequal pavement settlement which produces "bird baths".

Development of multiparameter procedures for the estimation of pavement skid numbers from surface texture measurements should continue. Although the Schonfeld method appears to be the most promising at this time, this procedure requires strengthening with respect to absolute description of textural parameters.

The extensive data included in this report offer reasonable conclusive proof that average water depths required to inundate the pavement asperities create a potential and definite hazard to high speed traffic. This conclusion appears to prevail irrespective of the value of the texture depth within the range of values studied under simulated rain where the skid number was determined by conventional procedures. This was verified for seven different finishes on portland cement concrete as well as for numerous bituminous surfaces.

Conclusions specific to TTI Annex Pads:

1. An examination of Figure 3-49 shows that a combination of maximum texture depths (TXD), maximum tire tread depth (TD), and minumum water depth (WD), for the maximum texture depth will give the highest skid number at all speeds of 20 to 60 mph, for the ASTM-14" tire at 24 psi tire inflation pressure. Considering the limiting values of the variables of TXD, TD, and WD, the change of any one of these variables from minimum to maximum test value will significantly affect the skid number at any speed from 20 to 60 mph. Various combinations will reduce the skid number until the minimum skid number will result from the combination of minimum texture depth, minimum tread depth, and maximum water depth for minimum texture.

2. The effects of the variables on the composite commercial tire inflated to 24 psi pressure are summarized on Figure 3-50. The combination of maximum pavement texture depth, maximum tire tread depth, and minimum water depth result in the highest skid number values at all speeds of 20 to 60 mph. Water depth and texture depth affect the skid number as long as the tread depth is not zero. When the tread depth becomes zero, there is negligible effect from either texture depth or water depth on the skid number.

3. The ASTM-14" tire at 24 psi inflation pressure as compared to the composite commercial tire gives higher skid numbers for all comparable conditions of speed, pavement texture depth, tire tread depth, and water depth. The effects are summarized in Figure 3-51 and to make comparisons curve A1 is compared with C1, curve A2 is compared with C2, etc.

4. The effects of tire inflation pressure are small with the 32 psi tire pressure generally giving slightly higher values of skid number than 24

psi tire inflation pressure, both for the ASTM-14" tire and for the composite commercial tire, all other conditions being equal. These results are summarized on Figure 3-52 and Figure 3-53.

5. For the two special surfaces tested (Pad No. 2 - Jennite flush seal, and Pad No. 9 - Painted Portland cement concrete), water depths generally had only a small effect on the skid numbers for the painted concrete surfaces whereas the effect was significant for the Jennite flush seal surface especially for the composite commercial tire. The higher tire pressures did not produce significantly higher skid numbers except in the case of ASTM-14" tire on painted concrete. The Commercial tire gave higher skid numbers on the Jennite flush seal surface whereas there was no significant difference between the ASTM-14" tire and the composite commercial tire on the painted concrete surface.

Conclusions Specific to East Bypass Experimental Surfaces:

1. The effects of pavement texture, tire tread depths, and water depths on the skid number for speeds of 20 to 60 mph for the ASTM tire at 24 psi inflation pressure are summarized on Figure 3-54 for transverse textured concrete pavements and on Figure 3-55 for longitudinally textured concrete pavements. The combination of maximum texture, maximum tire tread depth, and minimum water depth results in the maximum skid number at all speeds of 20 to 60 mph, whereas the combination of minimum texture depth, minimum tire tread depth, and maximum water depth results in the minimum skid number at all speeds of 20 to 60 mph, for both the transverse and longitudinally textured concrete pavements.

2. Comparison of the effects of transverse and longitudinal textured concrete pavements indicate that skid numbers are generally significantly higher for the transverse textured pavements, other combinations of variables being held equal. The effect is more pronounced at the higher values of speed. These effects are summarized in Figure 3-56 and the curves 1T (transverse) is to be compared with 1L (longitudinal), 2T with 2L, etc.

3. The effect of tire inflation pressure appears to be negligible for transversly textured concrete pavements, whereas there is a slight advantage to higher tire inflation pressures for longitudinal textured pavements. The effects are summarized on Figure 3-57 and Figure 3-58 where curves 1H and 1L are to be compared as are 2H and 2L, etc.

BIBLIOGRAPHY

1. Kummer, H. W. and Meyer, W. E. Tentative Skid-Resistance Requirements for Main Rural Highways. NCHRP Report 37, Highway Research Board, 1967.

2. Dearinger, J. A. and Hutchinson, J. W. Traffic Control & Roadway Elements -- Their Relationship to Highway Safety, Revised, Chap. 7, Cross Section and Pavement Surface. Highway Users Federation for Safety and Mobility, Washington, D. C., 1970.

3. Agg, T. R. Tractive Resistance and Related Characteristics of Roadway Surfaces. Bulletin 67, Iowa State College Engineering Station, Feb. 1924.

4. Moyer, R. A. Skidding Characteristics of Road Surfaces. HRB Proc., Vol. 13, 1934.

5. Traffic Speed Trends. U. S. Department of Transportation, March 1969.

6. Norman, O. K. Todays Speeds. Proc. First Int. Skid Prev. Conf. - Part I, 1959.

7. Highway Research Board Committee D-B4 Task Group. An Inventory of Existing Practices and Solutions to Slippery Pavements-1969. Presented at the 49th Annual Meeting, Jan. 1970.

8. Correlation Service Circular 363. Highway Research Board, Washington, D. C., 1958.

9. Department of Scientific and Industrial Research. Road Research Laboratory Great Britain, The Road Surface, Chap. 14, Research on Road Safety, 1963.

10. Sabey, B. E. The Road Surface and Safety of Vehicles. Proc., Institution of Mechanical Engineers, Vol. 183, Part 3A, 1968-69.

11. Traffic Control and Roadway Elements -- Their Relationship to Highway Safety. The Automotive Safety Foundation, 1963.

12. Sabey, B. E. Road Surface Characteristics and Skidding Resistance. Journal of the British Granite and Whinstone Federation, Vol. 5, No. 2, Autumn 1965.

13. Sabey, B. E. Accident Reports as a Guide to Slippery Lengths of Road. Roads and Road Construction, Great Britain, 1956.

14. Hutchinson, J. W., **et al.** An Evaluation of the Effectiveness of Televised, Locally Oriented Driver Re-Education. Presented at the 48th Annual Meeting of the Highway Research Board, Jan. 1969.

15. Shupe, J. W. Pavement Slipperiness. Highway Engineering Handbook, Chap. 20. New York: McGraw-Hill, 1960.

16. The State of the Art of Traffic Safety. Arthur D. Little, Inc.; For the Automobile Manufacturers Association, Inc., June 1966.

17. Gallaway, Bob M. Skid Resistance and Polishing Type Aggregates. Texas Transportation Researcher, Vol. 5, No. 1, January 1969.

18. Schonfeld, R. Skid Numbers from Stereo-Photographs. Report No. RR155, Department of Highways, Ontario, Canada, Jan. 1970.

19. Sabey, B. E. The Road Surface in Relation to Friction and Wear to Tires. Road Tar, Vol. 23, No. 1, Great Britain, March 1969.

20. Csathy, T. I., Burnett, W. C. and Armstrong, M. D. State of the Art of Skid Resistance Research. Special Report No. 95, Highway Research Board, 1968.

21. Rose, J. G., Hankins, K. D. and Gallaway, B. M. Macrotexture Measurements and Related Skid Resistance at Speeds from 20-60 MPH. Presented at 49th Annual Meeting of Highway Research Board, Jan. 1970. (Publication pending).

22. Sabey, B. E. Road Surface Texture and Change in Skidding Resistance with Speed. RRL Report No. 20, Road Research Laboratory, Ministry of Transport, Great Britain, 1966.

23. Gallaway, B. M. Skid Resistance Measured on Polishing Type Aggregates. American Society of Safety Engineers Journal, Sept. 1969.

24. Goodwin, W. A. Evaluation of Pavement Aggregates for Non-Skid Qualities. Bulletin No. 24, Engineering Experiment Station, University of Tennessee, 1961.

25. Hutchinson, J. W., Kao, T. Y. and Pendley, L. C. Pavement Dynamic Permeability Testing. STP 456, American Society for Testing and Materials, 1969.

26. Nichols, F. P., Jr. Further Studies on Skid Resistance of Virginia Pavements. Proceedings First International Skid Prevention Conference, Part II, Virginia Council of Highway Investigation and Research, 1959.

27. White, A. M. and Thompson, H. O. Tests for Coefficients of Friction by the Skidding Car Method on Wet and Dry Surfaces. Bulletin No. 186, Highway Research Board, 1958.

28. Mason, D. F. A Preliminary Report on Skid Resistance of Various Asphaltic Highway Surfaces. Unpublished Report, Department of Highways of British Columbia, 1962.

29. Moyer, R. A. and Shupe, J. W. Roughness and Skid Resistance Measurements of Pavements in California. Bulletin No. 37, Highway Research Board, 1951.

30. Moyer, R. A. A Review of the Variables Affecting Pavement Slipperiness. Proceedings, First International Skid Prevention Conference, Part II, Virginia Council of Highway Investigation and Research, 1959.

31. Shupe, J. W. and Goetz, W. H. A Laboratory Investigation of Pavement Slipperiness. Bulletin No. 219, Highway Research Board, 1959.

32. Shupe, J. W. and Lounsbury, R. W. Polishing Characteristics of Mineral Aggregates. Proceedings, First International Skid Prevention Conference, Part II, Virginia Council of Highway Investigation and Research, 1959.

33. Sabey, B. E. Pressure Distribution Beneath Spherical and Conical Shapes Pressed Into a Rubber Plane, and Their Bearing on Coefficients of Friction Under Wet Conditions. Proceedings, First International Skid Prevention Conference, Part II, Virginia Council of Highway Investigation and Research, 1959.

34. Stephens, J. E. and Goetz, W. H. Effects of Aggregate Factors on Pavement Friction, Bulletin No. 320, Highway Research Board, 1961.

35. Stephens, J. E. and Goetz, W. H. Designing Fine Bituminous Mixtures for High Skid Resistance, HRB Proc., Vol. 39, 1960.

36. Giles, C. G. Standards of Skidding Resistance: Some European Points of View. Proceedings, First International Skid Prevention Conference, Part II, Virginia Council of Highway Investigation and Research, 1959.

37. Zuk, W. The Dynamics of Vehicle Skid Deviation as Caused by Road Conditions. Proceedings, First International Skid Prevention Conference, Part I, Virginia Council of Highway Investigation and Research, 1959.

38. Finney, E. A. and Brown, M. G. Relative Skid Resistance of Pavement Surfaces Based on Michigan's Experience. Proceedings, First International Skid Prevention Conference, Part II, Virginia Council of Highway Investigation and Research, 1959.

39. Schulze, K. H. and Beckman, L. Friction Properties of Pavements at Different Speeds. American Society of Testing Materials, STP No. 326, 1962.

40. Kullberg, G. Skiddometer. Swedish State Road Institute, 1959.

41. Mahone, D. C. Variation in Highway Slipperiness Characteristics with Location. American Society of Testing Materials, STP No. 326, 1962.

42. Giles, C. G. Where Tyre Meets Road in Wet Conditions. Engineering, Vol. 195, No. 5070, June 21, 1963.

43. Giles, C. G. and Sabey, B. E. Rubber Hysteresis and Skidding Resistance. Engineering, Vol. 186, No. 4842, 1958.

44. Kummer, H. W. Unified Theory of Rubber and Tire Friction. Engineering Research Bulletin B-94, Pennsylvania State University, 1966.

45. Meyer, W. E. Friction and Slipperiness. Highway Research Record 214, 1968.

46. Meyer, W. E. and Schrock, M. O. Review of Test Methods for Tire Friction Characteristics. Journal of Materials, Vol. 4, No. 1, March 1969.

47. Moore, D. F. The Logical Design of Optimum Skid Resistant Surfaces. Highway Research Board Special Report 101, 1969.

48. Horne, Walter B. and Dreher, R. C. Phenomena of Pneumatic Tire Hydroplaning. NASA Technical Note D-2056, November 1963.

49. Keen, Harry M. Design for Safety. Highway Research Record 214, 1968.

50. Sugg, R. W. Joint NASA-British Ministry of Technology Skid Correlation Study-Results from British Vehicles. NASA SP-5073, November 1968.

51. Harris, A. J. Road Surface Texture and the Slipperiness of Wet Roads. Highway Research Record 214, 1968.

52. Giles, C. G. Some European Methods for the Measurement of Skidding Resistance. Proceedings, First International Skid Prevention Conference, Part I, Virginia Council of Highway Investigation and Research, 1959.

53. Gallaway, Bob M. and Rose, J. G. Macrotexture, Friction, Cross Slope and Wheel Track Depression Measurements on 41 Typical Texas Highway Pavements. Research Report No. 138-2, Texas Transportation Institute, Texas A&M University, June 1970.

54. Gallaway, B. M. and Rose, J. G. Highway Friction Measurements with Mu-Meter and Locked Wheel Trailer. Research Report No. 138-3, Texas Transportation Institute, Texas A&M University, June 1970.

55. Gallaway, B. M., Epps, J. A., and Hargett, E. R. Design and Construction of Full-Scale Stopping Pads and Spin-Out Curves to Predetermine Friction Values. Journal of Materials, JMLSA, Vol. 5, No. 2, June 1970.

56. Gallaway, B. M., Schiller, R. E. Jr., and Rose, J. G. The Effects of Rainfall Intensity, Pavement Cross Slope, Surface Texture, and Drainage Length on Pavement Water Depths. Research Report No. 138-6, Texas Transportation Institute, Texas A&M University, January 1971.

57. The Physics of Tire Traction-Theory and Experiment Plenum Press, New York. P. 241, 1974.

58. McCullough, B. F. and Hankins, K. D. Texas Highway Department Skid Test Trailer Development. Research Report 45-1, Texas Highway Department, April 1965.

59. McCullough, B. F. and Hankins, K. D. Skid Resistance Guideline for Surface Improvements on Texas Highways. Record 131, Highway Research Board, 1966.

60. Giles, C. G., et al. Development and Performance of the Portable Skid-Resistance Tester. Technical Paper No. 66, Road Research Laboratory (Great Britain), 1964.

61. DuBose, D. A. "Select Calling Program," Institute of Statistics, Texas A&M University, 1970.

62. Hocking, R. R., and R. N. Leslie, "Selection at the Best Subset in Regression Analysis," Technometrics 9, pp. 531 - 540, 1967.

63. LaMotte, L. R., and R. R. Hocking. "Computational Efficiency in the Selection of Regression Variable," Technometrics 12, pp. 83-93. 1970.

64. Ledbetter, W. B., Meyer, A. H., and Ballard, D. E., "Quality of Portland Cement Concrete Pavement as Related to Environmental Factors and Handling Practices During Construction," Texas Transportation Institute, Research Report 141-4F, Sept. 1974.